UNIVERSITÄT ZU LÜBECK

From the Institute of Anatomy
of the University of Lübeck
Director: Prof. Dr. med. Jürgen Westermann

“Analyzing the dynamics of the T cell receptor repertoire within different compartments of the murine spleen”

Dissertation
for Fulfillment of
Requirements
for the Doctoral Degree
of the University of Lübeck

from the Department of Natural Sciences

Submitted by
Lisa-Kristin Schierloh
from Elmshorn

Lübeck 2023

First referee:	Prof. Dr. med. Jürgen Westermann
Second referee:	Prof. Dr. med. vet. Jennifer Hundt
Date of oral examination:	21.10.2024

Approved for printing. Lübeck, 25.10.2024

Abstract

Effective humoral immunity is ensured by the tightly regulated interaction between T and B lymphocytes at different sites within secondary lymphoid organs (SLOs). Accordingly, the diversity of the local T cell receptor repertoire (TCR-R) has major effects on the immune response, as the highly variable T cell receptor (TCR) determines the T lymphocyte's specificity. However, little is known about the definite distribution of the TCR-R at these sites of interaction and its implications for a T cell dependent B cell response since recent research mainly dealt with the analysis of blood or whole SLOs instead of their distinct compartments. Hence, we asked if the TCR-Rs of T cell zone (TCZ) and B cell zone (BCZ) already differ at the naïve state and whether this affects the reaction to a blood-born antigen. Since antigen challenge results in the development of germinal centers (GCs), we further asked if the TCR-R of T follicular helper (Tfh) cells as characteristic T lymphocyte subset within this compartment holds special features and can also be exchanged between compartments. Aside from this, we monitored the current sleep status as further aspect that might have an effect on the underlying TCR-R as well as the predominant milieu. We therefore combined the precise isolation of TCZ, BCZ and GC from splenic cryosections of C57BL/6J mice by laser microdissection and deep sequencing of the CDR3β region of the TCR, both under steady-state conditions and after injection of sheep red blood cells (SRBC).

Analysis of the TCR-R within splenic TCZ and BCZ in unimmunized mice revealed that though the BCZ only harbors about 7 % of T lymphocyte numbers compared to those in the TCZ, they give rise to approximately 16,000 different TCR clonotypes (i.e. one third of TCZ clonotype numbers). The majority of these clonotypes is showing "public" characteristics while a minority present in fractions of highest copy number is holding more "private"-like features. Challenging the TCR-R of both compartments by injection with SRBC results in the induction of a "private" immune response with accumulating antigen-specific clonotypes displacing the former dominating naïve rather "public" ones. Though starting on different levels, this shifting effect can be similarly seen for the TCR-R of both TCZ and BCZ. During the peak of reaction 7 days post immunization, Tfh cells within the GC hold several thousands of antigen-specific "private" clonotypes. We did not only find the majority to proliferate but also detected Tfh cells with same TCR sequences in compartments proximal to the GC of origin as well as in distantly located TCZ and BCZ and even in another GC. Accordingly, these antigen-specific Tfh cells are likely able to migrate between anatomical locations by entering into circulation, thus shaping the underlying TCR-R and facilitating an effective immune response. However, short-term sleep deprivation did not affect the afore analyzed parameters of the TCR-R though sleep restriction dampened the immunization-induced increase in the expression of genes associated with T cell signaling, cell adhesion, and thus cell trafficking during the peak of GC reaction.

Taken together, we for the first time revealed an extensive insight into the TCR-R distribution within the splenic compartments by using an in-depth analysis tool. The knowledge we gained can be of consequence for further investigations regarding the biological role of the TCR-R.

Zusammenfassung

Effektive humorale Immunität wird gewährleistet durch die streng regulierte Interaktion zwischen T- und B-Lymphozyten an verschiedenen Stellen innerhalb sekundär lymphatischer Organe (SLOs). Demzufolge hat die Diversität des lokalen T-Zellrezeptor-Repertoires großen Einfluss auf die Immunantwort, da der hoch variable T-Zellrezeptor die Spezifität der T-Lymphozyten bestimmt. Über die genaue Verteilung des T-Zellrezeptor-Repertoires an diesen Interaktionsorten und seine Auswirkungen auf eine T-Zell abhängige B-Zellantwort ist jedoch wenig bekannt, da sich bisherige Analysen hauptsächlich mit Blut oder ganzen SLOs anstelle einzelner Kompartimente befasst haben. Deshalb haben wir uns gefragt, ob sich das T-Zellrezeptor-Repertoire der T-Zellzone und B-Zellzone bereits im naiven Zustand unterscheidet und ob dies die Reaktion auf ein Antigen beeinflusst. Da die Konfrontation mit einem Antigen in der Entstehung von Keimzentren resultiert, haben wir uns darüber hinaus mit der Frage beschäftigt, ob das T-Zellrezeptor-Repertoire von follikulären T-Helferzellen (Tfh-Zellen) als charakteristische T-Lymphozytensubpopulation in diesem Kompartiment besondere Eigenschaften aufweist und auch zwischen Kompartimenten ausgetauscht werden kann. Zusätzlich haben wir den Schlafstatus als weiteren Faktor untersucht, der einen Effekt auf das zugrundeliegende T-Zellrezeptor-Repertoire sowie das vorherrschende Milieu haben kann. Hierfür kombinierten wir die präzise Isolation von T-Zellzone, B-Zellzone und Keimzentrum von Gefrierschnitten der Milz von C57BL/6J-Mäusen mittels Lasermikrodissektion und die Sequenzierung der CDR3β-Region des T-Zellrezeptors – sowohl unter naiven Bedingungen als auch nach der Injektion von „sheep red blood cells“ (SRBC).

Die Analyse des T-Zellrezeptor-Repertoires von T-Zellzone und B-Zellzone der Milz unimmunisierter Tiere ergab, dass die B-Zellzone, obwohl sie im Vergleich zur T-Zellzone nur ca. 7 % der Anzahl an T-Lymphozyten enthält, ungefähr 16.000 verschiedene T-Zellrezeptor-Klonotypen beinhaltet und somit ein Drittel der Klonotypenanzahl der T-Zellzone. Die Mehrheit dieser Klonotypen zeigt sogenannte „public“ Charakteristika, während eine Minderheit in Fraktionen höchster Kopienanzahl eher „private“-ähnliche Merkmale aufweist. Die Konfrontation des T-Zellrezeptor-Repertoires beider Kompartimente mit der SRBC-Injektion bewirkt die Induktion einer „private“ Immunantwort, bei der akkumulierende Antigen-spezifische Klonotypen die zuvor dominierenden naiven, eher „public“ Klonotypen verdrängen. Obwohl das Ausgangslevel unterschiedlich ist, kann dieser Umverteilungseffekt sowohl beim T-Zellrezeptor-Repertoire der T-Zellzone als auch in der B-Zellzone beobachtet werden. Während des Reaktionshöhepunkts sieben Tage nach Immunisierung weisen die Tfh-Zellen im Keimzentrum mehrere Tausend Antigen-spezifische „private“ Klonotypen auf. Wir konnten nicht nur zeigen, dass die Mehrheit proliferiert, sondern entdeckten auch Tfh-Zellen mit gleichen T-Zellrezeptor-Sequenzen in Kompartimenten nahe des Ausgangskeimzentrums

sowie in entfernt liegenden T-Zellzonen und B-Zellzonen und sogar in anderen Keimzentren. Somit scheinen diese Antigen-spezifischen Tfh-Zellen die Fähigkeit zu besitzen, durch Eintritt in die Zirkulation zwischen anatomischen Orten zu migrieren und auf diese Weise dort das zugrundeliegende T-Zellrezeptor-Repertoire zu formen und eine effektive Immunantwort zu fördern. Einen Einfluss von kurzzeitigem Schlafentzug auf die zuvor analysierten Parameter des T-Zellrezeptor-Repertoires konnten wir allerdings nicht feststellen, obwohl eingeschränkter Schlaf den Immunisierungseffekt auf die Expression von Genen, welche in T-Zellsignaling, Zelladhäsion und somit Zellwanderung involviert sind, am Höhepunkt der Keimzentrumsreaktion abschwächt.

Zusammengefasst konnten wir mithilfe unserer detaillierten Analyse zum ersten Mal einen umfangreichen Einblick in die Verteilung des T-Zellrezeptor-Repertoires innerhalb der Kompartimente der Milz liefern. Dieses Wissen kann für weitere Untersuchungen in Bezug auf die biologische Rolle des T-Zellrezeptor-Repertoires von grundlegender Bedeutung sein.

Table of Contents

List of Abbreviations

°C	Degree Celsius
µl	Microliter
µm	Micrometer
aa	amino acid(s)
AID	Activation-induced deaminase
ANOVA	Analysis of variance
APAAP	Alkaline Phosphatase - Anti-Alkaline Phosphatase
APC	Antigen presenting cell
B4GALT1/*b4galt1*	β-1,4-galactosyltransferase 1 (protein/gene)
BCL6	B cell lymphoma 6
BCR	B cell receptor
BCZ	B cell zone
BLIMP1	B lymphocyte induced maturation protein 1
bp	base pair(s)
BSA	Bovine serum albumin
C	Constant
Ca	Calcium
CCL21	C-C motif chemokine ligand 21
CCR7	C-C motif chemokine receptor type 7
CD	Cluster of differentiation
CD40L/*cd40lg*	Cluster of differentiation 40 ligand (protein/gene)
CDI	Coding Diversity Index
cDNA	Complementary DNA
CDR	Complementary determining region
CIITA/*ciita*	class II MHC transactivator (protein/gene)
CNS	Central nervous system
CT	Cycle of threshold
CXCL12, CXCL13	C-X-C motif chemokine type 12/13
CXCR4, CXCR5	C-X-C motif chemokine receptor type 4/5
d	Day(s)
D	Diversity
DAB	3,3-Diaminobenzidine
DC	Dendritic cell
DEPC	Diethyl pyrocarbonate
DNA	Deoxyribonucleic acid
DNase	Deoxyribonuclease

D_{NC}	Nucleotide Coding Simpson Index
dNTP	Deoxynucleotide triphosphate
DTH	Delayed-type hypersensitivity
DTT	1,4-Dithiothreitol
DZ	Dark zone
e.g.	For example (lat.: exempli gratia)
EAE	Experimental autoimmune encephalomyelitis
EDTA	Ethylenediaminetetraacetic acid
et al.	And others (lat.: et alii)
FDC	Follicular dendritic cell
FoxP3	Forkhead box protein P3
g	Gravitational constant
g	Gram
GAPDH/*gapdh*	Glyceraldehyde 3-phosphate dehydrogenase (protein/gene)
GC	Germinal center
geomean	Geometric mean
h	Hour(s)
HIV	Human immunodeficiency virus
HPRT/*hprt*	Hypoxanthine phosphoribosyltransferase (protein/gene)
HS	High salt (washing solution)
i.a.	Amongst others (lat.: inter alia)
i.e.	This is (lat.: id est)
ICOSL/*icoslg*	Inducible T cell costimulator ligand (protein/gene)
ID	Identification
IFN	Interferon
Ig	Immunoglobulin
IL	Interleukin
ITAM	Immunoreceptor tyrosine-based activation motif
J	Joining
k	Kilo
LAT	Linker of activated T cell
Lck	Lymphocyte-specific protein tyrosine kinase
LD	Levenshtein distance
log	Logarithm
LS	Low salt (washing solution)
LZ	Light zone
M	Molar

mg	Milligram
MHC	Major Histocompatibility Complex
min	Minute(s)
ml	Milliliter
mln	Mesenteric lymph node
MLN51/*mln51*	Metastatic lymph node 51 (protein/gene)
mM	Millimolar
mm	Millimeter
mRNA	Messenger RNA
MS	Multiple Sclerosis
n	Sample size
NCBI	National Center for Biotechnology Information
ng	Nanogram
NGS	Next-generation sequencing
nM	Nanomolar
NP-OVA	4-hydroxy-3-nitrophenylacetyl-OVA
NREM	Non-REM
NT	No template
nt	nucleotide(s)
OLGA	Optimized Likelihood estimate of immunoGlobulin Amino-acid sequences
OVA	Ovalbumin
p.i.	Post injection
PALS	Periarteriolar lymphoid sheath
PBS	Phosphate buffered saline
PCR	Polymerase chain reaction
PD1	Programmed cell death protein 1
PFA	Paraformaledehyde
pg	Picogram
P_{gen}	Generation probability
pM	Picomolar
pMHC	Peptide-MHC complex
prdm1	PR domain zinc finger protein 1 gene
qRT-PCR	Quantitative real-time PCR
RAG	Recombination-activating gene
REM	Rapid eye movement
RHI	Repertoire Homogeneity Index

RNA	Ribonucleic acid
RORγt	RAR-related orphan receptor γ (isoform)
rpm	Revolutions per minute
sec	Second(s)
SLO	Secondary lymphoid organ
SRBC	Sheep red blood cells
ST6GAL1/*st6gal1*	ST6 β-galactoside α-2,6-sialyltransferase 1 (protein/gene)
SWS	Slow wave sleep
TAE	Tris base, acetic acid, EDTA
T-bet	T-box expressed in T cells
TBS	Tris buffered saline
TCR	T cell receptor
TCR-R	TCR repertoire
TCZ	T cell zone
TE	Tris, EDTA
Tfh	T follicular helper (cell)
TGF	Transforming growth factor
Th	T helper (cell)
TNF	Tumor necrosis factor
Treg	regulatory T (cell)
Tris	Tris(hydroxymethyl)aminomethane
U	Dalton
UV	Ultraviolet
V	Variable
ZAP70/*zap70*	Zeta chain associated protein kinase (protein/gene)

1. Introduction

1.1. The immune system

The immune system is the body's defense against invading pathogens like e.g. bacteria and viruses, as well as other harmful foreign substances, thereby also functioning as a control machinery for own tissues to prevent abnormal cell growth. Thus, a complex network of specialized cells, tissues and organs executes a series of coordinated events to both protect the individual against disease and to prevent the loss of self-tolerance. These main tasks involve recognizing potentially infectious agents, fulfilling effector functions to eliminate the infection, regulating the immune response to prevent overflowing reactions and building memory for long-lasting protective immunity. Accordingly, the immune system comprises two specialized domains that successively take effect as defense mechanism: the innate and the adaptive immune system [1-3].

Physical and chemical barriers like skin and oral or intestinal mucosa form the first line of defense against invading pathogens. Once the barriers are overcome, they are faced with components of the complement system as well as macrophages and neutrophils that sense characteristic surface patterns (i.e. pathogen-associated molecular patterns) and start to lyse or phagocytize the foreign agents, respectively. Hence, inflammation is induced by secretion of cytokines or complement fragments that enables the extravasation of further immune cells into the infected tissue. Innate immunity starts immediately after infection, but its wanting specificity faces the problem of missing certain pathogens that are not sensed by the pattern recognition receptors of rudimentary immune cells [1-3].

This is the timepoint where the adaptive immune system comes into play. Although it takes days to successfully initiate this defense mechanism, it scores with its efficient recognition of antigens by specific lymphocyte receptors. The adaptive immune system thus mainly consists of two types of lymphocytes that represent cellular and humoral immunity, respectively: T cells that function by direct cell contacts and B cells that produce antibodies to fight against infections. T lymphocytes are unable to detect antigens themselves, thus requiring the presence of antigen presenting cells (APCs) like dendritic cells (DCs) or B lymphocytes. DCs ingest antigen and present peptide fragments on their major histocompatibility complex (MHC). By getting in touch with T cells that recognize the presented peptide with their cognate T cell receptor (TCR), the APC initiates the lymphocyte's activation. Activated T lymphocytes then start to expand and become effector cells after second antigen encounter. Depending on their differentiation, these effector T cells are either able to directly eliminate virus-infected cells or to activate macrophages or B lymphocytes to disarm bacteria or produce antigen-specific antibodies, respectively. Accordingly, one of the fundamental components of adaptive immunity is the T cell dependent B cell response that relies on the complex interplay between

T and B cells. This effective interaction takes place in secondary lymphoid organs (SLOs), which serve as gathering places for immune cells and antigens, thus facilitating the generation of effective immune responses [1-3].

1.1.1. The spleen as SLO

SLOs including lymph nodes, Peyer's patches, tonsils, and the spleen, are structures organized to generate and coordinate immune responses by accumulation of lymphocytes and presentation of encountered antigen. While Peyer's Patches function to mount effective immune responses against pathogens invading the gastrointestinal tract, tonsils build a defense against ingested or inhaled pathogens. Furthermore, lymph nodes are distributed along the whole body and served by lymphatic vessels, thus covering the interception of antigens present in the tissue of their respective drainage area [2-5]. The spleen, known as the largest contiguous SLO, scans the blood for foreign pathogenic antigens and abnormal cells that have entered via the splenic artery located directly below the capsule [6, 7]. It is arranged of two functional regions, the red and the white pulp. While the red pulp functions to filter and remove damaged blood cells, the white pulp harbors different types of lymphocytes that are compartmentalized in anatomically distinct areas. T lymphocytes are mainly centered around a central arteriole, thus forming a compartment named as periarteriolar lymphoid sheath (PALS). This T cell zone (TCZ) is surrounded by accumulating B lymphocytes that form several follicles. During an ongoing immune response, the interaction of T and B cells gives rise to another, well-organized compartment within the B cell follicle, the germinal center (GC). The marginal zone that aside from B lymphocytes also contains specialized macrophages, forms the border between red and white pulp and hence represents a transition between the innate and the adaptive immune system [3, 4].

1.1.2. The T cell dependent B cell response

The T cell dependent B cell response is a complex and tightly regulated process that involves several distinct phases of antigen presentation and cell interaction. It is targeted on the production of extremely effective antibodies to fight infections. Furthermore, a second hallmark is the ability for creating immunological memory, i.e. resting memory T and B lymphocytes that speed up a secondary immune response when re-encountering their antigen [1, 8].

Naïve T lymphocytes circulate via the blood stream in search of their specific antigen, thereby continuously entering SLOs and scanning DCs in the TCZ. These immune cells are able to take up and process antigen, subsequently presenting small peptide fragments on their MHC class II molecules. Upon encountering with DCs, the engagement of the TCR with the cognate peptide-MHC complex (pMHC) triggers T cell activation, that is further facilitated by various co-stimulatory molecules. Once activated, antigen-specific T lymphocytes that bear cluster of differentiation (CD) 4 co-receptor undergo clonal expansion and differentiation into different

subsets. Activated T cells may either leave the SLO and adopt effector functions in peripheral tissues upon secondary encounter or they stay to interact with B lymphocytes. Like DCs, B cells are also able to take up, process and present antigen. In the B cell follicle, they take up unprocessed foreign antigen that is presented by follicular dendritic cells (FDCs) or a specialized subtype of macrophages residing e.g. in splenic marginal sinus, and express the peptide fragments on their MHC class II molecules. When relocated to the TCZ border, the B lymphocyte might thus cause a secondary contact between the activated T cell and its cognate antigen, finally inducing the differentiation into an effector T cell. This lymphocyte in turn produces cytokines that activate the respective B cell to proliferate, thus becoming either a short-lived plasma cell in extrafollicular foci or returning to the B cell zone (BCZ) to induce the development of secondary lymphoid follicles with GCs. During the precise coordinated machinery of the GC reaction, B cells are forced to become high-affinity antibody producing plasma cells or memory B cells. In this process, a specialized subtype of $CD4^+$ T lymphocytes takes over critical functions and will be examined more closely in section 1.3.1: T follicular helper (Tfh) cells [1, 2, 8, 9].

1.2. T lymphocytes

T cells play a pivotal role in adaptive immune responses, orchestrating a diverse array of immune reactions against pathogens, tumors, and self-antigens. Their function is based on their unique, membrane bound TCR [2].

1.2.1. The T lymphocyte receptor

The T lymphocyte's antigen receptor is a highly variable heterodimer consisting of an α and a β polypeptide chain that are linked by a disulfide bond (Figure 1A). A minority of T cells are also bearing an alternative heterodimeric receptor built by γ and δ chains, but in this study we will only focus on α:β TCRs [1, 2]. Each TCR chain consists of an amino-terminal variable region (i.e. the site of antigen-recognition) and a constant region that segues into stalk segment and transmembrane region to finally end in a short cytoplasmatic tail. Contrary to the B cell receptor (BCR), the TCR does not bind antigen by itself. It requires the presentation of processed short antigenic peptide fragments on MHC molecules on the surface of APCs. As the TCR recognizes features of both presented antigenic peptide and MHC complex, its specificity is determined by this unique combination. The domain by which the TCR contacts both components is termed complementary determining region (CDR) 3. This hypervariable region is one of the key determinants of TCR diversity and arises from the random recombination of certain gene segments during T cell development. Whereas two additionally CDRs (CDR1 + CDR2) are completely coded by the variable (V) gene segment and primarily interact with the MHC complex, the CDR3 domain spans the joining region of V, diversity (D) and joining (J) gene segment, with the D segment only occurring in the β chain. These DNA

fragments are multiply encoded in the respective chain locus and are randomly rearranged during a process called somatic recombination (Figure 1B) [1, 2, 10]. For the β chain, RAG (i.e. recombination-activating gene) enzymes first catalyze the combination of D and J gene segment to which in two consecutive steps a V and a constant (C) segment are added. In the α chain, V and J segment are directly combined without further placing a D segment in between. At the segment joining side, additional nucleotides can be inserted or deleted, thus further increasing the variability of the resulting TCR chain [1, 2]. Together with the combination of α and β chain, this process during T cell development results in a huge diversity of potentially generated TCR sequences that are theoretically said to reach more than 10^{15} unique TCRs, with only about 2 x 10^7 or 2 x 10^6 being simultaneously realized in a human's or mouse's repertoire, respectively [10-12].

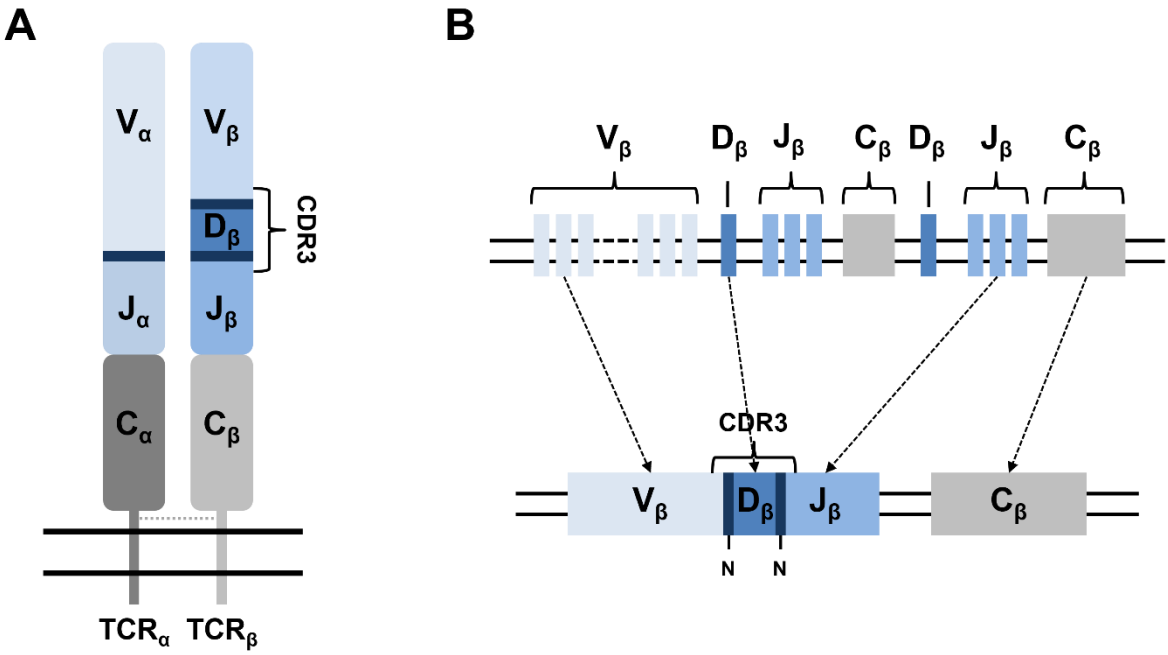

Figure 1: Structure and development of the TCR.
(A) The T cell receptor (TCR) consists of two polypeptide chains, mostly α and β chain. Each chain is composed of a constant and a variable part that is assembled out of single segments. **(B)** During somatic recombination in a T cell's maturation process, these variable (V), diversity (D), joining (J) and constant (C) segments that are multiply encoded on the respective gene locus, are randomly rearranged and additional nucleotides (N) inserted or deleted at the joining sites. The thusly hypervariable complementary determining region 3 (CDR3) that spans this joining region likely determines TCR specificity. Scheme exemplarily illustrates development of TCRβ chain, following graphical layout of [13].

1.2.2. Development and differentiation of T lymphocytes

The development of the TCR repertoire (TCR-R) occurs within the thymus, a specialized primary lymphoid organ [3]. T lymphocyte progenitors without expressed co-receptors developed from hematopoietic stem cells in the bone marrow migrate here for primary maturation. After TCR generation, T cells further undergo a series of distinct selection processes, termed positive and negative selection, which shape the functional repertoire of mature T cells [14]. Positive selection ensures that T cells expressing TCRs with moderate

affinity for self-MHC molecules survive, while those with insufficient or excessive affinity are eliminated. This applies to T lymphocytes expressing both co-receptors CD4 and CD8, i.e. representing a double positive state. In addition, a first lineage commitment of these cells takes place. There are two classes of MHC molecules that differ in both structure and expression, resulting in a MHC restriction for the respective TCR and a single positive state of the lymphocyte. Accordingly, $CD4^+$ T cells are specific for MHC class II molecules while $CD8^+$ T cells interact with MHC class I molecules [1, 2]. As a next step, negative selection eliminates T cells with high affinity for self-antigens presented by self-MHC molecules, preventing the development of autoimmune responses and thus maintaining self-tolerance [14]. Taken together, these selection processes ensure that the mature T cell repertoire is diverse, self-tolerant, and capable of mounting effective immune responses against foreign pathogens. The thusly formed naïve T lymphocytes are able to leave the thymus and migrate to SLOs for encountering antigen and further differentiation [1, 3].

As mentioned above, during maturation two types of naïve T lymphocytes are generated: $CD4^+$ T helper (Th) cells and $CD8^+$ cytotoxic T cells. Cytotoxic T cells interacting with MHC class I molecules expressed on all cells bearing a nucleus are especially responsible for eliminating virus-infected and tumor cells and play a critical role in cell-mediated immunity. They are armed with the ability to directly kill infected or cancerous cells through the release of cytotoxic molecules such as perforin and granzymes [1-3]. On the other hand, Th cells that only recognize antigenic peptides presented by MHC class II molecules expressed on a specialized type of cells, i.e. APCs like DCs and B cells, mainly take over help functions for other immune cells like macrophages or B lymphocytes [1-3]. The $CD4^+$ Th cells can further differentiate into various functional subsets, including amongst others Th1, Th2, Th17, and regulatory T (Treg) cells (Figure 2) [15-18]. These subsets exhibit unique cytokine profiles and effector functions, enabling tailored immune responses to combat specific pathogens. Factors affecting the differentiation of $CD4^+$ T lymphocytes into the different subsets are said to be both the cytokine milieu during activation and the TCR signaling strength [19-22]. Although these lymphocytes are producing different kinds of cytokines themselves, they retain a certain type of plasticity that allows them to take over features of other lineages [15, 21-23]. Of particular importance within the $CD4^+$ T cell lineage are Tfh cells, which play a crucial role during the GC reaction in the T cell dependent B cell response [23].

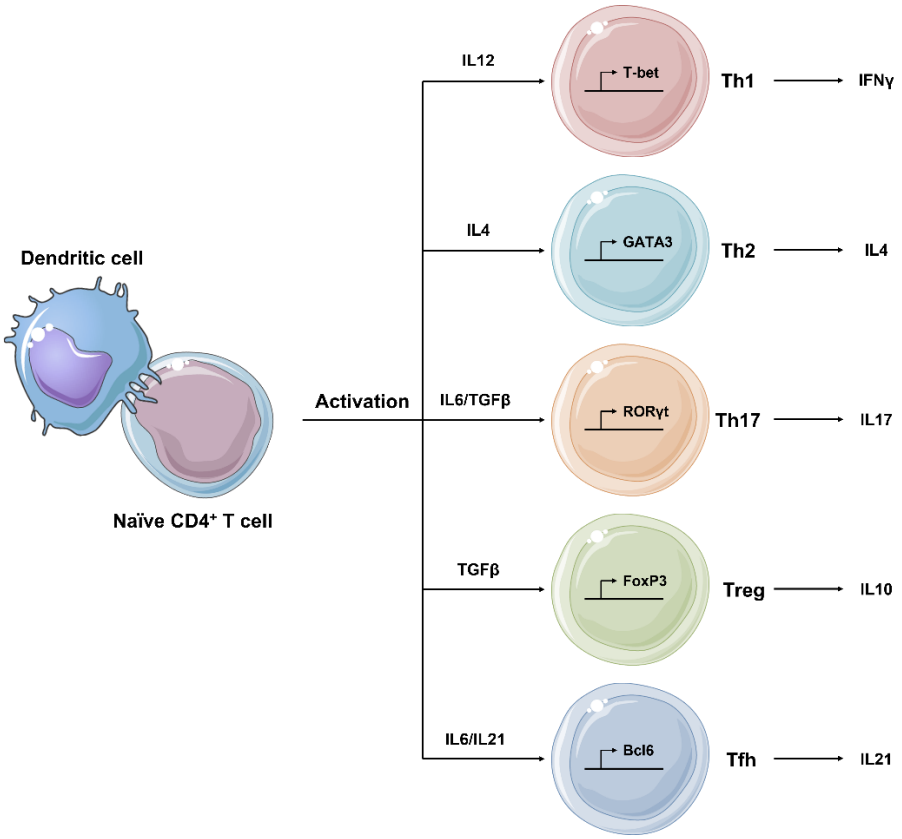

Figure 2: CD4⁺ T lymphocyte subsets.
Upon activation, lineage commitment of CD4⁺ T lymphocytes takes place. Depending on the predominant cytokine milieu, T cells differentiate into subsets that are characterized by both specific transcription factor and cytokine secretion. Graphical layout in the style of [24] and [25], partly generated by using [26]. Bcl6 – B cell lymphoma 6; CD – cluster of differentiation; FoxP3 – forkhead box protein P3; IFN – interferon; IL – interleukin; RORγt – RAR-related orphan receptor γ; T-bet – T-box expressed in T cells; TGF – transforming growth factor; Th – T helper cell; Tfh – T follicular helper cell; Treg – regulatory T cell.

1.3. The GC reaction

The GC is a specialized compartment in SLOs that originates in B cell follicles during a humoral immune response. It serves as a power station for the development of high-affinity antigen-specific antibodies. GCs are mainly composed of proliferating B lymphocytes, but also harbor specialized T cells, macrophages and FDCs. Two functional areas can be distinguished by means of the packing density of contained cells, namely the light zone (LZ) and the dark zone (DZ), in which different steps of the GC reaction take place (Figure 3). These sub compartments are surrounded by a peripheral mantle zone that mainly consists of resting B cells [1, 27, 28].

As mentioned in section 1.1.2, in the course of a T cell dependent B cell response, B lymphocytes that recognize by FDCs or macrophages within the follicle presented antigen with their BCR, internalize the foreign particle and start to present antigenic peptide fragments on their MHC class II molecule [1]. This process induces the expression of C-C motif chemokine receptor CCR7, which navigates the B lymphocyte to the TCZ border where the ligand CCL21 is highly expressed [29]. In turn, a specialized subset of CD4⁺ T lymphocytes,

i.e. Tfh cells, upregulates CXCR5 (i.e. C-X-C motif chemokine receptor type 5) upon activation and starts to migrate to the follicle border, attracted by the C-X-C motif chemokine CXCL13 that is expressed by FDCs [1, 28, 30]. The regulated migration of both cell types to the boundary increases the chance of interaction between appropriate T and B lymphocytes. Receiving T cell help results either in a primary focus of clonal B cell expansion or in the development of GCs. Together with their appropriate Tfh cells, these activated B lymphocytes return to the follicle center and start to undergo cycles of proliferation and affinity maturation [1, 8, 27, 28].

GC B cells, former named centroblasts, extensively proliferate in the DZ that is located proximal to the TCZ. The highly expressed chemokine CXCL12 there retains those CXCR4 expressing lymphocytes in this area. Besides the increased division rate in the DZ, B cells undergo diversification of their BCR. This process called somatic hypermutation induces point mutations in the variable region of immunoglobulin (Ig) genes, resulting in alterations of the respective amino acid sequence that consequently affects both antigen specificity and affinity [1, 2, 28]. Instead of a normal mutation rate of one base pair (bp) change per 10^{10} bp, the enzyme activation-induced deaminase (AID) introduces one point mutation per 10^{3} bp per cell division [1, 30]. Accordingly, the altered BCR will have an effect on the B cell's ability to bind a certain antigen, thus regulating the lymphocyte's fate. Mutations with a negative impact will result in the apoptosis of the respective B cell by tingible body macrophages, while B lymphocytes that received mutations that led to an improved BCR affinity are forced to clonally expand. After some cycles of proliferation and mutation, those B cells reduce their expansion rate, downregulate CXCR4 expression and move towards the GC LZ. Here, selection of the now termed centrocytes takes place by FDCs and Tfh cells. The newly assembled BCR is tested for its ability to bind antigen presented by FDCs. Appropriate B lymphocytes thus receive survival signals to undergo additional rounds of proliferation and mutation in the DZ. Furthermore, B cells also compete for limited Tfh cell help to experience additional co-stimulatory signals. Thereby, B lymphocytes with higher affinity of their BCR to bind the respective antigen as well as presenting the processed peptides to Tfh cells have an advantage over lower affinity B cell clones, thus receiving more positive selection signals. By means of the repetitive rounds of proliferation, mutation and selection, called cyclic-reentry, and thus bidirectional migration between DZ and LZ, both affinity and specificity of positively selected B cells is continuously refined. Competition between B lymphocytes causes an increased average affinity over time and effectuates that sometimes the clonal burst results in GCs being harbored by descendants of only a few single B cells. When these high-affinity B lymphocytes now exit the GC, they are forced to become a long-lived plasma cell, whereas clones with slightly lower affinity can still take the path of memory B cells. Moreover, since GCs are said to be open compartments, B lymphocytes can spread across other GCs, thus

increasing the overall efficiency of the affinity maturation process. In addition to affinity maturation, B lymphocytes also experience isotype switching. While early stages of the antibody response are dominated by IgM antibodies, especially IgG is becoming the predominant antibody class later. Taken together, the aim of the GC reaction is to achieve long-lived plasma cells producing high-affinity antibodies with maximum specificity against foreign pathogens while simultaneously maintaining self-tolerance and preventing overflowing of the immune response [1, 2, 23, 27, 28].

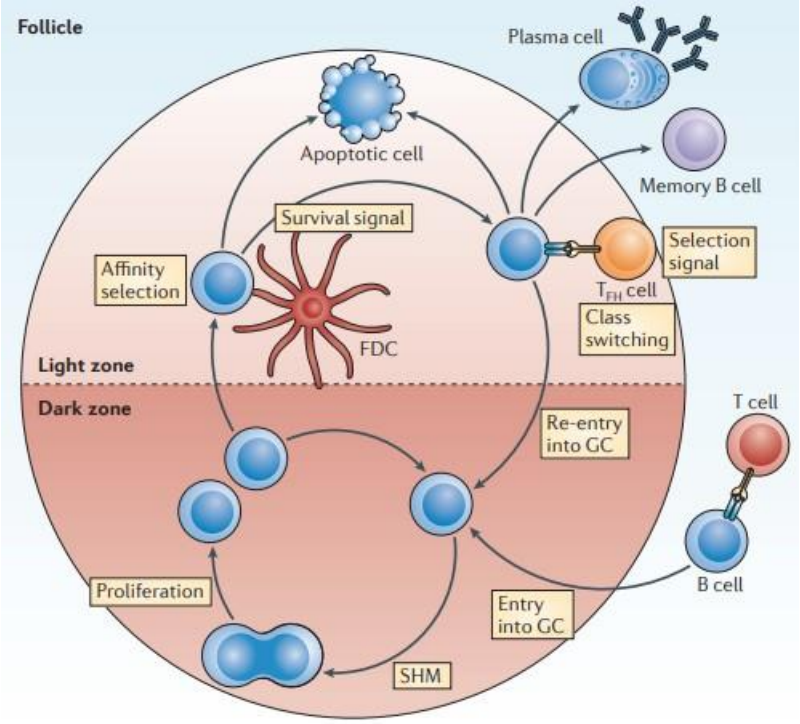

Figure 3: The GC reaction.
At the follicle border, interaction of cognate T and B cells takes place. Receiving co-stimulatory signals forces the B lymphocyte to return to the follicle to induce germinal center (GC) formation. In the GC dark zone, the B cell undergoes cycles of somatic hypermutation (SHM) and proliferation before migrating to the light zone where affinity selection of the mutated B cell receptor (BCR) occurs. While B cells with too low affinity for the antigen presented on follicular dendritic cells (FDCs) undergo apoptosis, the remaining lymphocytes receive survival signals to compete for the limited help of T follicular helper (Tfh) cells. Higher affinity B lymphocytes that are favored during interaction with Tfh cells can now re-enter the dark zone for further expansion and mutation or they can exit the GC to become an antibody-producing plasma cell or a memory B cell. Figure adapted from [31].

1.3.1. T follicular helper lymphocytes

Tfh cells are of particular importance within the $CD4^+$ T cell lineage and play a crucial role in the T cell dependent B cell response [16, 23]. They are amongst others characterized by the expression of transcription factor B cell lymphoma 6 (BCL6), programmed cell death protein PD1 and chemokine receptor CXCR5, which guides their migration to the B cell follicles within SLOs. BCL6 is also highly expressed in GC B cells and suppresses BLIMP1 (i.e. B lymphocyte induced maturation protein 1) as main regulator for effector and plasma cell differentiation [23, 32, 33]. Tfh cell differentiation is initiated in the TCZ by DCs producing interleukin 6 (IL6) that

increases IL21 production of T lymphocytes. Secretion of IL6 and IL21 in turn activates a signaling cascade to enhance BCL6 expression. Co-stimulatory signals like inducible T cell costimulator (ICOS) signaling received by interaction of T lymphocytes and DCs further strengthens the autocrine IL21 production and thus Tfh cell differentiation. Hence, Tfh cell conditioning due to follicular niches follows the principle of chance escape, i.e. getting away from an IL2-rich area that forces BLIMP1 induction and thus effector cell lineage, and chance encounter, i.e. staying in and being primed by an IL6-rich follicle surrounding [23, 30, 32-36]. Besides the cytokine milieu, TCR signaling strength is also said to affect T cell differentiation, with strong TCR signaling forcing Tfh cell development. However, Tfh cells, especially when present in GCs, are polarized the most, but still maintain a certain degree of plasticity that facilitates adopting characteristics of other T cell lineages [23, 24, 36].

Tfh cells that migrate to the follicle border experience a second antigen encounter when meeting cognate B lymphocytes that were likewise recruited to the boundary. Receiving activation signals from these T lymphocytes is important for further B cell differentiation and co-stimulatory signals form appropriate B lymphocytes are in turn essential for the Tfh cells. Especially CD40 and ICOS take over crucial functions in maintaining and strengthening lymphocyte differentiation and GC development during a T cell dependent B cell response. By interaction of CD40 on B lymphocytes and CD40L expressed on activated Tfh cells, both T cell growth and B cell proliferation can be increased. This contact-depending help during the immunological synapse drives the B cell response and causes the expression of further co-stimulatory molecules as well as cytokine secretion. In addition, ICOS expressed on Tfh cells encountering ICOSL presented by B lymphocytes facilitates the maintenance of entangled contacts between both lymphocytes and thus the exchange of additional co-stimulatory signals. This entanglement during formation of the immunological synapse between T and B cell allows an effective, specific and sensitive cytokine transfer despite short cell contacts. By doing so a selective and individual T cell help for antigen-specific B lymphocytes during the GC reaction can be ensured, thus regulating the competition of B cells of different affinity and consequently both affinity maturation and differentiation. Accordingly, the interplay between co-stimulatory signals and secretion of specialized cytokines by Tfh cells illustrates the critical function of this T cell subtype in mediating B cell maturation and consequently the generation of long-lived humoral immunity [23, 28, 30, 36, 37].

1.4. The antigen SRBC

To study such T cell dependent B cell responses in the spleen, the antigen of choice should fulfill certain requirements to mimic invading pathogens.

Sheep red blood cells (SRBC) are heterologous erythrocytes that are often used as thymus-dependent antigen to induce a T cell dependent immune response. Depending on application

site and dose, different types of immune responses can be generated. While high dosed injection of SRBC applied intravenously induces a humoral immune response, subcutaneous injection was shown to provoke a cellular one. Dose-dependency was especially illustrated by the so called delayed-type hypersensitivity (DTH) model. Here, primary intravenous injection of low dosed SRBC (10^5) resulted in a cellular immune response after subcutaneous DTH triggering, whereas intravenous injection of high doses (10^9) induced a humoral immune response [6, 38, 39].

Due to the multitude of studies using SRBC as antigen, the time course of antigen accumulation, uptake and presentation is well described. Intravenous injection of this non-replicating antigen effectuates that antigen uptake is timely restricted since blood-born antigens reach the spleen within seconds and are cleared from circulation within one hour. Furthermore, SRBC do not require adjuvants to induce an immune response and offer many different epitopes, thus ensuring antigen specificity of recruited T lymphocytes. Taken together, high dosed SRBC-injection is advantageous to directly and quickly induce a $CD4^+$ T cell dependent B cell response that is not disturbed by prolonged release of antigen or adjuvants [6, 39-44].

1.5. Sleep

Sleep is defined as a regularly occurring reversible state of inactivity and reduced responsiveness, in some degree comparable to a weakly pronounced unconsciousness. However, it is not a passive condition at all. The functions of sleep are multifarious: During sleep, energy storages are refilled, macromolecules synthesized and thus cell growth advanced as well as damaged cells repaired. In addition, it also effectuates memory formation and fulfills important tasks for an efficiently operating immune system (see section 1.5.1) [45-51]. Sleep is thereby associated with changes in neurophysiological, vegetative, and endocrine parameters, with characteristic patterns of distinct brain and body activity occurring during the different stages of sleep. For example, in contrast to slow wave sleep (SWS) that is accompanied with a reduced metabolic rate but still measurable muscle tonus, the so called rapid eye movement (REM) sleep is actually named for its typical eye fluctuations. Episodes of dreaming are mainly limited to this phase which is further characterized by suppressed muscle motion but increased brain activity almost comparable to wakefulness [46-49, 52].

According to the two-process model by Borbély [53], regulation of the sleep-wake cycle is subjected to both homeostatic and circadian components. Whereas the homeostatic component determines that the need for sleep increases after prolonged wakefulness, the circadian system mainly modulates the timing of sleep independent from the awake episode [46, 47]. Circadian rhythms thereby describe regularly occurring oscillations of biological parameters within approximately 24 hours (h). They are endogenously generated and

regulated by an “internal clock” consisting of the suprachiasmatic nuclei in the hypothalamus and numerous so called clock genes in the periphery but can be entrained to the environment by external stimuli like light or temperature. Besides body temperature and secretion of certain hormones the sleep-wake cycle is the most prominent circadian rhythm in humans. Moreover, sleep itself acts in concert with the “internal clock” in regulating the rhythms of other body parameters. For example, levels of growth hormone are elevated during sleep while cortisol levels are highest directly after the sleeping phase [45, 46, 52].

Considering the manifold spheres of sleep, it is no wonder that sleep deprivation can have severe consequences. Apart from alterations in memory, perception and concentration that e.g. can increase the probability of accidents, sleep deprivation is also associated with a higher risk for weight gain up to obesity, diabetes type II, hypertension and myocardial infarctions [51, 52, 54-57]. Accordingly, the relationship between sleep and the immune system is of prime importance.

1.5.1. Sleep and the immune system

There is a bi-directional relationship between sleep and the immune system, with immune parameters affecting sleep and sleep influencing immune responses [47, 58]. For example, immune activation during an infection on the one hand results in an increased need for sleep and accordingly enhanced sleep duration and intensity but can on the other hand also cause sleep disruptions when infections are overflowing. It is said that pro-inflammatory cytokines like interferon (IFN) γ or IL2 increase the amount of non-REM (NREM) sleep, i.e. sleep stages one to three including SWS. Anti-inflammatory cytokines like IL4 or IL10 in contrast dampen NREM sleep. In particular, cytokines IL1, tumor necrosis factor (TNF) and IL6 are rumored to regulate the sleep-wake cycle, with IL1 and TFN promoting sleep while too much IL6 is rather prejudicial. Accordingly, infections are able to alter sleep, whereas in turn healthy sleep affects various immune parameters, thus e.g. improving host defense mechanisms and outcome of vaccination responses [45-47, 52].

Experimental studies comparing the impact of sleep deprivation with regular sleep found out that sleep reduces the number of circulating leukocytes while promoting their distribution to other tissues, with e.g. higher numbers of T cells found within lymph node or spleen [52, 59, 60]. By especially facilitating the redistribution of APCs and T lymphocytes to SLOs and e.g. causing a shift towards increased Th1 cell activity, sleep enhances the chance of interaction and thus formation and efficiency of an immunological synapse. Thereby, the specific cytokine milieu predominant during SWS is extremely suited to favor and support APC – T cell interactions. This consequently promotes lymphocytes activation, proliferation and differentiation and thus the induction of an effective adaptive immune response including the formation of memory T and B cells. Hence, sleep does not only support psychological memory

consolidation but also the formation of immunological memory [52, 59]. Besides effects on distribution, activation and proliferation of immune cells, sleep furthermore increases the number of antigen-specific T lymphocytes and antibody titers following vaccination, e.g. shown for vaccinations against influenza, hepatitis A and B virus [61-63]. Thus, sleep does not only affect infection outcome but also the response to vaccination and hence is beneficial for both the innate and the adaptive immune system.

As a result of the strong regulatory interaction between sleep and the immune system, sleep restriction can stimulate inflammatory immune responses that can result in the emergence of infections or various diseases [46, 47, 64]. For example, sleep-deprived individuals are more prone to pulmonary infections or have an increased risk for cardiovascular diseases [46, 65]. In addition, prominent chronic infections that are associated with sleep disturbances are e.g. human immunodeficiency virus (HIV) or hepatitis C [46-48]. The correlation between sleep disorders and autoimmune diseases is moreover subject of today's research as well [46, 66].

1.6. Study aims

The T cell dependent B cell response represents an important part of the adaptive immune system. The precisely regulated interaction between T and B lymphocytes at different sites within SLOs thus facilitates the formation of effective humoral immunity. Although B cells are the source of antibodies to fight infections, T lymphocytes are pivotal in orchestrating those functions. As the highly variable TCR determines the T lymphocyte's specificity, the diversity of the TCR-R has major effects on the immune response. Despite this critical role, there are still questions remaining regarding its distribution within SLOs. By now, recent research mainly dealt with the analysis of blood or whole SLOs instead of their distinct compartments, with only a few studies focusing on the receptor repertoire of T lymphocytes within the TCZ. However, little is known about the TCR-R in the B cell follicle. Accordingly, we want to shed light on the distribution of the T lymphocytes' receptor repertoire within compartments of SLOs that are organized to generate effective immune responses. Choosing the spleen and its compartments for analysis, we're covering the largest contiguous SLO that is also easily reached by a blood-born antigen. Thus, challenging the present repertoire with inducing a T cell dependent B cell response finally results in the development of GCs that let us turn our attention to Tfh cells as characteristic T lymphocyte subset here. Since interaction of T and B cells requires detailed regulation of their migrational movements to specific locations, questioning the ability of Tfh cells to distribute within splenic compartments will be of note. Regarding the strong interaction between sleep and the immune system, we finally wondered in which way the parameters of the T cell dependent B cell response will be affected by short-term sleep deprivation, in particular the predominant TCR-R in the splenic compartments.
In detail, we want to address the following questions:

1. Does the TCR-R within splenic TCZ and BCZ differ at the naïve state?
2. How does the TCR-R within splenic TCZ and BCZ respond to the injection of a multiepitopic blood-born antigen (i.e. SRBC)?
3. Analyzing the TCR-R of Tfh cells during the GC reaction:
    a. How is the TCR-R of Tfh cells within the GC structured?
    b. Are Tfh cells able to distribute to other locations?
4. Analyzing the impact of sleep on the T cell dependent B cell response:
    a. Does short-term sleep deprivation affect the regulation of key functions of T and B lymphocytes?
    b. Does short-term sleep deprivation affect the predominant TCR-R?

2. Materials and Methods

2.1. Materials

2.1.1. Antibodies

Antibodies used for immunohistochemical and immunofluorescence staining are denoted in Table 1.

Table 1: Utilized antibodies.

Antibody	Manufacturer
Alexa Fluor 488 rat anti-mouse CD4 monoclonal antibody (GK1.5)	BioLegend, USA
Alexa Fluor 594 rat anti-mouse/human Ki67 monoclonal antibody (11F6)	BioLegend, USA
Biotin hamster anti-mouse TCRβ chain monoclonal antibody (H57-597)	BD Biosciences, Germany
Biotin rabbit anti-rat IgG polyclonal antibody	BIOZOL, Germany
ExtrAvidin®-Alkaline Phosphatase	Sigma-Aldrich GmbH, Germany
ExtrAvidin®-Peroxidase	Sigma-Aldrich GmbH, Germany
Normal Mouse Serum	Thermo Fisher Scientific, USA
Rat anti-mouse CD45R (B220) monoclonal antibody (RA3-6B2)	BD Biosciences, Germany
Rat anti-mouse Ki67 monoclonal antibody (16A8)	BioLegend, USA

2.1.2. Primer

Sequences, concentrations and NCBI accession number or ID of used primers for quantitative real-time PCR (qRT-PCR) are denoted in Table 2. Primer for housekeeping genes were purchased from biomers.net GmbH, Germany, while TaqMan assays were received from Thermo Fisher Scientific, USA.

Table 2: Utilized oligonucleotides.

Primer		Sequence	Concentration (mM)	Accession Number or ID
βactin	for rev	5'GATGCTCCCCGGGCTGTATT 5'GGGGTACTTCAGGGTCAGGA	0.25 0.25	NM_007393
b4galt1		TaqMan		Mm00480753_m1
cd40lg		TaqMan		Mm01303060_m1
ciita		TaqMan		Mm00482914_m1

gapdh	for rev	5'GACGGCCGCATCTTCTTGT 5'CACACCGACCTTCACCATTTT	0.25 0.25	NM_008084.3
hprt	for rev	5‘GCTTTCCCTGGTTAAGCAGTAC 5‘CCAACAACAAACTTGTCTGGAATTC	0.25 0.25	NM_013556
icoslg		TaqMan		Mm00497237_m1
mln51	for rev	5'CCAAGCCAGCCTTCATTCTTG 5'TAACGCTTAGCTCGACCACTCTG	0.125 0.125	NM_138660.2
st6gal1		TaqMan		Mm00486119_m1
zap70		TaqMan		Mm00494260_m1

2.1.3. Reagents and Kits

Reagents and kits for the experiments are denoted in Table 3.

Table 3: Utilized reagents and kits.

Name	Manufacturer
Acetic acid 100 %	Carl Roth GmbH & Co. KG, Germany
Acetone 99.8 %	Carl Roth GmbH & Co. KG, Germany
Agarose peqGOLD	VWR International GmbH, Germany
Agilent RNA 6000 Pico Kit	Agilent Technologies Inc., USA
Aquatex	Merck KGaA, Germany
Bovine Serum Albumin (BSA) (IgG-free)	Sigma-Aldrich Inc., USA
Chloroform 99 %	Carl Roth GmbH & Co. KG, Germany
Diethyl pyrocarbonate (DEPC)	Sigma-Aldrich Inc., USA
N,N-Dimethylformamide	Sigma-Aldrich Inc., USA
1,4-Dithiothreitol (DTT) 0.1 M	Sigma-Aldrich Inc., USA
5x DNA Loading Buffer Blue	Bioline Reagents, UK
DNase I	Thermo Fisher Scientific, USA
dNTP Mix 10 mM each	Thermo Fisher Scientific, USA
Ethylenediaminetetraacetic acid (EDTA)	Sigma-Aldrich Inc., USA
Ethanol 99.8 %	Carl Roth GmbH & Co. KG, Germany
Fast Blue RR Salt	Sigma-Aldrich Inc., USA
Fast Red RR Salt	Sigma-Aldrich Inc., USA

Formaldehyde 37 %	Merck KGaA, Germany
Formamide 99 %	Sigma-Aldrich Inc., USA
Glycerol 99.5 %	Sigma-Aldrich Inc., USA
Hoechst Dye (33258)	Thermo Fisher Scientific, USA
Hydrochloric acid 37 %	Sigma-Aldrich Inc., USA
HyperLadder 100 bp	Bioline Reagents, UK
innuPREP RNA Mini Kit 250	Analytik Jena, Germany
Isoflurane Baxter	Baxter Deutschland GmbH, Germany
Isopropanol 99.95 %	Carl Roth GmbH & Co. KG, Germany
Levamisole	Sigma-Aldrich Inc., USA
Liquid DAB + substrate chromogen system	Agilent Technologies, Inc., USA
Liquid nitrogen	University Medical Center Schleswig-Holstein, campus Lübeck, Germany
Methanol 99.9 %	Carl Roth GmbH & Co. KG, Germany
MinElute Gel Extraction Kit (250)	QIAGEN GmbH, Germany
Mineral Oil	Biotech, Ireland
MiSeq Reagent Kit v2 300 cycles	Illumina INC, USA
Mowiol 4-88	Sigma-Aldrich Inc., USA
MTBIvc reagent system (i1-18)	iRepertoire Inc., USA
Multiplex PCR Kit	QIAGEN GmbH, Germany
Naphthol AS-MX phosphate	Sigma-Aldrich Inc., USA
OneStep RT-PCR Kit	QIAGEN GmbH, Germany
Paraformaldehyde (PFA)	AppliChem GmbH, Germany
PerfeCTa NGS Quantification Kit	Quantabio, USA
PhiX Control v3	Illumina INC, USA
QuantiFluor RNA System	Promega Corporation, USA
Qiazol Lysis Reagent	QIAGEN GmbH, Germany
Random Hexamer Primer	Thermo Fisher Scientific, USA
Revert Aid 5x buffer	Thermo Fisher Scientific, USA
Revert Aid H-RT (200 U/UL)	Thermo Fisher Scientific, USA

RNeasy Plus Universal Mini Kit	QIAGEN GmbH, Germany
Roti-GelStain	Carl Roth GmbH & Co. KG, Germany
Sheep red blood cells (SRBC) in Alsever's solution	Labor Dr. Merk, Germany
Sodium azide (NaN_3)	Sigma-Aldrich Inc., USA
Sodium chloride (NaCl)	Carl Roth GmbH & Co. KG, Germany
Sodium hydroxide (NaOH)	Carl Roth GmbH & Co. KG, Germany
SYBR Green PCR Master Mix	Thermo Fisher Scientific, USA
TaqMan Universal PCR Master Mix	Thermo Fisher Scientific, USA
Tissue freezing medium	Leica Instruments GmbH, Germany
Toluidine blue	Merck KGaA, Germany
Tris base	Sigma-Aldrich Inc., USA
Trisodium citrate	Sigma-Aldrich Inc., USA
Triton-X-100	Carl Roth GmbH & Co. KG, Germany
Tween 20	Serva Electrophoresis GmbH, Germany

2.1.4. Solutions and Buffers

Solutions and buffers for the experiments are denoted in Table 4.

Table 4: Utilized solutions and buffers.

Name	Composition
APAAP-substrate	0.5 mM Naphthol AS-MX phosphate, 250 mM N,N-Dimethylformamide, 1 mM Levamisole, Tris Buffer 0.1 M
DEPC-H_2O	0.1 % DEPC in Aqua bidest.
Fast Blue staining solution	3 mM Fast Blue RR Salt, APAAP-substrate
Fast Red staining solution	1.5 mM Fast Red RR Salt, APAAP-substrate
Immunofluorescence blocking solution	5 % BSA, 5 % normal mouse serum, PBS
Library dilution buffer (TrisHCl)	10 mM Tris, 0.1 % Tween 20, laboratory grade H_2O, pH adjusted to 8.5
NaOH (1 M)	1 M NaOH, laboratory grade H_2O
PBS	2.5 mM KCl, 1.5 mM KH_2PO_4, 140 mM NaCl, 6.5 mM Na_2HPO_4, laboratory grade H_2O, pH adjusted to 7.25

PFA 4 %	4 % PFA in PBS
TAE Buffer	40 mM Tris base, 20 mM acetic acid, 1 mM EDTA, laboratory grade H_2O, pH adjusted to 7.6
TBS-Tween	50 mM Tris base, 0.05 % Tween 20, 0.8 % NaCl, laboratory grade H_2O, pH adjusted to 7.6
Toluidine blue solution (0.1 %)	0.1 % Toluidine blue, 1 % Methanol, 15 % Ethanol in DEPC-H_2O
Tris Buffer (0.1 M)	0.1 M Tris base, laboratory grade H_2O, pH adjusted to 8.2

2.1.5. Consumables and operating materials

Consumables for the experiments are denoted in Table 5.

Table 5: Utilized consumables and operating materials.

Name	Manufacturer
CryoPure Tube 1.6 ml	Sarstedt AG & Co., Germany
Gauge needle 16/18 size	B. Braun SE, Germany
Gloves, Touch N Tuff gloves	Ansell, Belgium
Gloves, Micro-Touch	Ansell, Belgium
Gloves, Roti Protect, nitrile	Carl Roth GmbH & Co. KG, Germany
MembraneSlide 1.0 Pen NF	Carl Zeiss Microscopy GmbH, Germany
MicroAmp Optical Adhesive Film	Thermo Fisher Scientific, USA
MicroFine Insuline syringes 1 ml	BD Biosciences, Germany
Microtube 500	Carl Zeiss Microscopy GmbH, Germany
Omnifix 1 ml Syringes	B. Braun SE, Germany
PARAFILM M	Sigma-Aldrich Inc., USA
Pipette tips 10/20/100/200/1000 µl	Nerbe plus, Germany
Reaction tubes 0.2/0.5/1.5/2/5 ml	Sarstedt AG & Co., Germany
Reaction tubes 15/50 ml	Nerbe plus, Germany
Safe Seal Tubes 1.5 ml	Sarstedt AG & Co., Germany
Scalpel blades	Dimeda Instrumente GmbH, Germany
Surgical instruments (stainless steel)	
Superfrost Plus Microscope Slides	Thermo Fisher Scientific, USA

Thermanox coverslips	Thermo Fisher Scientific, USA
96 Well Multiply® PCR Plates	Sarstedt AG & Co., Germany

2.1.6. Instruments

Devices used for the experiments are denoted in Table 6.

Table 6: Utilized instruments.

Name	Manufacturer
ABI PRISM 7900 HT	Applied Biosystems, Germany
AccuBlock Digital Dry Baths	Labnet International INC, USA
Agilent 2100 Bioanalyzer	Agilent Technologies Inc., USA
Agilent Pico Chips	Agilent Technologies Inc., USA
AxioCamHR digital camera	Carl Zeiss Microscopy GmbH, Germany
AxioCamIC	Carl Zeiss Microscopy GmbH, Germany
Axiophot optical microscope	Carl Zeiss Microscopy GmbH, Germany
Axiovert 200M	Carl Zeiss Microscopy GmbH, Germany
Calibration slide universal	Carl Zeiss Microscopy GmbH, Germany
Centrifuge 5417R (Rotor: F-45-30-11)	Eppendorf AG, Germany
EBOX VX 5	VILBER LOURMAT GmbH, Germany
Eppendorf Research plus/reference pipettes	Eppendorf AG, Germany
Fluorescence microscope BZ-X	Keyence GmbH, Germany
FTSS 355-50	CryLaS GmbH, Germany
Galaxy Mini Microcentrifuge	VWR International GmbH, Germany
Heraeus Megafuge 1.0 R (Rotor: 75002704)	Thermo Fisher Scientific, USA
Humidity chamber	Sigma-Aldrich Inc., USA
Hyrax Cryostat C50	Carl Zeiss Microscopy GmbH, Germany
IKA MS3 basic	IKA works INC, USA
Leica Cryostat CM3050 S	Leica Biosystems, Germany
MiniSpin Plus Centrifuge (Rotor: F-45-12-11)	Eppendorf AG, Germany
MiSeq System	Illumina INC, USA
Neubauer improved counting chamber	Glaswarenfabrik Karl Hecht GmbH, Germany

PALM MicroBeam	Carl Zeiss Microscopy GmbH, Germany
PerfectBlue Gel System Mini L	VWR International GmbH, Germany
PowerPac Basic Power Supply	Bio-Rad Laboratories Inc., USA
Power Supply LNG 350-6 Economy Line	Heinzinger electronic GmbH, Germany
Primus 96 Plus Thermal Cycler	Eurofins Genomics GmbH, Germany
Scales, Kern 440-51N	Kern & Sohn GmbH, Germany
Scales, OHAUS® Adventurer™ AR0640	Ohaus GmbH, Germany
StepOne Plus Real-Time PCR System	Thermo Fisher Scientific, USA
Thermo Mixer C	Eppendorf AG, Germany
Titramax 100	VWR International GmbH, Germany
Quantus Fluorometer	Promega Corporation, USA
Vacuum Centrifuge Concentrator 5301 (Rotor: F-45-48-11)	Eppendorf AG, Germany
Vortexer Merck Eurolab	Merck KgaA, Germany

2.1.7. Software

Software for data generation, processing, analysis and visualization is denoted in Table 7.

Table 7: Utilized software.

Name	Developer
ABI 7900 HT detection System 2.4	Applied Biosystems, Germany
Adobe Photoshop CS 8.0.1	Adobe Systems Incorporated, USA
Apache Commons Text 1.4	Apache Software Foundation, USA
AxioVision 4.9.1.2	Carl Zeiss Microscopy GmbH, Germany
Clono Suite	Institute of Anatomy, University of Lübeck, Germany [67]
Eclipse IDE	Eclipse.org Foundation Inc., Canada
FASTX Barcode splitter	Hannon Lab, Howard Hughes Medical Institute, USA
GraphPad Prism 5.0	GraphPad Software, Inc., USA
ImageJ 1.52a	National Institutes of Health, USA
Java 8.0	Oracle Corporation, USA

KIEL	Markus Schilhabel, Institute of Clinical Molecular Biology, Kiel University, Germany
Microsoft Excel 16.0	Microsoft Germany GmbH, Germany
Microsoft Word 16.0	Microsoft Germany GmbH, Germany
Microsoft PowerPoint 16.0	Microsoft Germany GmbH, Germany
MiTCR	Pirogov Russian National Research Medical University, Russia [68]
OLGA 1.2.4	Joseph Henry Laboratories, Princeton University, USA [69]
PALMRobo 4.8	Carl Zeiss Microscopy GmbH, Germany
Pear 0.9.8	The Exelixis Lab, Heidelberg Institute for Theoretical Studies, Germany [70]
Python 3.10.5	Python Software Foundation, USA
R 4.2.2	R Foundation for Statistical Computing, Austria (R Core Team 2022)
R Packages: dplyr, emmeans, ggplot2, readr, readxl, rio, rlist, rstatix, openxlsx, stats, stringr, tidyverse	
R Studio 2022.12.0	R Foundation for Statistical Computing, Austria (R Core Team 2022)
Step One Software 2.3	Thermo Fisher Scientific, USA

2.2. Methods

2.2.1. Animal experiments

2.2.1.1. Mice

8- to 12-week-old female C57BL/6J mice were obtained from Charles River Laboratories or Janvier and kept in the central animal facility of the Universities of Lübeck or Tübingen, respectively. The mice were housed in groups of four to five animals per cage under a 12 h light – 12 h dark cycle (50 lux) and had *ad libitum* access to food and water. Room temperature and humidity were kept constant at approximately 20 °C and 50-60 %, respectively.

All experiments were conducted in accordance with the German Animal Welfare Act and approved by the Animal Research Ethics Board of the respective Ministry of Environment (Kiel, Germany, no. 72-5/15 and 25-3/18; Stuttgart, Germany, no. M11/14).

2.2.1.2. Immunization

SRBC were washed twice in PBS and centrifuged for 10 minutes (min) at 700*g*. Subsequently, cells were counted to obtain a concentration of 10^9 cells per 200 µl PBS and this suspension

was injected into the tail vein of the mice about 1.5 h before the switch to the light cycle. To not disturb the animals' circadian rhythm, the injection procedure was carried out under dim red light. Control mice were injected with 200 µl PBS only.

2.2.1.3. Sleep deprivation

For sleep deprivation experiments half of the SRBC- and PBS-injected C57BL/6J mice were kept awake by gentle handling for the first 6 h of their sleeping phase, i.e. at the beginning of the light cycle. New stuff to investigate like paper towel or chocolate paper was put in the cage every 10 to 15 min to keep the mice awake. When mice adopted a sleeping posture, their nest was disturbed or they were gently touched with a plastic pipette. After 6 h of sleep restriction the mice were allowed to recover for the rest of the light phase. Control animals of both groups were free to sleep during the whole period without any disturbances.

2.2.1.4. Tissue isolation

Mice were sacrificed 3, 4, 7 or 10 days (d) after injection of SRBC or PBS by exposure to an overdose of inhaled isoflurane followed by total blood withdrawal or cervical dislocation. Spleens and mesenteric lymph nodes (mlns) were taken, snap frozen in liquid nitrogen and finally stored at -80 °C until further analysis.

2.2.2. Histological analysis

For immunohistochemical staining and laser microdissection splenic cryosections were prepared using the Leica CM3050 S or the Hyrax C50 cryostat. At a temperature of -20 °C serial sections of 12 µm thickness were mounted on glass or membrane-covered slides, respectively. For immunofluorescence staining, the thickness of the serial sections was reduced to 7 µm. All slides were dried at room temperature for 2 h before further processing.

2.2.2.1. Toluidine blue staining

The membrane-covered slides for laser microdissection were stained with toluidine blue afterwards. For this, the sections were fixed in 75 % ethanol for 2 min before being washed in DEPC treated water. Finally, the slides were incubated in 1 % toluidine blue solution and then washed twice using DEPC treated water and dehydrated by 99,8 % ethanol. After drying the stained slides were stored at -80 °C.

2.2.2.2. Ki67/B220 staining

As a control staining, cryosections on glass slides were stained for proliferating cells and B cells using the markers Ki67 and B220, respectively. First, cryosections were fixed using chloroform and acetone for 10 min each at room temperature. After purging for 10 min in TBS-Tween, fixation for 45 min in 4 % PFA at 4 °C and a subsequent washing step for another 10 min in TBS-Tween, the primary anti-mouse Ki67 antibody was applied overnight. Unbound

antibodies were washed away by TBS-Tween (10 min at room temperature) before the samples were incubated with the secondary biotinylated anti-rat IgG antibody for 30 min. After purging in TBS-Tween for 10 min again, ExtrAvidin Alkaline Phosphatase was added for 30 min, followed by a further washing step. To visualize proliferating cells, we applied Fast Red staining solution for 25 min. After the next washing step, the primary anti-mouse B220 antibody was added for 1 h and remaining substances were washed away afterwards. The secondary biotinylated anti-rat IgG antibody was applied for 30 min then. Following purging in TBS-Tween for 10 min, the samples were incubated with ExtrAvidin Alkaline Phosphatase for 30 min and washed again. To visualize B lymphocytes, we used Fast Blue staining solution for 10 min. After the last washing step, the slides were finally covered using Aquatex and cover slips and stored in the dark at room temperature.

2.2.2.3. TCRβ/B220 staining

As a control staining and to assess the number of T cells in different splenic compartments, cryosections on glass slides were stained for T and B lymphocytes using the markers TCRβ and B220, respectively. First, cryosections were fixed using a methanol-acetone solution (1:1) for 10 min at -20 °C. After purging for 10 min in TBS-Tween, the primary biotinylated anti-mouse TCRβ antibody was applied for 1 h. Unbound antibodies were washed away by TBS-Tween (10 min at room temperature) before the samples were incubated with ExtrAvidin Peroxidase for 30 min. After purging in TBS-Tween for 10 min again, DAB substrate was added for 5 min to visualize T cells. After the next washing step, the primary anti-mouse B220 antibody was added for 1 h and remaining substances were washed away afterwards. The secondary biotinylated anti-rat IgG antibody was applied for 30 min then. Following purging in TBS-Tween for 20 min, the samples were incubated with ExtrAvidin Alkaline Phosphatase for 30 min and washed again. To visualize B lymphocytes, we used Fast Blue staining solution for 25 min. After the last washing step, the slides were finally covered using Aquatex and cover slips and stored in the dark at room temperature.

Examination of the splenic sections stained for TCRβ and B220 was performed using the Axiophot light microscope. The ImageJ software was then used to quantify the number of T lymphocytes present in the different splenic compartments. A calibration slide was used to adjust the right magnification by means of the function “Set scale”. Using the functions “Rectangle” and “Measure”, selections with a known area were transferred in TCZ, BCZ and GC regions. Within these sectors, TCRβ positive cells were separately counted and number of T cells denoted in relation to an area of one mm^2 after averaging over several representative compartments per animal. In addition, these counts were further used for extrapolating the frequency of T lymphocytes present in our sequencing samples. Therefor the T cell counts per mm^2 were put in relation to the total area of TCZs, B cell follicles and GCs isolated via laser

microdissection and then doubled in order to consider the cryosections' thickness of 12 µm, as lymphocytes are said to have an average size of 6 to 8 µm [71].

2.2.2.4. Immunofluorescence staining

To assess the number of proliferating T cells within the different splenic compartments, cryosections were stained in a humid chamber for proliferating cells and $CD4^+$ T lymphocytes using the markers Ki67 and CD4, respectively. First, cryosections were fixed using 4 % PFA in PBS for 10 min at room temperature. After three washes with PBS, 0.5 % Triton-X-100 in PBS was used to permeabilize the tissue. Sections were again washed in PBS and subsequently blocked in blocking solution containing 5 % BSA and 5 % normal mouse serum in PBS for 1 h at room temperature. Both antibodies were applied at a concentration of 1:25 in blocking solution at 8 °C overnight. On the next day sections were washed, counterstained with Hoechst Dye (1:10,000 in PBS) and cover slipped with Moviol.

Examination of the splenic sections stained for Ki67 and CD4 was performed using the Keyence microscope. The ImageJ software was then used to quantify the number of proliferating T lymphocytes present in the different splenic compartments. A calibration slide was used to adjust the right magnification by means of the function "Set scale". Using the functions "Rectangle" and "Measure", selections with a known area were transferred in TCZ, BCZ and GC regions. Within these sectors, cells positive for both Ki67 and CD4 were separately counted and their number denoted in relation to an area of one mm^2 after averaging over several representative compartments per animal. In addition, these counts were further set in relation to the total number of $CD4^+$ T cells within the corresponding area to obtain the relative number of proliferating T lymphocytes for all compartments analyzed.

2.2.3. Laser microdissection

To analyze the different splenic compartments, we used the Zeiss Axiovert 200M PALM Microbeam System to precisely isolate TCZ, BCZ and GC from cryosections stained with toluidine blue. Control stained slides were used to ensure correct identification. Compartments were marked using PALM Robo Software (version 4.8) and then dissected by a pulsed UV laser. Isolated tissues were sampled in tubes whose lids were wetted with inert mineral oil, and lysis buffer was added afterwards. For deep sequencing, separated compartments were dissected and 200 µl Lysis solution RL (Analytik Jena) per tube was added, while compartments were pooled and lysed in 300 µl QIAzol Lysis Reagent (Qiagen) for gene expression analysis. An isolated area of at least one million $µm^2$ per compartment was required to facilitate further processing. Therefor up to three slides per animal covering 15 stained serial sections each were used for dissection and sampled in individual tubes. After incubation for 30 min at room temperature the samples were swirled, spun down and then stored at -20 °C.

2.2.4. Gene expression analysis

2.2.4.1. RNA isolation

For gene expression analysis total RNA was isolated from dissected samples using the RNeasy Plus Universal Mini Kit (Qiagen). One to three single tubes per sample were pooled and filled to 900 µl QIAzol Lysis reagent. After swirling for 1 min, the samples were sheared using a disposable syringe. 100 µl gDNA Eliminator Solution were added, followed by swirling for 15 seconds (sec). After addition of 180 µl chloroform, the samples were swirled for 15 sec, incubated for 3 min and spun for 15 min at 12,000*g* at 4 °C. The upper hydrous phase was then transferred into a new tube and the same volume of 70 % ethanol was added. Half of the solution was applied to a RNeasy Mini spin column, centrifuged for 15 sec at 6,000*g* and the flow through discarded. This step was repeated with the second half of the solution. Afterwards two washing steps were conducted using 700 µl of Buffer RWT and 500 µl of Buffer RPE with subsequent centrifugation for 15 sec at 6,000*g* and flow through refusal each. Finally, another 500 µl of Buffer RPE were added and spun for 2 min at 6,000*g* before the column was transferred to a new tube for drying for 1 min at 12,000*g*. To elute the bound RNA, the column was transferred into a new tube and 40 µl of RNase-free water were applied on the filter and centrifuged for 1 min at 6,000*g*. To increase the RNA yield, the previous step was repeated by re-applying the filtrate on the filter and spinning it down again. The sample volume was then reduced to 11 µl via evaporation in a vacuum centrifuge for around 15 min at 240*g* and 60°C.

2.2.4.2. RNA quantification

To quantify the RNA concentration, 1 µl of the dispensed RNA was diluted 1:100 with 1x TE buffer. 100 µl QuantiFluor RNA dye solution (1 µl dye diluted 1:1000 with 1x TE buffer) was then added and mixed carefully. After incubation for 5 min at room temperature in the dark, the RNA concentration was measured using the Quantus Fluorometer.

In addition, the quality of the extracted RNA was randomly tested using the Agilent RNA 6000 Pico Kit. For this purpose, the samples had to be diluted with RNase-free water to adjust a concentration in the range of 200 to 5,000 pg/µl. All reagents and used chips were kindly provided by the Department for Infectious Diseases and Microbiology (University of Lübeck).

To prepare the gel, 550 µl of RNA gel matrix were pipetted into a spin filter, centrifuged for 10 min at 1,500*g* at room temperature and stored as 65 µl aliquots at 4 °C. Then 1 µl RNA dye concentrate was added to an aliquot of filtered gel, thoroughly mixed and centrifuged for 10 min at 13,000*g* at room temperature. 9 µl of this gel-dye mix were loaded on a RNA Pico Chip that was placed on the chip priming station of the Agilent 2100 Bioanalyzer. After closing the priming station, the plunger of the prepared syringe was pressed down for 30 sec. The clip was released then and after another 5 sec the plunger was slowly pulled back to the 1 ml position. Afterwards 9 µl gel-dye mix were pipetted into two more wells. After adding 9 µl RNA

conditioning solution into the designated well, 5 µl of RNA marker were pipetted in all eleven sample wells and the well marked with the ladder symbol. Here 1 µl of the aliquoted ladder was added as well. Finally, the samples were loaded on the chip (1 µl each) and after mixing for 1 min at 2,400 rpm using the IKA vortexer, the run was started on the prior cleaned Agilent 2100 Bioanalyzer instrument.

2.2.4.3. cDNA synthesis

To transcribe the isolated RNA into complementary DNA (cDNA), a mastermix containing the following reagents per sample was prepared: 4 µl RevertAid 5x buffer, 1 µl dNTP mix (10 mM each), 1 µl random hexamer primer (250 ng/µl), 3.5 µl RNase-free water and 0.5 µl RevertAid Reverse Transcriptase (200 U/µl). 10 µl of this mastermix were then added to the remaining 10 µl of the RNA sample and incubated for 10 min at room temperature. Reverse transcription of messenger RNA (mRNA) into cDNA was in progress for 1 h at 42 °C and stopped by incubation at 70 °C for 10 min. The transcribed cDNA was stored at -20 °C until further progressing.

2.2.4.4. qRT-PCR

For gene expression analysis, qRT-PCR was performed using the StepOnePlus System. First, 5 µl of transcribed cDNA (diluted 1:10 with laboratory grade water) were loaded on a 96 well plate. 15 µl mastermix containing the following reagents were added afterwards: 2 µl primer-(probe)-mix (used concentrations denoted in Table 2), 10 µl SYBR Green PCR Master Mix or TaqMan Universal PCR Master Mix and 3 µl laboratory grade water. Samples were run in technical duplicates under the conditions shown in Table 8. If SYBR Green based reagents were used an additional dissociation step to generate a melting curve was conducted at the end.

Table 8: Used conditions for qRT-PCR.

	Temperature	Time	Number of cycles
Initial denaturation and activation	95 °C	10 min	1
Denaturation Annealing and elongation	95 °C 60 °C	45 sec 1 min	50
Dissociation curve (optional)	95 °C 60-95 °C	15 sec 15 sec per 0.5 °C	1

To analyze the relative expression of several genes, the ΔCT method was used. First, for each sample the cycle of threshold (CT) was determined via the Step One software. This threshold denotes the cycle where the specific fluorescence signal stands out against the background noises. The geometric mean (geomean) of the CT values of four independent housekeeping genes, *βactin*, *gapdh* (i.e. glyceraldehyde 3-phosphate dehydrogenase), *mln51* (i.e. metastatic

lymph node 51) and *hprt* (i.e. hypoxanthine phosphoribosyltransferase), was used as reference. The relative expression of target genes was then denoted as: $2^{\Delta CT} = 2^{((\text{geomean(reference genes)} - \text{CT(target gene)})}$.

2.2.5. Deep sequencing

2.2.5.1. RNA isolation

For deep sequencing, total RNA was isolated from dissected samples using the innuPREP RNA Mini Kit (Analytik Jena). One to three single tubes per sample were pooled and filled to 700 µl Lysis solution RL. For analysis of mlns, five 12 µl thick cryosections were stored in 700 µl Lysis solution RL and processed likewise. After swirling for 1 min, the samples were sheared using a disposable syringe. After addition of 700 µl 70 % ethanol, half of the solution was applied to a Spinfilter R, centrifuged for 1 min at 10,000*g* and the flow through discarded. This step was repeated with the second half of the solution. Afterwards two washing steps were conducted using 500 µl of Washing solution with high salt (HS) and 700 µl of Washing solution with low salt (LS) concentration with subsequent centrifugation for 1 min at 10,000*g* and flow through refusal each. Finally, the column was transferred to a new tube for drying for 2 min at 12,000*g*. To elute the bound nucleic acids, the column was transferred into a new tube and 60 µl of RNase-free water were applied on the filter and centrifuged for 1 min at 6,000*g*. To increase the RNA yield, the previous step was repeated by re-applying the filtrate on the filter and spinning it down again. The sample volume was then reduced to 8 µl via evaporation in a vacuum centrifuge for around 25 min at 240*g* and 60 °C.

2.2.5.2. DNA digestion

To digest genomic DNA, 1 µl 10x DNase reaction buffer and 1 µl DNase I were carefully interspersed with the nucleic acid solution. After incubation for 15 min at room temperature 1 µl Stop solution was added and subsequently incubated for 10 min at 70 °C to terminate the reaction. Finally, 1 µl of the sample was used for quantifying the RNA concentration using the Quantus Fluorometer (see 2.2.4.2).

2.2.5.3. Amplicon rescued multiplex PCR

TCR sequencing libraries were prepared using an amplicon rescued multiplex PCR with two consecutive PCR steps.

Using the Qiagen One-Step-RT-PCR-Kit, reverse transcription and multiplex-nested PCR were performed in the first step, with gene-specific primers targeting the TCRβ V and C segments. A mastermix of 5 µl 5x Buffer, 1 µl dNTPs, 1 µl Enzyme Mix and 2.5 µl MTB-x-Primer containing barcodes was added into precooled tubes. A total amount of 200 ng RNA was applied and filled up with RNase-free water to 15.5 µl to obtain a total solution of 25 µl per sample. For the negative control, only 1.5 µl of MTB-x-Primer were used and instead of the probe, 16.5 µl

RNase-free water were added to the mastermix. Reverse transcription and first PCR were run under the following conditions:

Table 9: Reverse transcription and multiplex-nested PCR.

	Temperature	Time	Number of cycles
Reverse transcription	50 °C	40 min	1
Denaturation	95 °C	15 min	
Denaturation	94 °C	30 sec	15
Annealing	60 °C	2 min	
Elongation	72 °C	30 sec	
Denaturation	94 °C	30 sec	10
Elongation	72 °C	2 min	
Final elongation	72 °C	10 min	1

For the next exponential amplification PCR step, using the Qiagen Multiplex PCR Kit, 1 µl PCR product was added to 2.5 µl communal Illumina primer, 9 µl laboratory grade water and 12.5 µl multiplex PCR mastermix. Amplification was conducted under the following conditions:

Table 10: Amplification PCR.

	Temperature	Time	Number of cycles
Initial denaturation	95 °C	15 min	1
Denaturation	94 °C	30 sec	40
Annealing	55 °C	30 sec	
Elongation	72 °C	30 min	
Final elongation	72 °C	5 min	1

2.2.5.4. Gel electrophoresis

Gel electrophoresis was performed to verify correct amplification during amplicon rescued multiplex PCR. 8 g agarose was dissolved in 400 ml 1x TAE buffer at 95 °C to receive a 2 % gel. 1 µl Roti GelStain per 10 ml gel solution was added after cooling down to 60-65 °C and the solution was poured into a gel-tray. 25 µl of the second PCR product cDNA was mixed with 6 µl 5x DNA Loading Buffer Blue and loaded onto the gel. In addition, 5 µl HyperLadder (100-1,000 bp) was filled into the first lane to estimate product size. Electrophoresis was performed by 110 Volt for 40 min and gel was monitored under minimal exposure of UV light, capturing a photo using the EBOX VX5. Positively amplified samples were expected to show a product band at approximately 280 bp with corresponding negative controls only holding considerably smaller unspecific bands (see example in Figure 4). Correct samples were cut out, weighted, and stored at -20 °C until further processing.

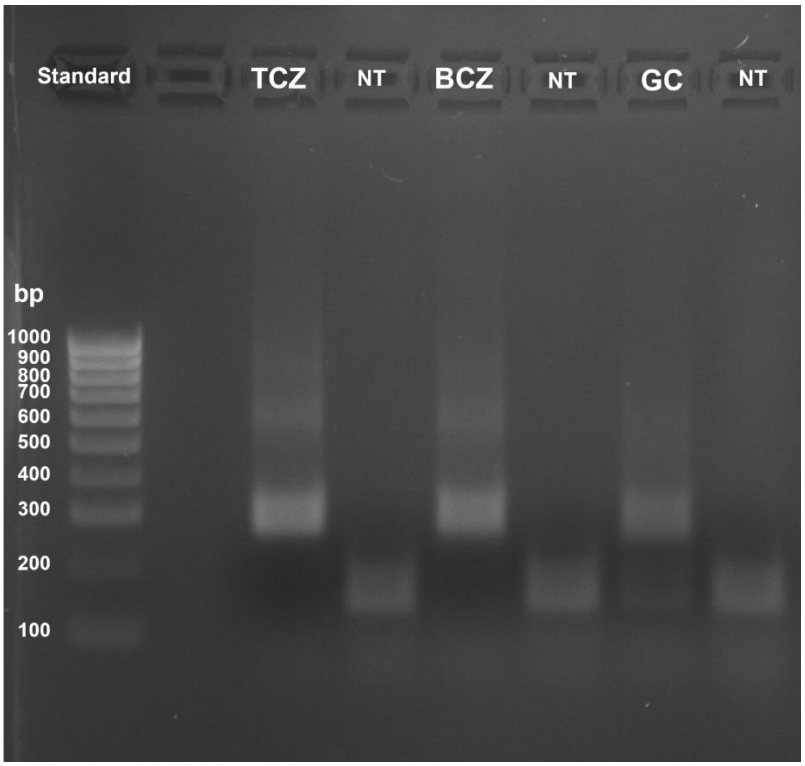

Figure 4: Representative PCR product gel.
2 % agarose gel showing correct amplification of splenic compartment samples, i.e. T cell zone (TCZ), B cell zone (BCZ) and germinal center (GC), with product bands at approximately 280 bp. For corresponding no template (NT) controls, only small unspecific bands were detected. bp – base pairs.

2.2.5.5. DNA gel extraction

DNA gel extraction was performed using the MinElute Gel Extraction kit (Qiagen). The weighted gel slices were dissolved in buffer QG (volume (ml) = weight (mg) x 3) for 10 min at 50 °C in a thermomixer. Isopropanol was added (volume (ml) = weight (mg) x 1) and mixed with the sample. 700 µl of the mixed sample solution was then transferred to a spin column to allow binding of the DNA at 12,000*g* for 1 min. Flow through was discarded and two washing steps were conducted. First, the column was washed using 500 µl buffer QG at 12,000*g* for 1 min and after discard of flow through, the samples were incubated with 750 µl buffer PE for 3 min before spinning at 12,000*g* for 1 min again. The flow through was discarded again and the column was dried at 12,000*g* for 1 min. To elute the bound DNA, the column was transferred into a new collection tube and incubated with 10 µl buffer EB for 1 min before centrifugating at 12,000*g* for 1 min again. Eluted samples were stored at -20 °C until further processing.

2.2.5.6. Sequencing library quantification

Using the PerfeCTa NGS Quantification Kit, the concentration of TCR sequencing libraries was determined by qRT-PCR. Samples were stepwise diluted 1:10,000 with 1x Dilution buffer, and 4 µl of this dilution were then added to a 96 well plate already containing a master mix of 10 µl PerfeCTa SYBR Green SuperMix, 0.6 µl Illumina Primer Mix and 5.4 µl laboratory grade

water. In addition, 4 µl of standards 1-5 and 4 µl laboratory grade water as negative control were added into the lowest row of wells. Probes were run in technical duplicates on the ABI PRISM 7900 under the following conditions:

Table 11: PCR conditions for sequencing library quantification.

	Temperature	Time	Number of cycles
Initial denaturation	95 °C	5 min	1
Denaturation	95 °C	20 sec	35
Annealing	60 °C	30 sec	
Elongation	72 °C	45 sec	
Dissociation curve	95 °C 60-95 °C	15 sec 15 sec per 0.5 °C	1

Amplification results were analyzed using the ABI 7900 detection system, with a standardized baseline setting from three to eight and a threshold set to 0.2. By means of standard amplification curves, the CT values of each sample were converted to the raw concentration, and taking both standard and amplicon fragment length as well as dilution factor into account, the absolute library concentration was calculated as:

$$\text{library concentration (nM)} = \text{raw concentration (pM)} \times 1.52 \times 10{,}000$$

Considering both molecular size and weight of the samples, probes were normalized to a library concentration of 2 nM using library dilution buffer.

2.2.5.7. Next-Generation Sequencing

The TCR sequencing libraries were analyzed using Illumina MiSeq platform and MiSeq Reagent Kit v2 (300 cycles). Deep sequencing was performed by combining six individual samples bearing a unique barcode in one library. For this, 5 µl of each individual 2 nM sample were combined for building the sample pool. 5 µl of this sample pool were denatured by 5 µl 0.2 M NaOH for 5 min at 25 °C and filled up with 990 µl HT1 buffer afterwards. PhiX Control was used as internal sequencing control. To obtain a 10 pM PhiX library, 2 µl of PhiX 10 nM stock solution were diluted with 3 µl library dilution buffer, denatured by 5 µl 0.2 M NaOH for 5 min at 25 °C and diluted with appropriate amounts of HT1 buffer. For sequencing, 510 µl of the 10 pM sample pool and 90 µl of 10 pM PhiX library were loaded into the MiSeq reagent cartridge. The flow cell that was stored in buffer in the fridge was rinsed using laboratory grade water. Sequencing was conducted as 150 bp paired-end sequencing using Illumina PE Read 1/2 Sequencing Primer and FASTQ files were supposed to be generated. Individual sequencing runs were assessed based on PhiX sequencing quality, density of clusters (k/mm^2) and the cluster passed filter (%). Runs displaying a cluster density of 750 k/mm^2 ± 150 k/mm^2 and a cluster past filter rate > 90 % were categorized as successful sequencing runs.

2.2.5.8. Data processing

Two separate FASTQ files, containing information of forward and reverse read, respectively, result from each sequencing run. Using the software ClonoCalc (version 2.1) and the embedded links to FASTX Barcode splitter and programs KIEL and PEAR, data demultiplexing, processing and TCR detection were performed. The received assembled reads were used by MiTCR to extract TCR sequences that were mapped against murine TCR gene locus. Finally, tables containing detailed information about the TCR of the respective sample were given as result, i.e. CDR3 nucleotide sequence, CDR3 amino acid sequence, read count, read frequency, VDJ segment usage and number of nucleotide insertions (see example in Figure 5).

Read.count	Percentage	CDR3.nucleotide.sequence	CDR3.amino.acid.sequence	V.segments	...
76233	0.0469427454052047	GCCAGCAGTACTACTGGGGGGATTCAAAACACCTTGTAC	ASSTTGGIQNTLY	TRBV19	
29051	0.0178890204605171	GCCAGCAGGTACTGGGGGGCCCAAGACACCCAGTAC	ASRYWGAQDTQY	TRBV14	
24025	0.014794110927814	GCCAGCAGTTGGACTGGGGGGATGGACACCCAGTAC	ASSWTGGMDTQY	TRBV14	
22260	0.0137072594902451	GCCAGCTCTCTCGAATCGGGGGGGCAGTGGCACCGGGCAGCTCTAC	ASSLESGGSGTGQLY	TRBV12-2	
20312	0.0125077203398858	GCAAGCAGCTTAGAGGGACAGCTCTCTGAACAGTAC	ASSLEGQLSEQY	TRBV16	

Figure 5: Representative sequencing output table.
Exemplary output table containing detailed information about the T cell receptor (TCR) sequences that are found in the respective sample. Shown are first entries of the five most frequent sequences, specifying copy number (= read count), percentaged frequency, nucleotide and amino acid sequence of complementary determining region 3 (CDR3) as well as used variable (V) gene segment.

2.2.5.9. Data evaluation

Most data analysis was conducted using the open-access statistical software R (version 4.2.2), when not specified otherwise. A list of all R packages for this study can be seen in Table 7.

After excluding non-functional sequences, each data set contained up to two million nucleotide sequences that are coding for a large number of different amino acid sequences. In the following, unique CDR3β amino acid sequences are denoted as clonotype to which V and J segment of the coding nucleotide sequence (= clone) with highest frequency is assigned. In addition, the frequency of each individual clonotype is termed copy number and can be determined by summing up the values of all coding nucleotide sequences. Be aware that clonotypes still can differ in sequences outside the CDR3β region or in their α chain since these analyses are restricted to CDR3β TCR sequences only. Furthermore, the amino acid or nucleotide sequence length is determined as number of amino acids or nucleotides within the noted CDR3β region, respectively.

To assess the homogeneity or diversity of the present TCR sequences, we calculated indices that were developed by Martin Meinhardt during his doctoral thesis on the basis of the commonly used Simpson index [72, 73] and are already published in [74].

The Repertoire Homogeneity Index (RHI) is defined as

$$\mathrm{RHI}_R(X) = \frac{\sum_{\substack{i=1,\ldots,m \\ j<i}} \mathbb{1}(x_i R x_j)}{\binom{m}{2}} \quad ,$$

with x denoting a clonotype in a TCR-R data set X,

Ω the set of all possible TCRβ sequences,

$R \subset \Omega \times \Omega$ a similarity criterion of two sequences and

$\mathbb{1}(\cdot)$ the indicator function.

The RHI thus reflects the probability by which a randomly sampled pair of clonotypes within a data set is similar in respect of the similarity criterion R, with R given a flexible definition of similarity within a variety of sequence parameters. Here, we have chosen the Levenshtein distance (LD) as similarity criterion, implying that two clonotypes are similar if LD of their CDR3β regions is at maximum one, i.e. the number of conversion steps to transfer one sequence into another by displacing one amino acid at a time [75, 76]. The calculation of $\mathrm{RHI}_{\mathrm{LD}}$ was performed in Java with the required software developed using Eclipse IDE for Java Developers and the Apache Commons Text library being applied.

Furthermore, due to the degeneracy of the genetic code, an amino acid sequence can be encoded by a multitude of different nucleotide sequences. To assess this variety in the TCR-R, the Coding Diversity Index (CDI) is defined as

$$\mathrm{CDI}(X) = \frac{1}{m}\sum_{i=1}^{m} D_{\mathrm{NC}}(x_i) \quad .$$

For each clonotype x in a TCR-R data set X that is encoded by several nucleotide sequences $x^{(1)}, \ldots, x^{(m_x)}$, first the Nucleotide Coding Simpson Index (D_{NC}) is defined as

$$D_{\mathrm{NC}}(x) = 1 - \sum_{i=1}^{m_x} \left(\frac{v_X(x^{(i)})}{v_X(x)} \right)^2 \quad ,$$

with $v_X(x)$ denoting the copy number of the clonotype.

As $D_{NC}(x)$ quantifies the coding diversity of the clonotype x, the mean values of these indices result in a measurement of the heterogeneity of the nucleotide coding of the total clonotypes in X, thus given the CDI(X).

In addition, we used OLGA (Optimized Likelihood estimate of immunoGlobulin Amino-acid sequences, version 1.2.4), a free python 2.7 software, to compute the generation probability (P_{gen}) of amino acid and nucleotide CDR3β sequences from a generative model of V(D)J recombination [69]. P_{gen} thus is the sum of occurrence probabilities of all possible recombination events resulting in a given nucleotide sequence, as well as further summing up the probabilities of all single nucleotide sequences leading to an amino acid sequence [69, 77]. As the ClonoCalc software we used for generating the TCR sequence data files cuts of the conserved cysteine and phenylalanine in the V and J region, respectively, we had to modify the V and J gene anchors in the python code for OLGA to be able to compute P_{gen} for our data sets.

Finally, to compare the TCR-R between two samples, we calculated the Jaccard index [78] as

$$J(A,B) = \frac{|A \cap B|}{|A \cup B|} \quad ,$$

with A denoting all TCRβ clonotypes of sample A and B representing all TCRβ clonotypes of sample B. Thus, the ratio of sequences being identical between the two samples is divided by the number of sequences that are exclusively present in only one of the samples. Accordingly, the clonal overlap between two TCR-R ranges from 0 (= no TCR sequences shared) to 1 (= all sequences shared, i.e. an identical repertoire).

Jaccard indices determined between different compartments and animals were further used for multidimensional scaling analysis to visualize the level of similarity within the data set. Thereby, higher clonal overlap between the compartments' TCR sequences results in clustering, while repertoire differences cause separation between the analyzed compartments.

All parameters were applied both on the total data set and on TCR sequences that were grouped in ten categories according to their frequency ($\log_2$ of their copy number), i.e. using the fractioning strategy introduced by Meinhardt *et al*. [74].

2.2.6. Data visualization and statistics

Most data were visualized using GraphPad Prism (version 5.0). Scatterplots and Clustering analysis were illustrated using the open-access statistical software R (version 4.2.2). In addition, R software was also used for statistical analysis of all data sets. A list of all R packages used in this study is shown in Table 7.

qRT-PCR data were denoted by median and interquartile ranges and ANOVA including Holm's method as post-hoc test was performed for evaluating differences between analyzed groups. Deep sequencing data were presented as arithmetic mean ± standard deviation and analyzed using Mann-Whitney-U for unpaired or its analog, Wilcoxon signed-rank test, for paired samples. Statistical significance is denoted as * $p < 0.05$, ** $p < 0.01$ and *** $p < 0.001$.

3. Results

3.1 The TCR-R of splenic TCZ and BCZ in naïve mice

We first focused our analyses on the TCR-R of naïve mice where we compared the repertoire found in splenic TCZ and BCZ. Since T cells are also present in B cell follicles (Figure 6A), we used the determined numbers of on average 16,000 and 1,100 T cells per mm^2 TCZ or BCZ, respectively (Figure 6B), to estimate the total number of T cells found in our samples isolated out of splenic cryosections (Figure 6C). Using deep sequencing to characterize the TCR-R, e.g. to determine the number of unique TCRs present in the different compartments, we focused on the CDR3 region of the TCRβ chain as this variable domain spans the joining region of the V, D and J segments and the subsequent nucleotide additions, and thus is the site of antigen recognition that determines the TCR specificity. A set of T cells bearing identical CDR3β chains on the amino acid level is thus referred to as a clonotype. Accordingly, we detected on average 54,000 different T cell clonotypes in the TCZ but only about 16,000 different T cell clonotypes in the BCZ (Figure 6D). With other words, while 15 times more T cells were found in the TCZ compared to the BCZ, this ratio was extenuated to a 3-fold difference in clonotype number.

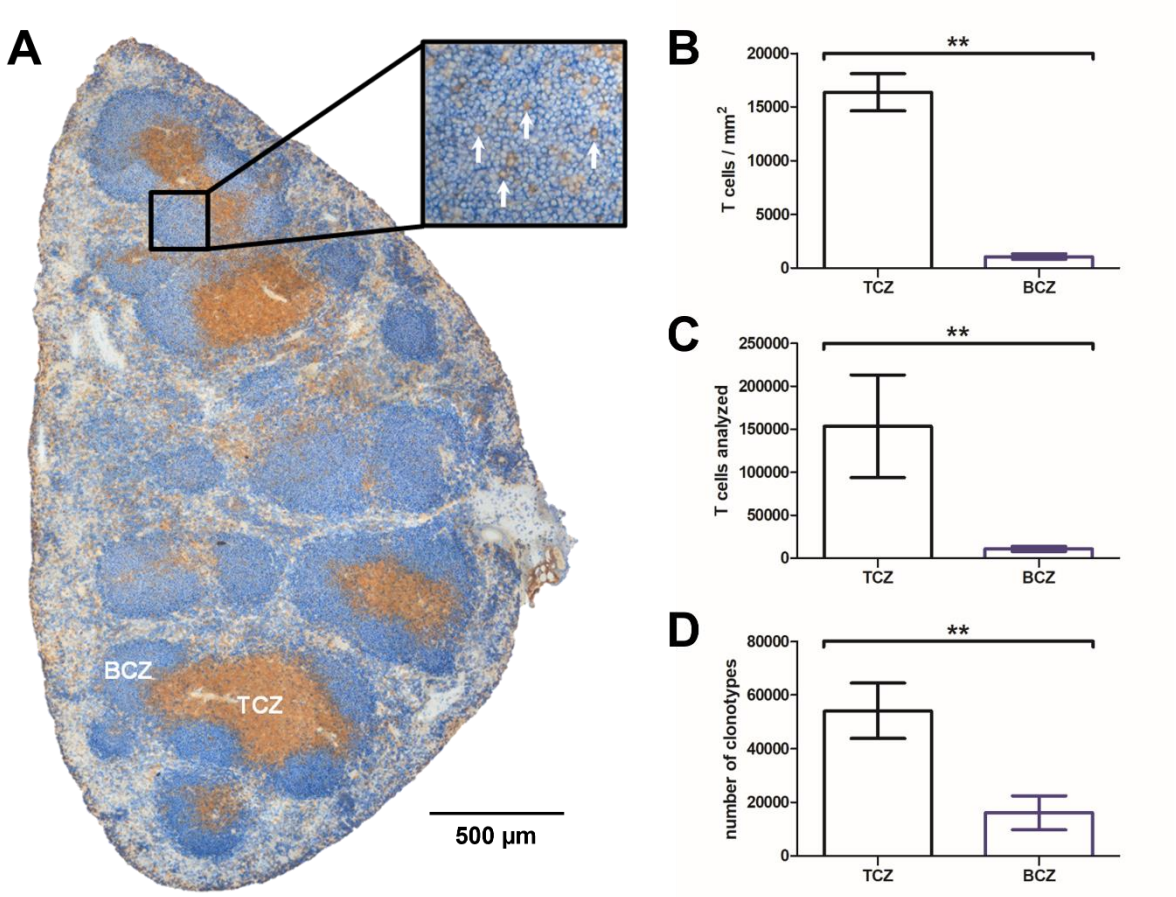

Figure 6: Analyzing the TCR-R of splenic TCZ and BCZ in naïve mice.
(A) Representative cryosection of a naïve spleen stained for B cells (blue, B220) and T cells (brown, TCRβ) to indicate clear structured splenic compartments, i.e. T cell zone (TCZ) and B cell zone (BCZ). Magnification highlights incidence of T cells in B cell follicle and **(B)** cryosections were quantified with ImageJ to assess those numbers. Splenic compartments were isolated to perform deep sequencing of the complementary determining region 3 (CDR3) β chain, **(C)** number of analyzed T cells was extrapolated and **(D)** number of detected T cell clonotypes was determined to analyze the T cell receptor repertoire (TCR-R). Displayed are means and standard deviations for PBS-injected mice (n = 8) and data were analyzed using Mann-Whitney-U, with ** $p < 0.01$ indicating significant differences between TCZ and BCZ.

3.1.1 With respect to the TCZ, the TCR-R of BCZs features more "public" characteristics

We further analyzed these T cells by determining various parameters of the underlying TCR-R. Calculating both length and generation probability of the CDR3β amino acid sequences provides details about their origination. According to this, TCR sequences with fewer nucleotide additions and a consequently shorter CDR3β amino acid sequence length are predicted to be closer to the germline and therefore more likely to be generated. Within the B cell follicle, we found a higher generation probability (P_{gen}) (Figure 7A) as well as a reduced sequence length of T cell clonotypes (Figure 7B) compared to their counterparts in the TCZ. To obtain information about the relationship between these clonotypes, we determined the probability by which two TCR sequences are similar, i.e. differing in at most one amino acid,

by using the repertoire homogeneity index on the basis of Levenshtein distance (RHI_{LD}). An increase in value consequently reflects a homogenization of the underlying TCR-R as found in the BCZ, indicating a higher sequence similarity and thus appearance of sequence families here (Figure 7C). In addition, we computed the coding diversity index (CDI). This index describes the heterogeneity of nucleotide coding of the CDR3β amino acid sequences, with usage of different nucleotides leading to high values, while homogenization is represented by data that show a tendency towards 0. Contrary to our expectations, TCR amino acid sequences present in the B cell follicles were coded by only a few dominant nucleotide sequences, resulting in a reduced CDI value (Figure 7D). Finally, we also found V and J segments differentially used by T cell clonotypes of TCZ and BCZ (Figure 7E+F). Taken together, most of these parameters indicate that the TCR-R in the B cell follicle is mainly built by clonotypes holding “public” characteristics.

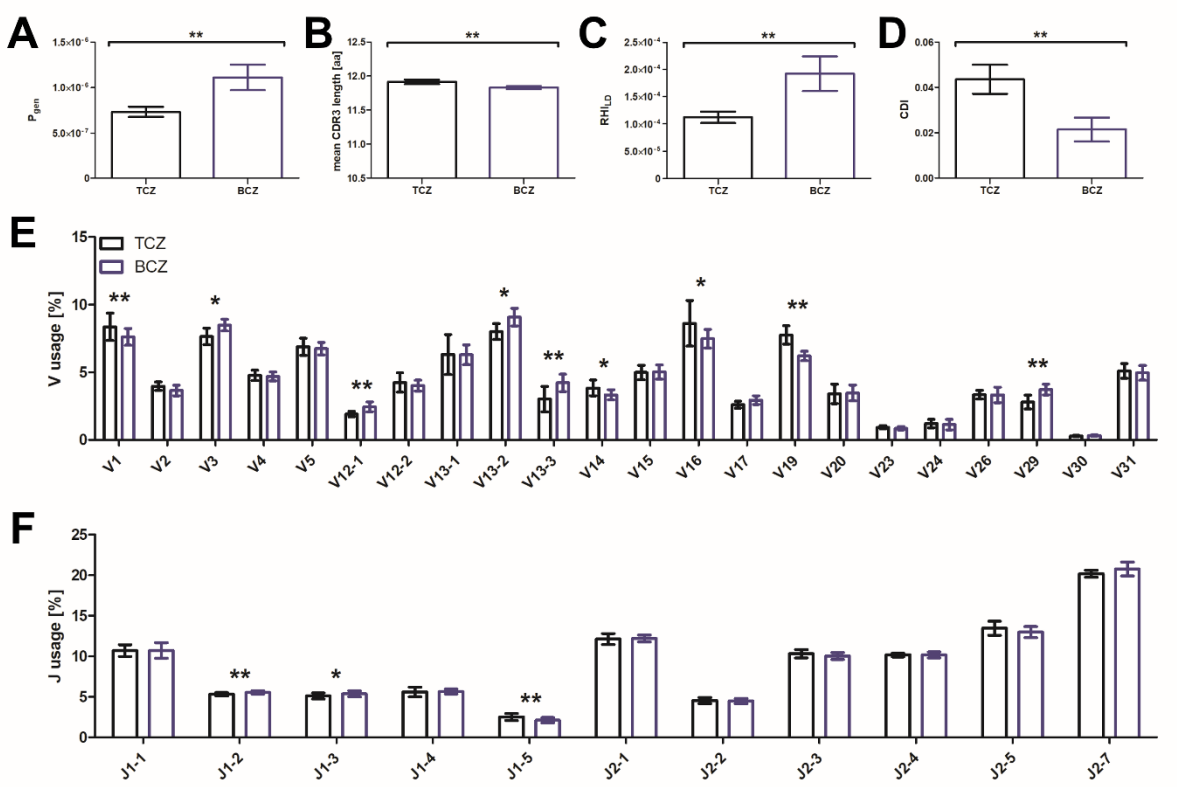

Figure 7: The TCR-R differs between splenic TCZ and BCZ of naïve mice.
Deep sequencing of the complementary determining region 3 (CDR3) β chain of splenic compartments was performed, i.e. T cell zone (TCZ) and B cell zone (BCZ). **(A)** Generation probability, **(B)** mean length and **(C)** homogeneity of CDR3β amino acid sequence, **(D)** heterogeneity of nucleotide coding as well as distribution of used **(E)** V and **(F)** J segments were determined to analyze the T cell receptor repertoire (TCR-R) in naïve mice after injection of PBS (n = 8). Displayed are means and standard deviations and data were analyzed using Mann-Whitney-U, with * $p < 0.05$ and ** $p < 0.01$ indicating significant differences between TCZ and BCZ. aa – amino acids; CDI – coding diversity index; P_{gen} – generation probability; RHI_{LD} – repertoire homogeneity index based on Levenshtein distance.

3.1.2 Fractioning the T cell clonotypes according to their copy number reveals that also "private" features can be detected in high copy clonotypes of BCZs

To investigate even small changes in the underlying repertoire, we grouped the detected T cell clonotypes into ten fractions according to their frequency (log_2 of their copy number) and analyzed these categories separately.

For the TCZ we found the expected distribution pattern of many clonotypes with only few copies and just a few clonotypes that occur in large copy numbers. A similar pattern was found in the B cell follicle, but with fewer clonotypes being detected in general (Figure 8A). Nevertheless, no significant difference between TCZ and BCZ could be detected for T cell clonotypes with highest frequency (last three fractions). Interestingly, the effects found for the total repertoire were particularly reflected in fractions of low copy numbers. T cell clonotypes showed a higher generation probability, a reduced sequence length and more homogenous sequences in the BCZ than in TCZ here. However, oppositional effects were found for high copy clonotypes, where the TCR sequences present in the B cell follicle had a reduced probability of being generated, were longer and more heterogenous than in the TCZ. The repertoire found in the medium fractions exhibited a crossover between these two effects (Figure 8B-D). In addition, nucleotide coding was reduced for all fractions in the BCZ, even though the values likewise increased with copy number for both compartments (Figure 8E).

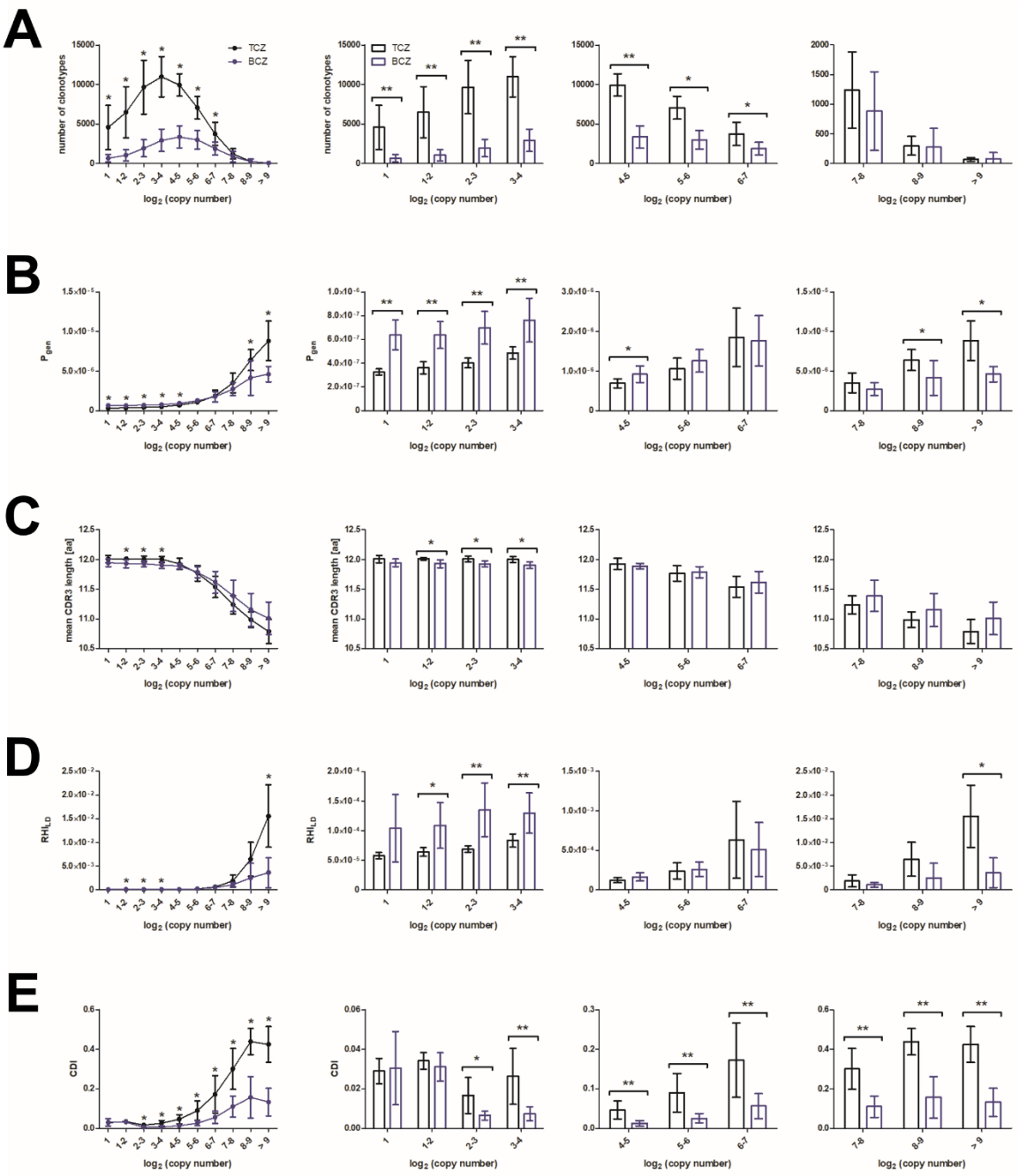

Figure 8: Low copy T cell clonotypes reflect differences found in the total repertoire, while also "private" features can be detected in high copy clonotypes within BCZs.

Deep sequencing of the complementary determining region 3 (CDR3) β chain of splenic compartments was performed, i.e. T cell zone (TCZ) and B cell zone (BCZ). **(A)** Number of detected T cell clonotypes, **(B)** generation probability, **(C)** mean length and **(D)** homogeneity of CDR3β amino acid sequence as well as **(E)** heterogeneity of nucleotide coding were determined to analyze the T cell receptor repertoire (TCR-R) in naïve mice after injection of PBS (n = 8). Clonotypes are grouped in fractions according to their frequency (log_2 of their copy number). All fractions shown in the left panel are presented separately in the right panel to show more details. Displayed are means and standard deviations. Within each fraction data were analyzed using Mann-Whitney-U, with * $p < 0.05$ and ** $p < 0.01$ indicating significant differences between TCZ and BCZ. aa – amino acids; CDI – coding diversity index; P_{gen} – generation probability; RHI_{LD} – repertoire homogeneity index based on Levenshtein distance.

Furthermore, differences in V segment usage were also nearly exclusively present for T cell clonotypes with low or medium copy numbers (Figure 9A+B), but not for high frequent ones (Figure 9C).

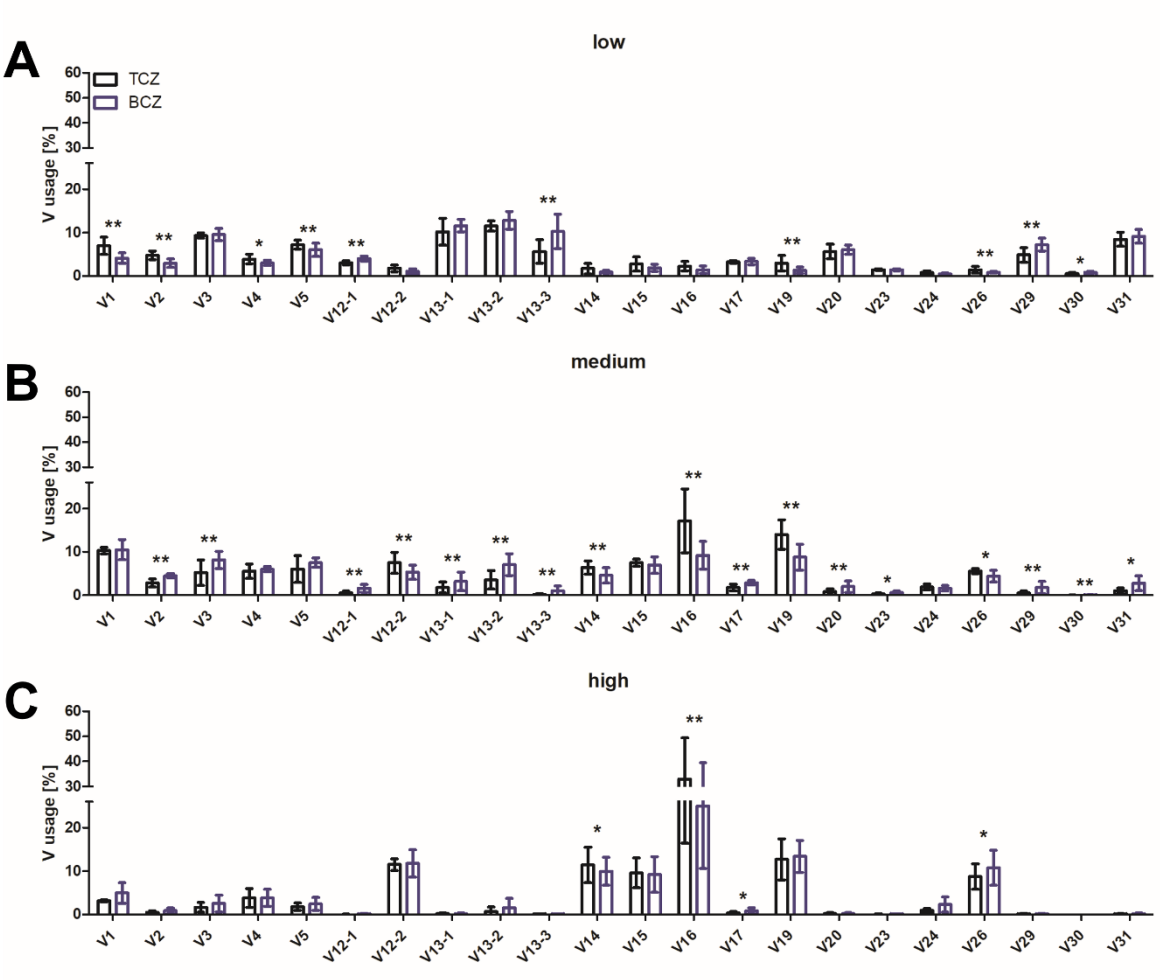

Figure 9: High copy T cell clonotypes do not differ in V segment usage for TCZ and BCZ.
Deep sequencing of the complementary determining region 3 (CDR3) β chain of splenic compartments was performed, i.e. T cell zone (TCZ) and B cell zone (BCZ). Distribution of used V segments was determined to analyze the T cell receptor repertoire (TCR-R) in naïve mice after injection of PBS (n = 8). Clonotypes are grouped in fractions according to their frequency (log_2 of their copy number). Fractions of **(A)** lowest (equivalent to fractions 1-4 in Figure 8, **(B)** medium (equivalent to fractions 5-7 in Figure 8) and **(C)** highest copy number (equivalent to fractions 8-10 in Figure 8) are separately shown. Displayed are means and standard deviations. Within each panel data were analyzed using Mann-Whitney-U, with * $p < 0.05$ and ** $p < 0.01$ indicating significant differences between TCZ and BCZ.

3.1.3 Compartments within the same spleen show a higher clonal overlap

We extended our analyses of the receptor repertoire to T cells of distinct compartments, because we were interested to know to what extent the TCR-R diversity differs between compartments of different mice compared to compartments of the same spleen. Therefore, we estimated the Jaccard index as a measure of similarity both between compartments of different animals (“between”) and within distant zones of the same slice (“within”), with the calculated value representing the percentage of clonal overlap (1 = all TCR sequences shared; 0 = no TCR sequences shared).

In the TCZ, high copy T cell clonotypes showed a higher Jaccard index both within and between compartments, but almost no significant difference in the clonal overlap of the predominant TCR-R could be detected between TCZs from the same mouse and those of different animals (Figure 10A). In contrast to that we found a higher amount of diversity between BCZs of different mice than within the same spleen. While the clonal overlap remained at low levels throughout all fractions for different animals, it was increased within the fractions of numerically dominant clonotypes for “within” comparisons (Figure 10B).

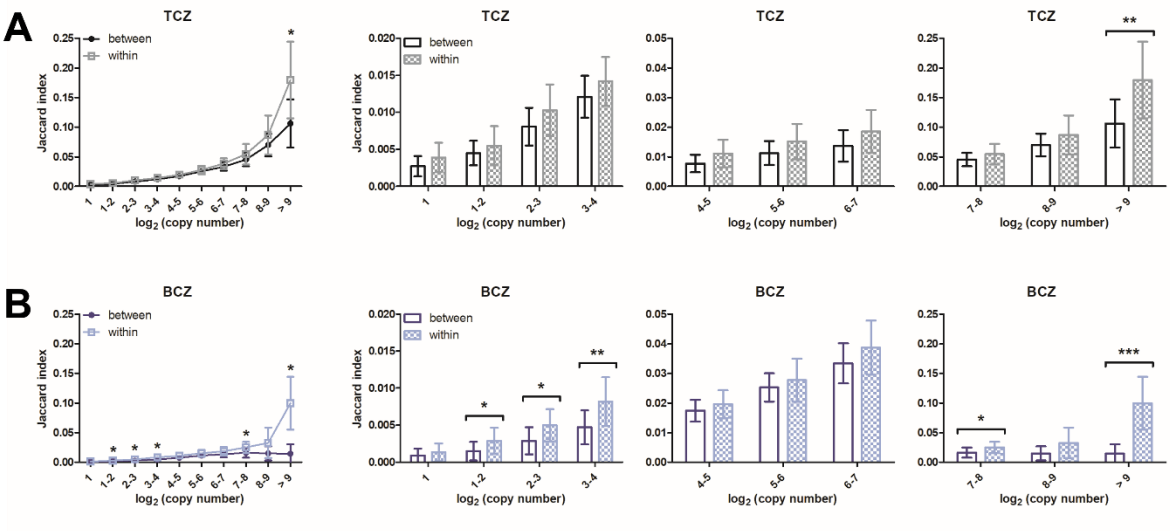

Figure 10: Clonal overlap is higher between compartments within the same spleen.
Deep sequencing of the complementary determining region 3 (CDR3) β chain of splenic compartments was performed, i.e. T cell zone (TCZ) and B cell zone (BCZ), with two independent compartments each being isolated to analyze the T cell receptor repertoire (TCR-R) in naïve mice after injection of PBS (n = 8). Jaccard index indicating clonal overlap (1 = 100 %; 0 = 0 %) was determined for T cell clonotypes in **(A)** TCZ and **(B)** BCZ, both between different animals (“between”) and within distant zones of the same mouse (“within”). Clonotypes are grouped in fractions according to their frequency (log_2 of their copy number). All fractions shown in the left panel are presented separately in the right panel to show more details. Means and standard deviations are displayed and within each fraction data were analyzed using Mann-Whitney-U, with * $p < 0.05$, ** $p < 0.01$ and *** $p < 0.001$ indicating significant differences for indices measured between or within animals.

3.2 The effect of immunization on the TCR-R in splenic TCZ and BCZ after SRBC-injection

Immunization is known to have a strong impact on the composition of lymphocytes that are recruited into a T cell dependent B cell response, raising the question how this might variably affect the TCR-R of splenic compartments. To investigate if an antigen challenge influences both distribution and diversity of the TCR-R in the different splenic compartments, we compared the TCR specificities of naïve and immunized mice 3, 4, 7 and 10 d after injection of SRBC, using the aforementioned parameters.

3.2.1 Overall immunization effects on the TCR-R can be detected at late timepoints

For the TCZ, the total number of different T cell clonotypes notably decreased 7 d after SRBC-injection (Figure 11A, left panel). Furthermore, immunization induced a noticeable shift in the distribution of clonotypes towards fewer low copy clonotypes that already started earlier in both compartments (Figure 11A+B, right panel), although we did not detect any significant differences in the total number for the B cell follicle (Figure 11B, left panel). In addition, multidimensional scaling revealed that TCR sequences in TCZs and B cell follicles form two independent clusters, even if BCZs were scattered to a greater extent in general (Figure 11C). Especially for the TCZ one could see that 7 d after immunization these compartments diverged from their cluster, showing a growth in variance between the different animals that already slightly started after 3 d.

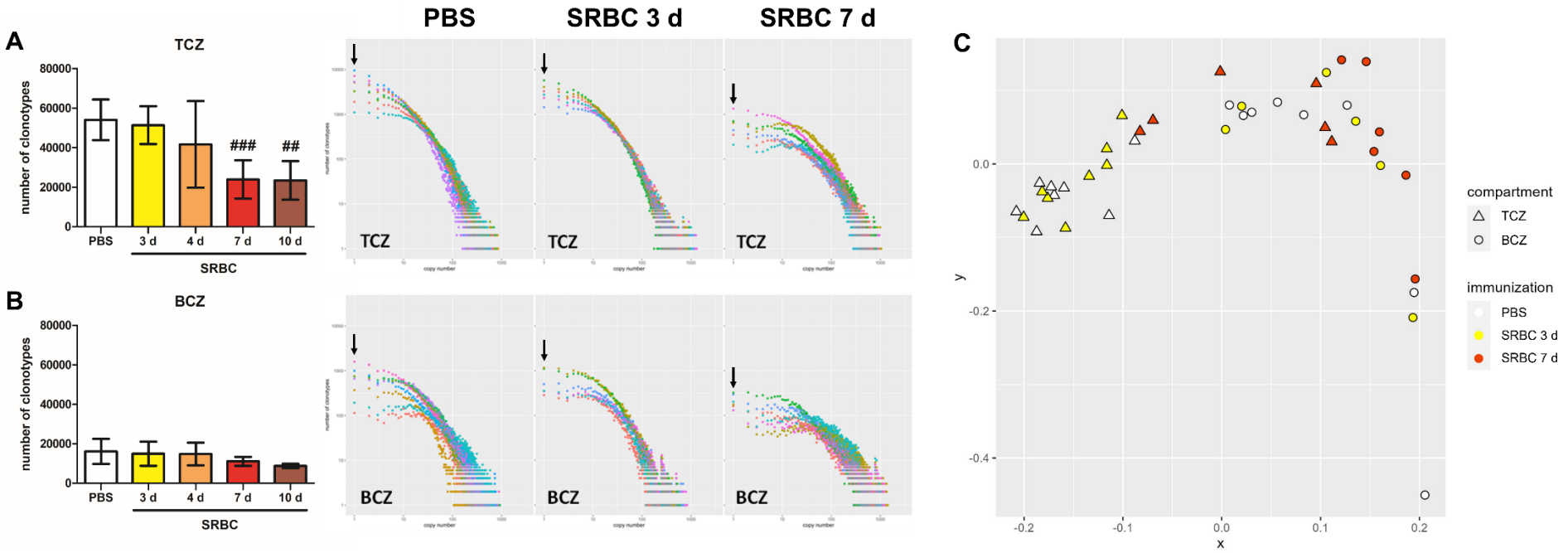

Figure 11: Immunization reduces total number of different T cell clonotypes at late timepoints.
Deep sequencing of the complementary determining region 3 (CDR3) β chain of splenic compartments was performed, i.e. T cell zone (TCZ) and B cell zone (BCZ). Number of detected T cell clonotypes within **(A)** TCZ and **(B)** BCZ (left panel) and distribution of these clonotypes relative to their copy number (right panel) were determined to analyze the T cell receptor repertoire (TCR-R) in naïve mice (n = 8) or 3 (n = 8), 4 (n = 8), 7 (n = 6) and 10 (n = 4) days (d) after SRBC-injection. Displayed are means and standard deviations, while in scatterplots each dot represents a single clonotype, colors show affiliation to different animals and arrows highlight decrease in low copy clonotypes. Data were analyzed using Mann-Whitney-U, with ## $p < 0.01$ and ### $p < 0.001$ indicating significant differences between PBS and SRBC. For **(C)**, Jaccard indices were determined between different compartments and animals and used for clustering analysis by multidimensional scaling. Here, each dot or triangle represents a single BCZ or TCZ, respectively, and colors show affiliation to different timepoints of immunization.

3.2.2 Fractioning the T cell clonotypes according to their copy number reveals early immunization effects in high copy clonotypes present in the TCZ

To analyze these shifts in the predominant TCR-R in more detail, we used our fractioning strategy to separately look at the different categories.

Although we could not detect any differences in the total TCR-R in the TCZ at early stages, immunization already resulted in more different clonotypes occurring in highest copy number 3 d after SRBC-injection here (Figure 12A, left panel). In addition, both generation probability (Figure 12B, left panel), homogeneity (Figure 12D, left panel) and nucleotide coding (Figure 12E, left panel) of CDR3β amino acid sequences were reduced, as well as mean sequence length increased for high copy clonotypes (Figure 12C, left panel). The T cell clonotypes showed a similar distribution for all fractions in the B cell follicle, though on a lower level (take notice of the different scaling), but almost no significant differences between naïve and immunized animals could be detected (Figure 12A-E, right panel). Thus, all parameters are pointing towards a beginning “private” immune response 3 d after SRBC-injection starting in the TCZ.

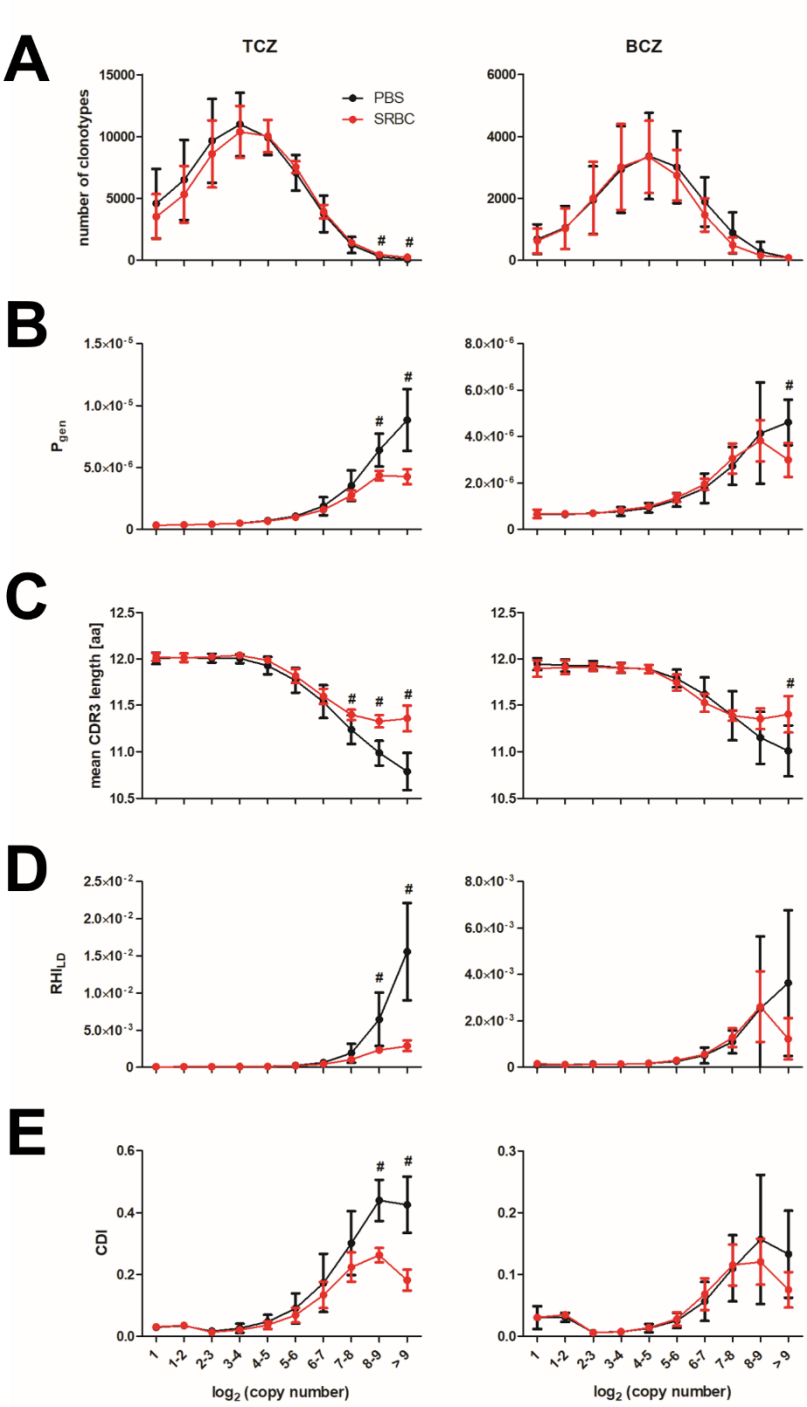

Figure 12: Immunizations alters the TCR-R of high copy clonotypes in the TCZ 3 d after SRBC-injection.

Deep sequencing of the complementary determining region 3 (CDR3) β chain of splenic compartments was performed, i.e. T cell zone (TCZ) and B cell zone (BCZ). **(A)** Number of detected T cell clonotypes, **(B)** generation probability, **(C)** mean length and **(D)** homogeneity of CDR3β amino acid sequence as well as **(E)** heterogeneity of nucleotide codings were determined to analyze the T cell receptor repertoire (TCR-R) in naïve mice or 3 days (d) after SRBC-injection (n = 8 each). Clonotypes are grouped in fractions according to their frequency (log_2 of their copy number). Displayed are means and standard deviations. Immunization effects within each fraction were analyzed using Mann-Whitney-U and displayed as #. aa – amino acids; CDI – coding diversity index; P_{gen} – generation probability; RHI_{LD} – repertoire homogeneity index based on Levenshtein distance.

3.2.3 Immunization induces a shift in the TCR-R of TCZ and BCZ 7 d after SRBC-injection

7 d after immunization the effects that are characteristic for a “private” immune response, known to be induced by injection of a high dosage of SRBC, were even more pronounced. In the TCZ immunization induced a noticeable shift towards high copy clonotypes, while the overall number of different T cell clonotypes was reduced (Figure 13A, left panel). Like in naïve mice, generation probability increased with growing copy number but was still significantly lower after SRBC-injection here (Figure 13B, left panel). In addition, we detected a drop in CDR3β amino acid sequence length for numerically dominant clonotypes, but they nevertheless remained slightly longer than at the naïve state in the top fractions after immunization (Figure 13C, left panel). Repertoire homogenization measured by RHI_{LD} followed the same pattern with overall more homogenous high copy TCR sequences, but a reduced level compared to PBS after SRBC-injection (Figure 13D, left panel). Finally, immunization induced homogenization of nucleotide coding for CDR3β amino acid sequences of reacting T cell clonotypes, even if a higher degree of heterogeneity was also detected for clonotypes that occur in high copy numbers (Figure 13E, left panel). However, when separately looking at the T cell clonotypes that only appear in low copy numbers, oppositional effects were detected. After immunization, TCR sequences had a higher generation probability and a shorter mean length than at the naïve state here (Figure 13B+C, left panel). In addition, higher values for RHI_{LD} were also found after SRBC-injection in low fractions (Figure 13D, left panel). All effects detected for T cell clonotypes in the TCZ were also present in the B cell follicle, but on a lower level (take notice of the different scaling) (Figure 13A-E, right panel). Consequently, high frequent T cell clonotypes are featuring “private” characteristics, while low copy TCR sequences are more prone to “public” properties, resulting in the same patterns for both TCZ and B cell follicle.

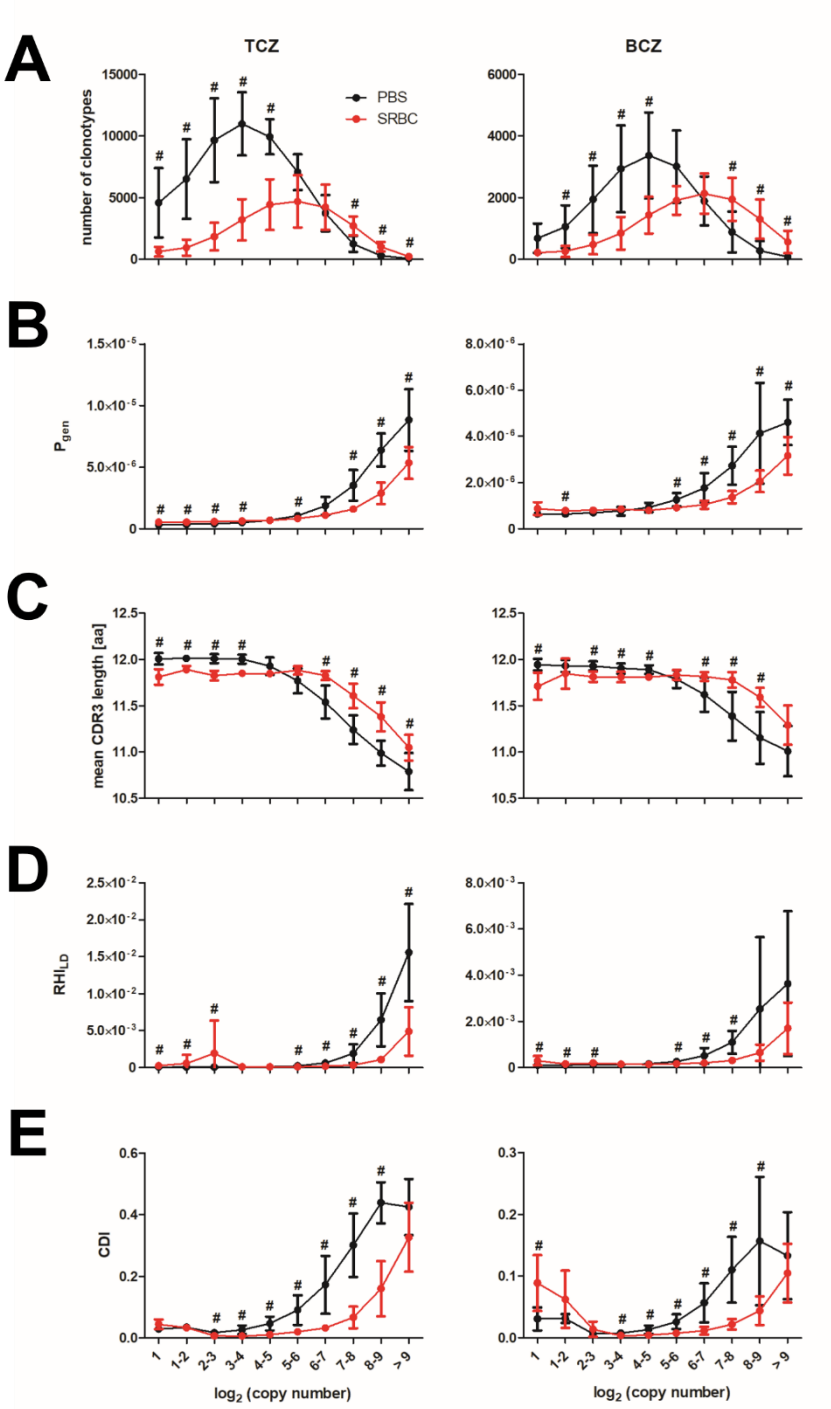

Figure 13: Immunizations induces a shift in the TCR-R of TCZ and BCZ 7 d after SRBC-injection.

Deep sequencing of the complementary determining region 3 (CDR3) β chain of splenic compartments was performed, i.e. T cell zone (TCZ) and B cell zone (BCZ). **(A)** Number of detected T cell clonotypes, **(B)** generation probability, **(C)** mean length and **(D)** homogeneity of CDR3β amino acid sequence as well as **(E)** heterogeneity of nucleotide codings were determined to analyze the T cell receptor repertoire (TCR-R) in naïve mice (n = 8) or 7 days (d) after SRBC-injection (n = 6). Clonotypes are grouped in fractions according to their frequency (log_2 of their copy number). Displayed are means and standard deviations. Immunization effects within each fraction were analyzed using Mann-Whitney-U and displayed as #. aa – amino acids; CDI – coding diversity index; P_{gen} – generation probability; RHI_{LD} – repertoire homogeneity index based on Levenshtein distance.

3.3 The TCR-R during the GC reaction

During an ongoing T cell dependent B cell response, proliferation of T and B cells causes the formation of GCs within B cell follicles (Figure 14A). For the generation of high-affinity antibodies, B lymphocytes need the help of a specialized subset of T cells found in GCs, namely Tfh cells. Thus, we determined those numbers and the underlying TCR-R and compared it to the other splenic compartments. About 3,600 T cells were counted per mm^2 in the GC, and thus approximately twice as much as found in the B cell follicle after immunization (Figure 14B). In addition, we used the determined numbers to estimate the total number of T cells found in our samples isolated out of splenic cryosections. No difference between BCZ and GC could be detected here, whereas much more T cells were present in the samples isolated from single TCZs (Figure 14C). Using deep sequencing we characterized the underlying TCR-R and determined the number of T cell clonotypes present in the different compartments 7 d after immunization. We detected about 11,000 different T cell clonotypes for on average 19,000 T cells present in the BCZ sample, while we found only 2,000 different T cell clonotypes for on average 12,500 T cells sampled from GCs surrounding a single TCZ (Figure 14D).

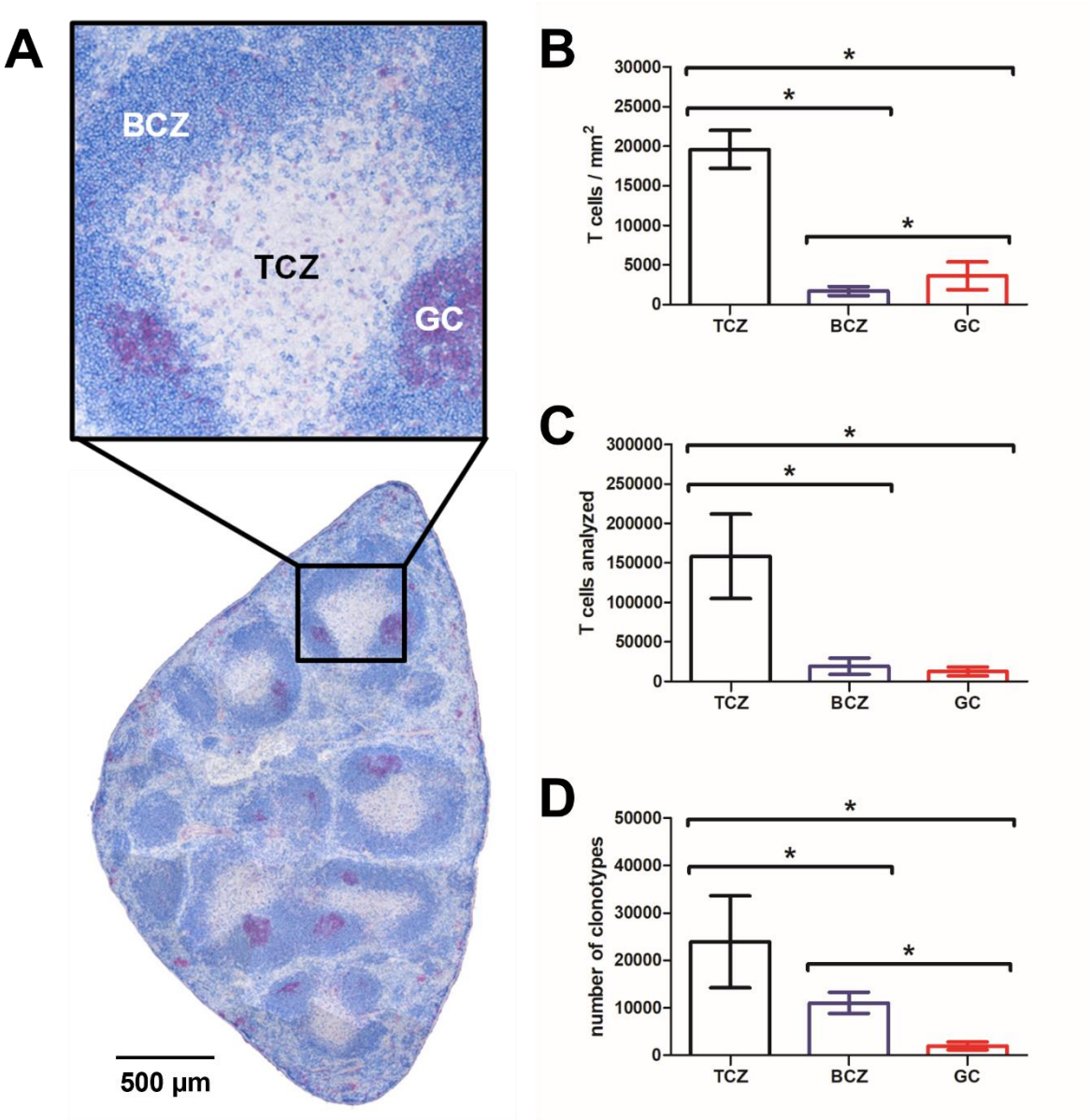

Figure 14: A multitude of Tfh cells is located in GCs surrounding a single TCZ.
(A) Representative cryosection of an immunized spleen stained for B cells (blue, B220) and proliferating cells (red, Ki67). Magnification highlights clear structured splenic compartments, i.e. T cell zone (TCZ), B cell zone (BCZ) and germinal center (GC). **(B)** Cryosections stained for B cells and T cells were quantified with ImageJ to assess number of T cells. Splenic compartments were isolated to perform deep sequencing of the complementary determining region 3 (CDR3) β chain, **(C)** number of analyzed T cells was extrapolated and **(D)** resulting number of detected T cell clonotypes determined to analyze the T cell receptor repertoire (TCR-R). Displayed are means and standard deviations 7 days (d) after SRBC-injection (n = 6) and data were analyzed using Mann-Whitney-U, with * $p < 0.05$ indicating significant differences between compartments. Tfh – T follicular helper cell.

3.3.1 The TCR-R of Tfh cells shows mainly "private" characteristics

Using the afore introduced parameters we further analyzed the TCR-R of these Tfh cells in the GC compared to the other splenic compartments. In total, Tfh cell clonotypes were significantly fewer, had both an equal generation probability and CDR3β amino acid sequence length, as well as a higher homogeneity and the same nucleotide coding level compared to the repertoire of surrounding B cell follicles (Figure 15A-E, left panel). Fractioning the TCR-R reveals that GC clonotypes were indeed on an overall lower level than T cell clonotypes of the other

compartments but showed a noticeable shift towards high copy clonotypes (Figure 15A, right panel). Generation probability also only slightly increased with growing copy number but was still significantly lower compared to TCZ and BCZ here (Figure 15B, right panel). However, the drop in CDR3β amino acid sequence length for numerically dominant clonotypes that was striking for T cell clonotypes of TCZ and B cell follicles was diminished for the GC. Here, TCR sequences showed an almost constant length cross all fractions (Figure 15C, right panel). Finally, both repertoire homogenization and heterogeneity of nucleotide coding were significantly reduced in the TCR-R repertoire of GCs (Figure 15D+E, right panel). Interestingly, when separately looking at the T cell clonotypes that only appear in lower copy numbers, oppositional effects were detected for RHI_{LD} and CDI. TCR sequences in the GC had higher values of homogenization and were more diversely nucleotide coded than their counterparts present in the other compartments here (Figure 15B, D+E, right panel).

Nevertheless, despite the variances in fractions of lowest copy number, highlighting the effects of a “private” immune response is even more pronounced in GC high frequent T cell clonotypes than for B cell follicles.

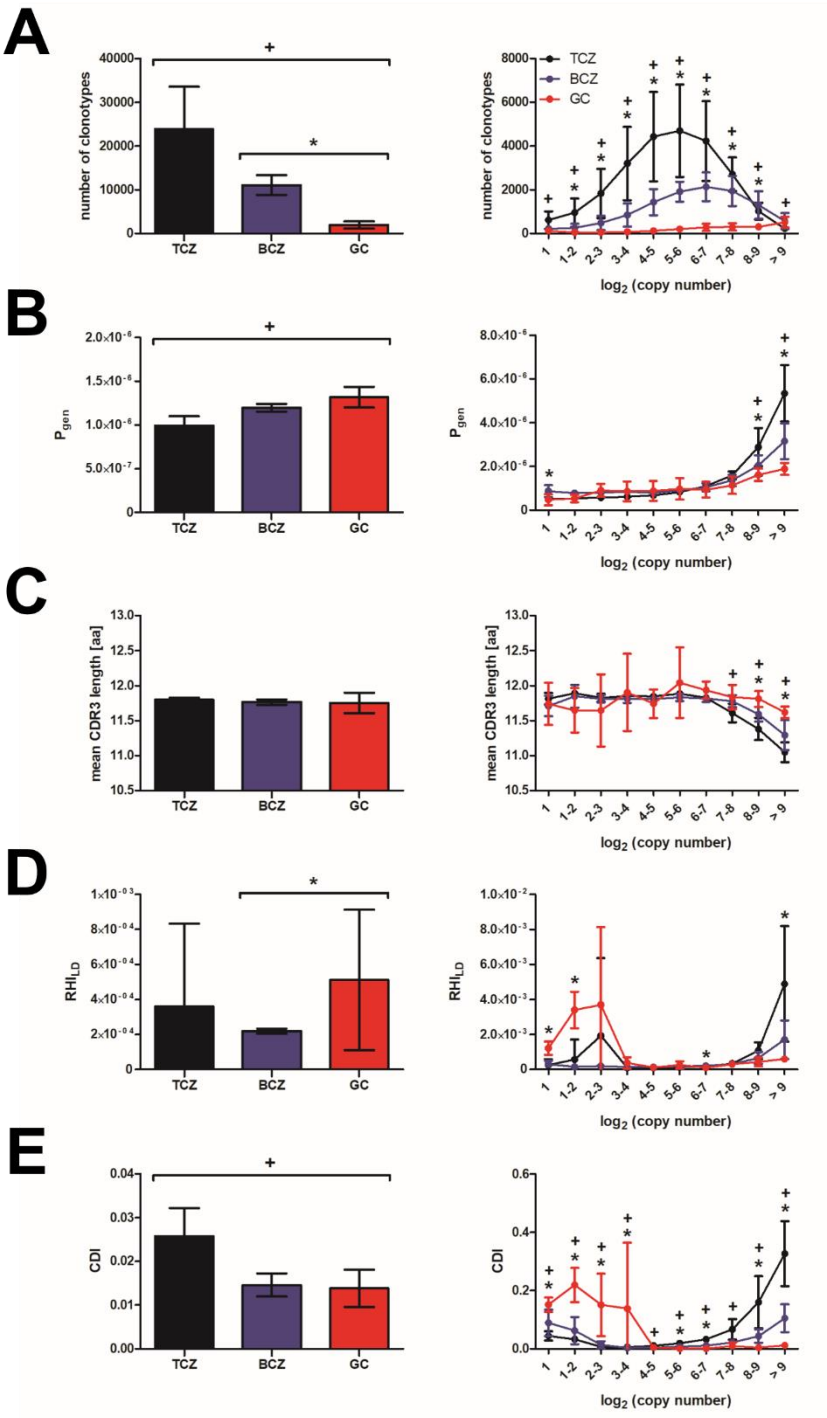

Figure 15: The TCR-R within GCs shows mainly "private" characteristics when compared to surrounding BCZs and TCZ.

Deep sequencing of the complementary determining region 3 (CDR3) β chain of splenic compartments was performed, i.e. T cell zone (TCZ), B cell zone (BCZ) and germinal center (GC). **(A)** Number of detected T cell clonotypes, **(B)** generation probability, **(C)** mean length and **(D)** homogeneity of CDR3β amino acid sequence as well as **(E)** heterogeneity of nucleotide coding were determined to analyze the T cell receptor repertoire (TCR-R) 7 days (d) after SRBC-injection (n = 6). Clonotypes are analyzed in total (left panel) or grouped in fractions according to their frequency (log_2 of their copy number) (right panel). Displayed are means and standard deviations. Data were analyzed using Mann-Whitney-U, with * and + displaying differences between GC and BCZ or GC and TCZ, respectively. aa – amino acids; CDI – coding diversity index; P_{gen} – generation probability; RHI_{LD} – repertoire homogeneity index based on Levenshtein distance.

3.3.2 Tfh cells proliferate within the GC

When taking a closer look at the number of different T cell clonotypes in the GC, we found no significant difference between 4, 7 and 10 d after SRBC-injection, i.e. beginning and peak of GC development, respectively (Figure 16A). This clearly revealed that a multitude of different Tfh clones were found in GCs surrounding one single TCZ, occurring in frequencies with partly more than 1,000 copies. Accordingly, many clonotypes were detected in the high copy fractions with a maximum increase 7 d after immunization (Figure 16B). To further analyze these hints pointing towards proliferation of Tfh cells within GCs, we quantified immunofluorescent stained splenic cryosections (Figure 16C). Counting the number of GC T cells that were positive for both T cell marker CD4 and proliferation marker Ki67 demonstrates that more than 70 % of Tfh cells are proliferating (Figure 16D).

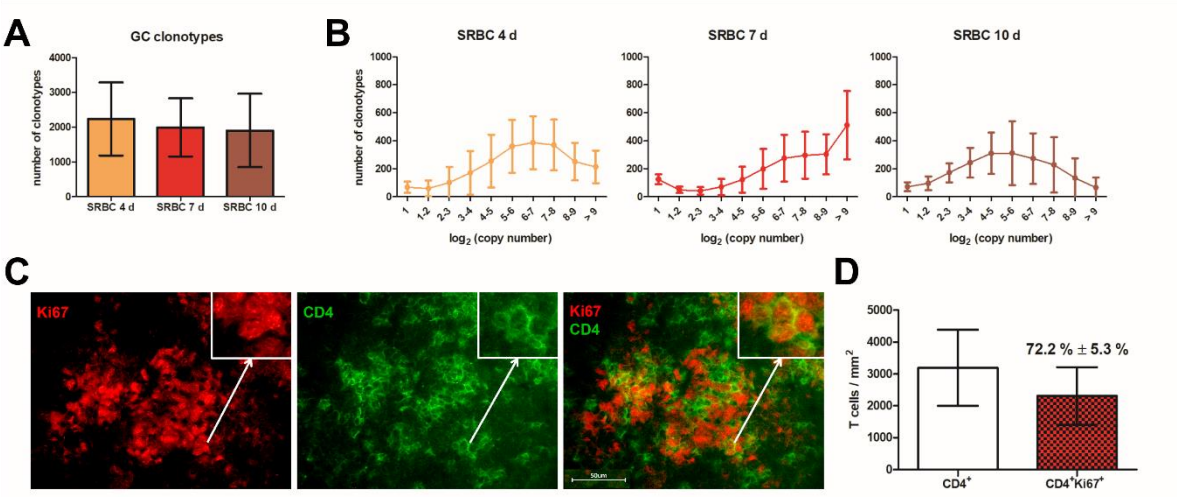

Figure 16: Most Tfh cells proliferate within the GC.
Deep sequencing of the complementary determining region 3 (CDR3) β chain of germinal centers (GCs) was performed. Numbers of detected T cell clonotypes were determined to analyze the T cell receptor repertoire (TCR-R) 4 (n = 8), 7 (n = 6) and 10 (n = 4) days (d) after SRBC-injection **(A)** in total or **(B)** grouped in fractions according to their frequency (log_2 of their copy number). **(C)** Representative cryosections highlighting GC area stained for T cells (green, CD4) and proliferating cells (red, Ki67) were quantified with ImageJ to assess **(D)** number of proliferating T follicular helper (Tfh) cells within GCs. For (A), (B) and (D) means and standard deviations are displayed. Numbers above the graph indicate percentage of proliferating $CD4^+$ T cells. CD – cluster of differentiation.

3.3.3 Tfh cells can be detected in compartments outside the GC, holding "public" characteristics

It is commonly accepted that T cells can enter the circulation and migrate to infected tissues or other lymphatic organs. Since we found clear evidence that Tfh cells are proliferating within the GC, which seems to be also limited in size, we hypothesize that these cells are able to migrate to other splenic compartments as well.

To answer this question, we did not only isolate one TCZ and the adjacent B cell follicles and GCs, but also analyzed a second, separated set of TCZ, BCZs and GCs from serial splenic

sections. To investigate possible migration patterns, we had to switch from amino acid sequence level (= T cell clonotype) to nucleotide sequence level (= T cell clone). Only if two TCR sequences have identical nucleotide sequences and VJ segment usage, they can be related. Hence, each Tfh cell clone was tested to be either exclusively present in the GC (GC_{in}) or also found in at least one of the remaining compartments (GC_{+out}). Most of GC-affiliated Tfh cell clones (also named GC clones here) were resident only in the original GC. Nevertheless, 20-30 % of GC clones could be identified in other compartments in the course of GC reaction (Figure 17A-C, left panel). This partition applied not only to high copy clones but was observable throughout all fractions (Figure 17A-C, right panel). Thus, it is reasonable to restrict further analyses on the total repertoire.

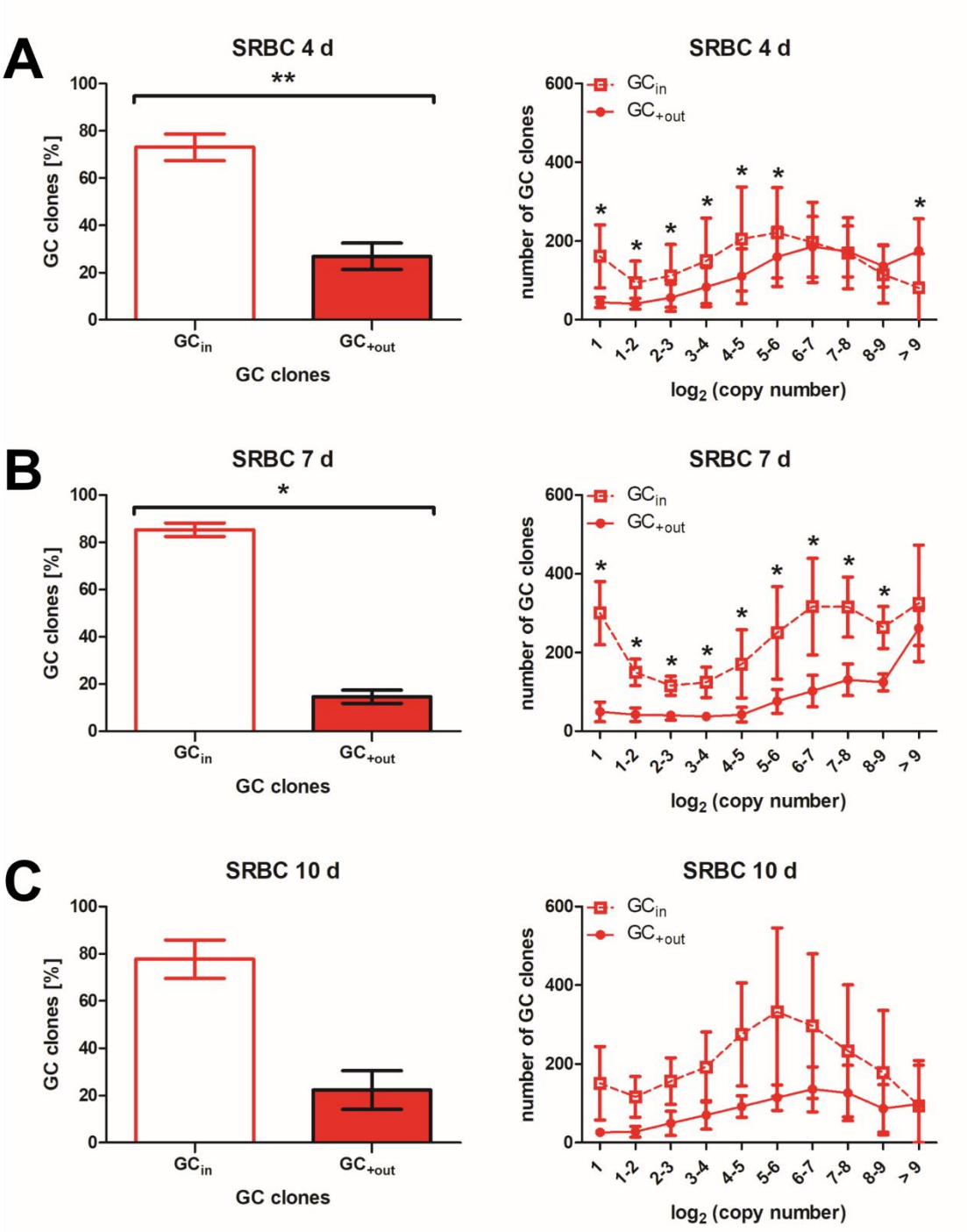

Figure 17: Tfh cell clones can be detected outside the GC.
Deep sequencing of the complementary determining region 3 (CDR3) β chain of germinal centers (GCs) was performed. Each T follicular helper (Tfh) cell clone was tested to be either exclusively present in the GC (GC_{in}) or also found in other splenic compartments (GC_{+out}). **(A)** Total percentage (left panel) and number (right panel) of Tfh cell clones grouped in fractions according to their frequency (log_2 of their copy number) within GCs classified as "GC_{in}" or "GC_{+out}" were assessed **(A)** 4 (n = 8), **(B)** 7 (n = 6) and **(C)** 10 (n = 4) days (d) after SRBC-injection. Displayed are means and standard deviations. Data were analyzed using Mann-Whitney-U, with * $p < 0.05$ and ** $p < 0.01$ indicating significant differences between Tfh cell subgroups.

We further analyzed these two identified subgroups of Tfh cell clones at the peak of GC reaction (i.e. 7 d after SRBC-injection) to characterize the underlying TCR-R using our toolkit of standard parameters. GC clones also present outside the original GC (= GC_{+out} clones) were

determined to have a higher generation probability (Figure 18A), a reduced nucleotide sequence length (Figure 18B) and an increased copy number (Figure 18C) compared to their residential counterparts (= GC_{in} clones). Thus, these clones seem to hold special features that are characteristic for “public” clones. In addition, we also found differences in the distribution of V and J segments with those antigen-specific “public”-like Tfh cell clones preferentially using e.g. segments V3 and J2-7 (Figure 18D+E).

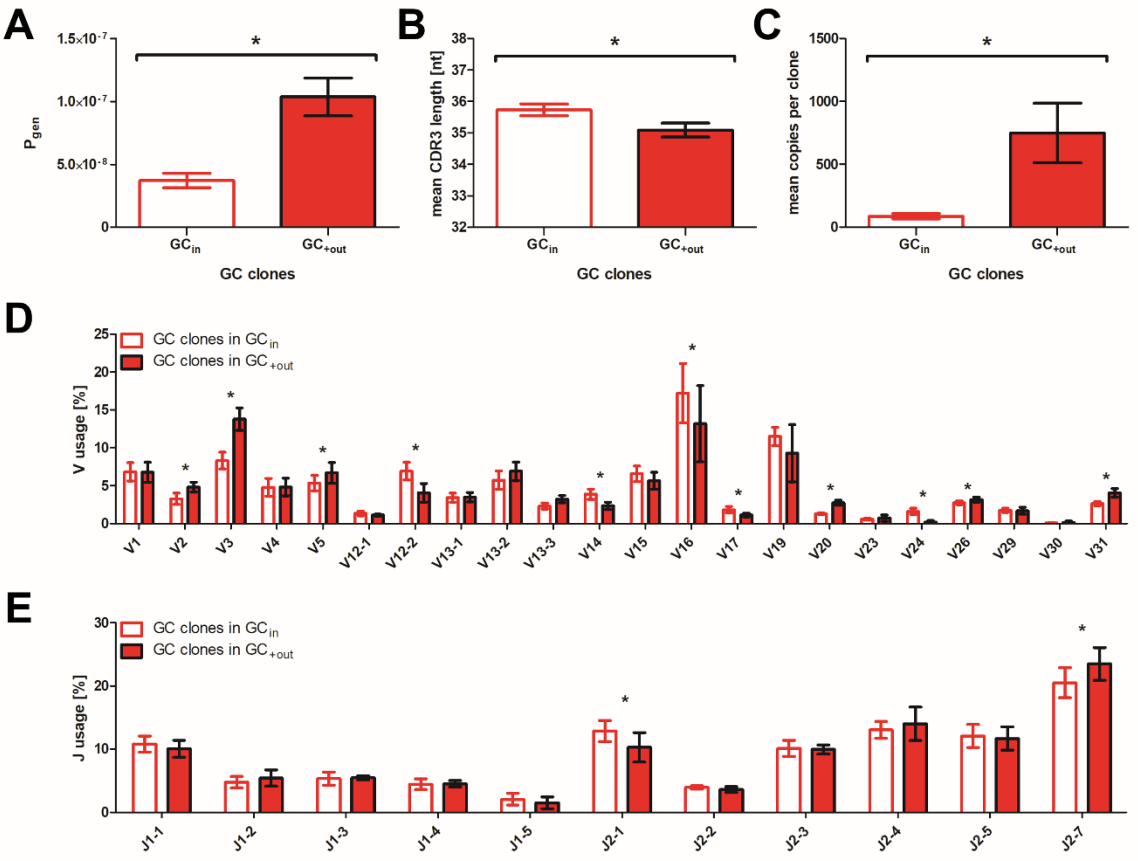

Figure 18: Tfh cell clones found outside the GC hold “public” characteristics.
Deep sequencing of the complementary determining region 3 (CDR3) β chain of germinal centers (GCs) was performed. Each T follicular helper (Tfh) cell clone was tested to be either exclusively present in the GC (GC_{in}) or also found in other splenic compartments (GC_{+out}) and thus assigned in subgroups. For each subgroup **(A)** generation probability, **(B)** mean length and **(C)** copy number of CDR3β nucleotide sequences as well as distribution of used **(D)** V and **(E)** J segments were determined 7 days (d) after SRBC-injection (n = 6). Displayed are means and standard deviations. Data were analyzed using Mann-Whitney-U, with * $p < 0.05$ indicating significant differences between Tfh cell subgroups. nt – nucleotides; P_{gen} – generation probability.

3.3.4 Allocation of GC associated clones highlights the distribution of antigen-specific T cell clones

In the next step, we analyzed how these “public”-like Tfh cell clones contribute to the different splenic compartments and determined the percentage of those GC_{+out} clones in adjacent BCZs and TCZ as well as in distantly located compartments (Figure 19A, right panel). 40 % of GC clones were found in the surrounding B cell follicles (BCZ1) while only 30 % could be detected in the near TCZ (TCZ1). A lower amount of Tfh clones was identified in distant TCZ

and BCZs (TCZ2 and BCZ2, respectively), and we also determined that 30 % of these clones were present in the mln. Surprisingly, 40 % of Tfh clones of the original GC could be noted for a second set of GCs (GC2) as well.

We wondered if this allocation is only due to the fact that these GC clones are considered to be a “public” subgroup. Therefore, we used the same criterion for grouping T cell clones of BCZs and TCZ. T cell clones present in the B cell follicle were predominantly resident in the original BCZ (BCZ_{in}) while around 15 % of these clones were also found in other compartments (BCZ_{+out}) (Figure 19B, left panel). The percentage of T cell clones exclusively present in the TCZ (TCZ_{in}) was even higher with only 10 % being identified outside (TCZ_{+out}) (Figure 19C, left panel). However, when looking at their appearance in all compartments, the distributional pattern clearly differs between GC, BCZ and TCZ clones (Figure 19A-C, right panel). The lowest amount of TCZ clones was detected in GCs, regardless of being close or distant to the original TCZ. While 20-30 % of T cell clones found in the TCZ were also identified in a second TCZ and in different BCZs, even up to 50 % were determined outside the spleen in the mln (Figure 19C, right panel). The distribution of T cell clones identified from B cell follicles illustrates a pattern in between (Figure 19B, right panel). Even though a similar ratio of resident and shared T cell clones could be found for all splenic compartments, their distribution definitely differs.

To complement this finding, we further determined the generation probability of the different clonal subgroups within all compartments and detected the following pattern: The probability of sequences being generated was highest for mln and TCZs and followed by B cell follicles, regardless of being near or distantly located to the compartment of origin. Clones present in GCs held the lowest P_{gen} levels. Surprisingly, this pattern was independent of whether the T cell clones were determined of GCs, BCZs or TCZ (Figure 19D-F). Thus, for T cell clones identified from TCZ and BCZ, generation probability of detected sequences could mostly account for the observed distributional pattern (Figure 19E-F), whereas the opposite distribution was identified for GC clones (Figure 19D).

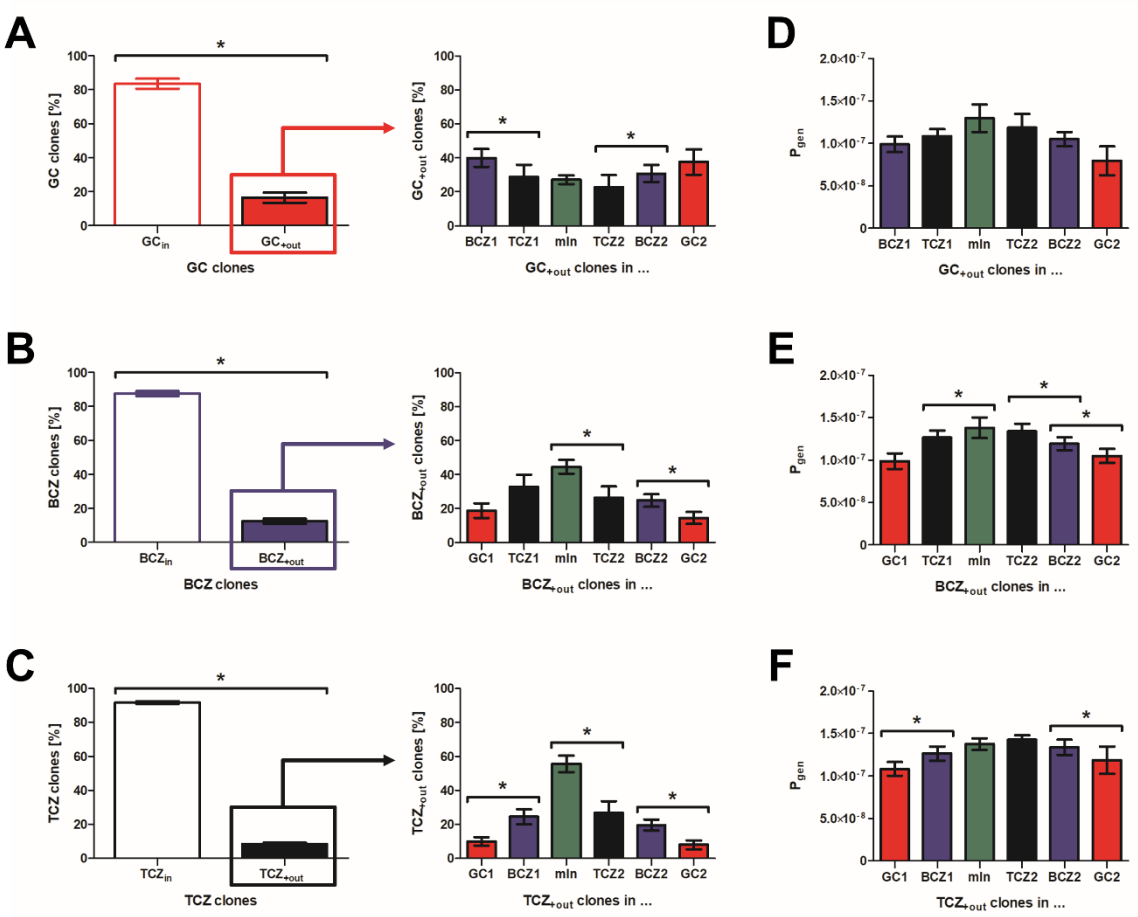

Figure 19: Allocation of Tfh cell clones highlights the distribution of antigen-specific T cell clones, independent of generation probability.
Deep sequencing of the complementary determining region 3 (CDR3) β chain of splenic compartments was performed, i.e. T cell zone (TCZ), B cell zone (BCZ) and germinal center (GC), with two independent compartments each being isolated. Left panel: Each T cell clone was tested to be either exclusively present in **(A)** GC (GC_{in}), **(B)** BCZ (BCZ_{in}) or **(C)** TCZ (TCZ_{in}) or also found in other splenic compartments besides their original one (GC_{+out}, BCZ_{+out} and TCZ_{+out}, respectively). Right panel: Percentage of T cell clones outside original GC, BCZ and TCZ, respectively, found in near or distant compartments (marked with number 1 or 2, respectively) or in mesenteric lymph node (mln). **(D)-(F)** For each subgroup the generation probability of the respective CDR3β nucleotide sequences were determined. Displayed are means and standard deviations 7 days (d) after SRBC-injection (n = 6). Data were analyzed using Mann-Whitney-U, with * $p < 0.05$ indicating significant differences between T cell subgroups (A-C, left panel) or T cell clones found in neighboring compartments (A-C, right panel, and D-F). P_{gen} – generation probability.

3.4 Analyzing the molecular composition of splenic compartments during a T cell dependent B cell response

The previous results have shown that different T cell clonotypes are recruited into the splenic compartments and that immunization affects the diversity of the underlying TCR-R. We wondered what parameters might influence these effects in TCZ, BCZ and GC. To pursue this question, it will be beneficial to first evaluate the functional state of relevant cell types and the underlying splenic milieu before further analyzing the impact of sleep on the T cell dependent B cell response.

Thus, we assessed the mRNA-expression of a set of genes that are involved in key functions of T and B lymphocytes by qRT-PCR to characterize the molecular composition of the splenic compartments both in the naïve state and during a T cell dependent B cell response against SRBC.

To assess antigen presentation, we examined the mRNA-expression of the gene for class II MHC transactivator (*ciita*) as the master control factor for the expression of MHCII genes. T cell activation was analyzed via the gene of the zeta chain associated protein kinase (*zap70*) coding for a part of the TCR signaling machinery. In addition, the co-stimulatory molecules cluster of differentiation 40 ligand (*cd40lg*), which is expressed by activated T cells, and inducible T cell costimulator ligand (*icoslg*), which is expressed by APCs, were determined to monitor cell-cell interaction. Finally, the mRNA-expression of β-1,4-galactosyltransferase 1 (*b4galt1*) and ST6 β-galactoside α-2,6-sialyltransferase 1 (*st6gal1*), which are coding for enzymes involved in glycosylation processes, was measured to investigate modifications of key molecules as well as trafficking of lymphocytes involved in the immune response.

3.4.1 Immune cell interaction is reduced 3 d after SRBC-injection

In the naïve state, the relative mRNA-expression of *ciita* was highest in the BCZ, while we detected an increased expression of *zap70* in the TCZ here (Figure 20A). Overall levels of *cd40lg* were higher in the TCZ as well, whereas *icoslg*-expression was increased in the B cell follicle (Figure 20B). For the glycosylation markers *b4galt1* and *st6gal1* no difference between the splenic compartments could be determined (Figure 20C). These effects of compartmentalization also stayed robust 3 d after SRBC-injection. However, two-way ANOVA revealed a significantly reduced expression of both *cd40lg* and *icoslg* here, demonstrating a decreased interaction of immune cells after immunization (Supplement Table 1 and Figure 20B).

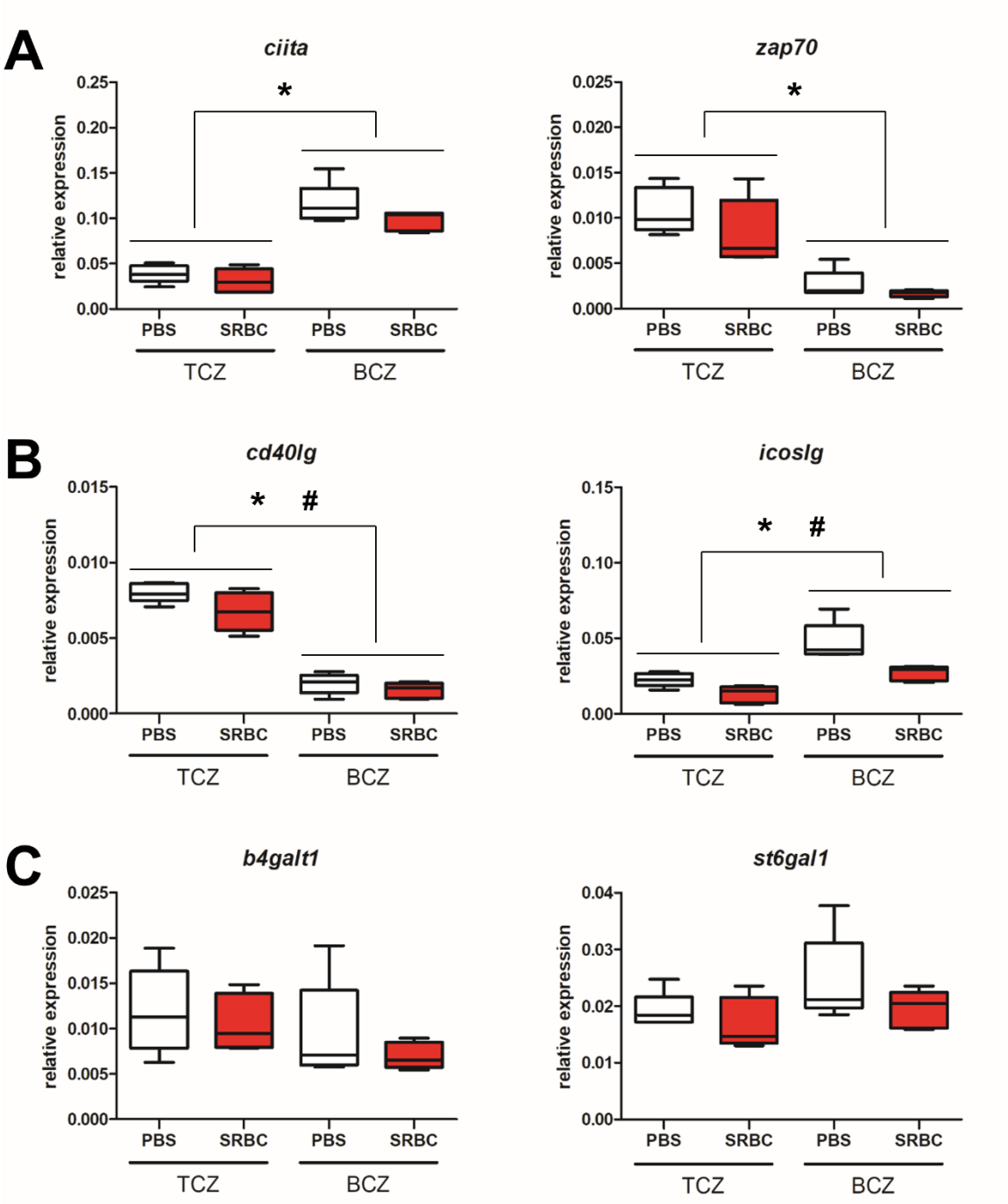

Figure 20: The expression of genes involved in the T cell dependent B cell response during the first proliferation period 3 d after SRBC-injection.
Mice were injected with either PBS or SRBC, and splenic cryosections were subjected to laser microdissection 3 days (d) later. mRNA-expression levels of genes involved e.g. in **(A)** activation, **(B)** interaction and **(C)** modification of T and B lymphocytes were assessed by qRT-PCR in splenic compartments, i.e. T cell zone (TCZ) and B cell zone (BCZ). Boxplots show medians and interquartile ranges, whiskers indicate minima and maxima (n = 5 per group). Data were analyzed by two-way ANOVA (see Supplement Table 1 for details), with * indicating significant differences between compartments. Significant immunization effects are displayed as #.

3.4.2 Immunization increases expression of genes involved in activation, interaction and modification of T and B lymphocytes 7 d after SRBC-injection

7 d after immunization, the former observed differences in mRNA-expression levels between splenic compartments were still detectable for *ciita*, *zap70*, *cd40lg* and *icoslg* (Figure 21A+B). In addition, *b4galt1*-expression was increased in the TCZ, while the relative mRNA-expression of *st6gal1* showed higher levels in the B cell follicle (Figure 21C). In contrast to the 3 d timepoint where we found no significant differences between naïve and immunized animals, expression levels of both *ciita* and *zap70* were significantly increased 7 d after SRBC-injection (Figure 21A). The same was also true for *cd40lg* where a significant interaction between compartment and immunization status was demonstrated by two-way ANOVA (Supplement Table 2 and Figure 21B, left panel). An immunization-induced expression increase could also be detected for both *icoslg* (Figure 21B, right panel) and for the glycosylation markers *b4galt1* and *st6gal1* (Figure 21C).

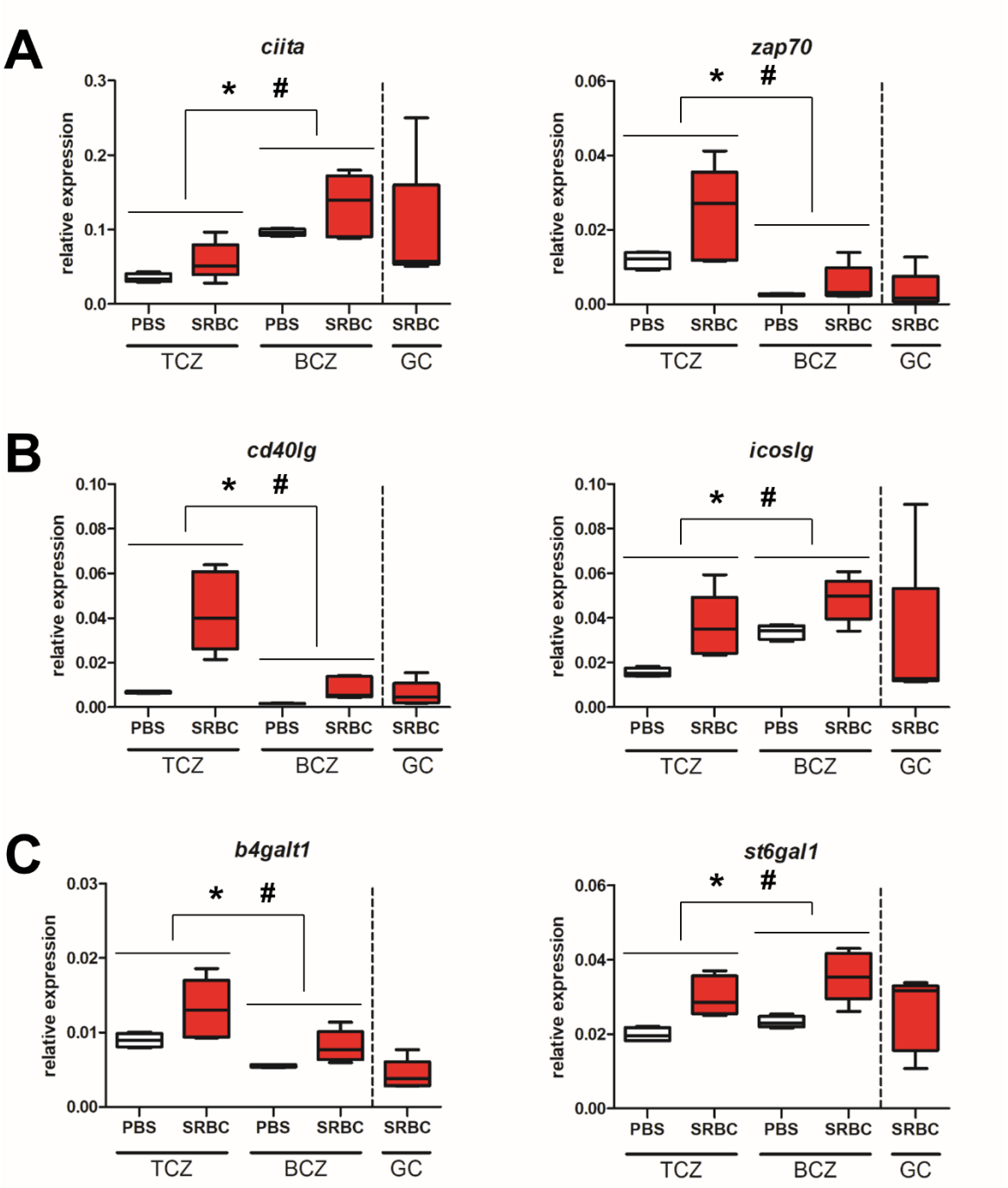

Figure 21: Immunization increases the expression of genes involved in the T cell dependent B cell response during the GC reaction 7 d after SRBC-injection.
Mice were injected with either PBS or SRBC, and splenic cryosections were subjected to laser microdissection 7 days (d) later. mRNA-expression levels of genes involved e.g. in **(A)** activation, **(B)** interaction and **(C)** modification of T and B lymphocytes were assessed by qRT-PCR in splenic compartments, i.e. T cell zone (TCZ), B cell zone (BCZ) and germinal center (GC). Boxplots show medians and interquartile ranges, whiskers indicate minima and maxima (n = 5 per group). Data were analyzed by two-way ANOVA (see Supplement Table 2 for details), with * indicating significant differences between compartments. Significant immunization effects are displayed as #.

3.5 The effect of sleep on a T cell dependent B cell response

3.5.1 Sleep deprivation dampens the immunization-induced effects on T cell signaling and modification

As injection of high dosed SRBC induced changes in the expression of a diverse set of genes that were still detectable 7 d after immunization, we wondered about whether sleep deprivation might affect these functions. To investigate this, we injected mice with either PBS or SRBC 1.5 h prior to the sleeping phase and then allowed them to sleep normally ("sleep") or subjected them to 6 h of sleep deprivation ("awake"). mRNA-expression of the aforementioned genes was assessed in the different splenic compartments 7 d later using qRT-PCR.

Three-way ANOVA revealed a significant effect for sleep(deprivation) 7 d after immunization for two genes, *zap70* and *b4galt1* (Supplement Table 3 and Figure 22A+B). Here, we also found a significant interaction with the immunization status, highlighting that the effect for sleep(deprivation) was only detected after SRBC-injection and not in the naïve state. Thus, we could determine that 6 h of sleep deprivation at the beginning of the sleeping phase decreased both *zap70*- and *b4galt1*-expression and so lowered the immunization-induced expression changes back to naïve like levels (Figure 22A+B).

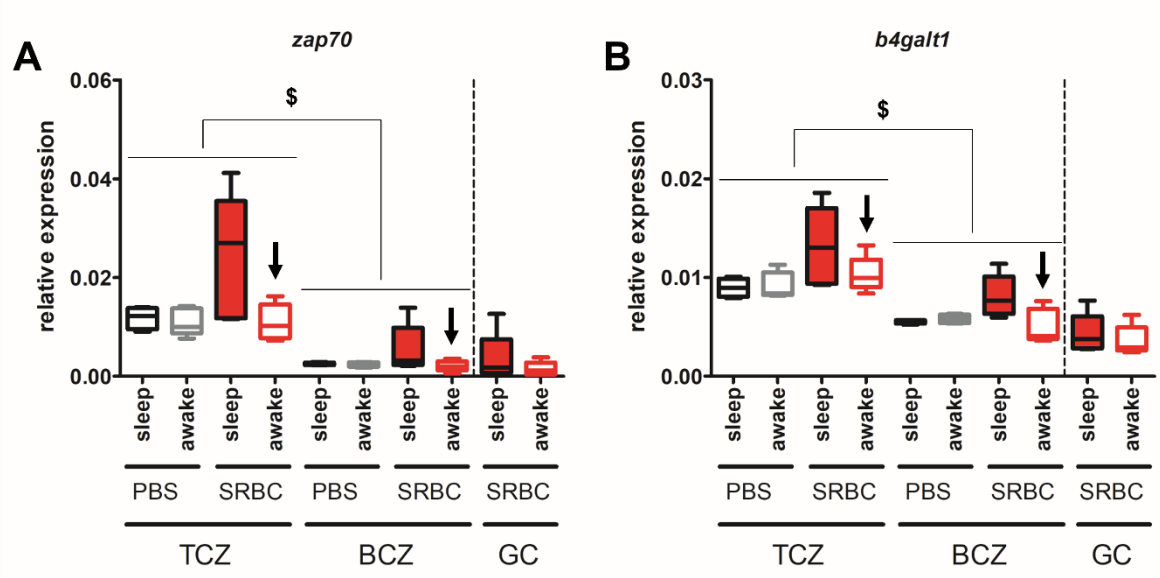

Figure 22: Sleep deprivation dampens immunization-induced expression changes in genes involved in TCR signaling and glycosylation 7 d after SRBC-injection.
Mice were injected with either PBS or SRBC 1.5 hours (h) prior to the sleeping phase and were allowed to sleep normally ("sleep") or subjected to 6 h of sleep deprivation ("awake"). mRNA-expression levels of genes for **(A)** T cell receptor (TCR) signaling and **(B)** glycosylation were assessed by qRT-PCR in splenic compartments, i.e. T cell zone (TCZ), B cell zone (BCZ) and germinal center (GC) 7 days (d) after immunization. Boxplots show medians and interquartile ranges, whiskers indicate minima and maxima (n = 5 per group). Data were analyzed by three-way ANOVA (see Supplement Table 3 for details) and a significant interaction for sleep(deprivation) and immunization is displayed as $. Arrows highlight sleep deprivation-induced reduction of immunization effect.

3.5.2 Sleep deprivation does not affect the TCR-R recruited into an immune response

Due to the fact that *zap70* and *b4galt1* are coding for proteins that are involved in important T cell functions, we further wondered if sleep deprivation might also have an effect on the composition of the TCR-R. Hence, we compared the repertoire found in splenic compartments of SRBC-injected mice with normal sleep ("sleep") to that of sleep-deprived animals ("awake"). As before we determined the number of detected T cell clonotypes (Figure 23A), their generation probability (Figure 23B), mean CDR3 sequence length (Figure 23C) and repertoire homogeneity (Figure 23D) as well as heterogeneity of nucleotide coding (Figure 23E). No differences in the TCR -R of mice with normal sleep and those with sleep deprivation could be observed in the splenic compartments 7 d after immunization.

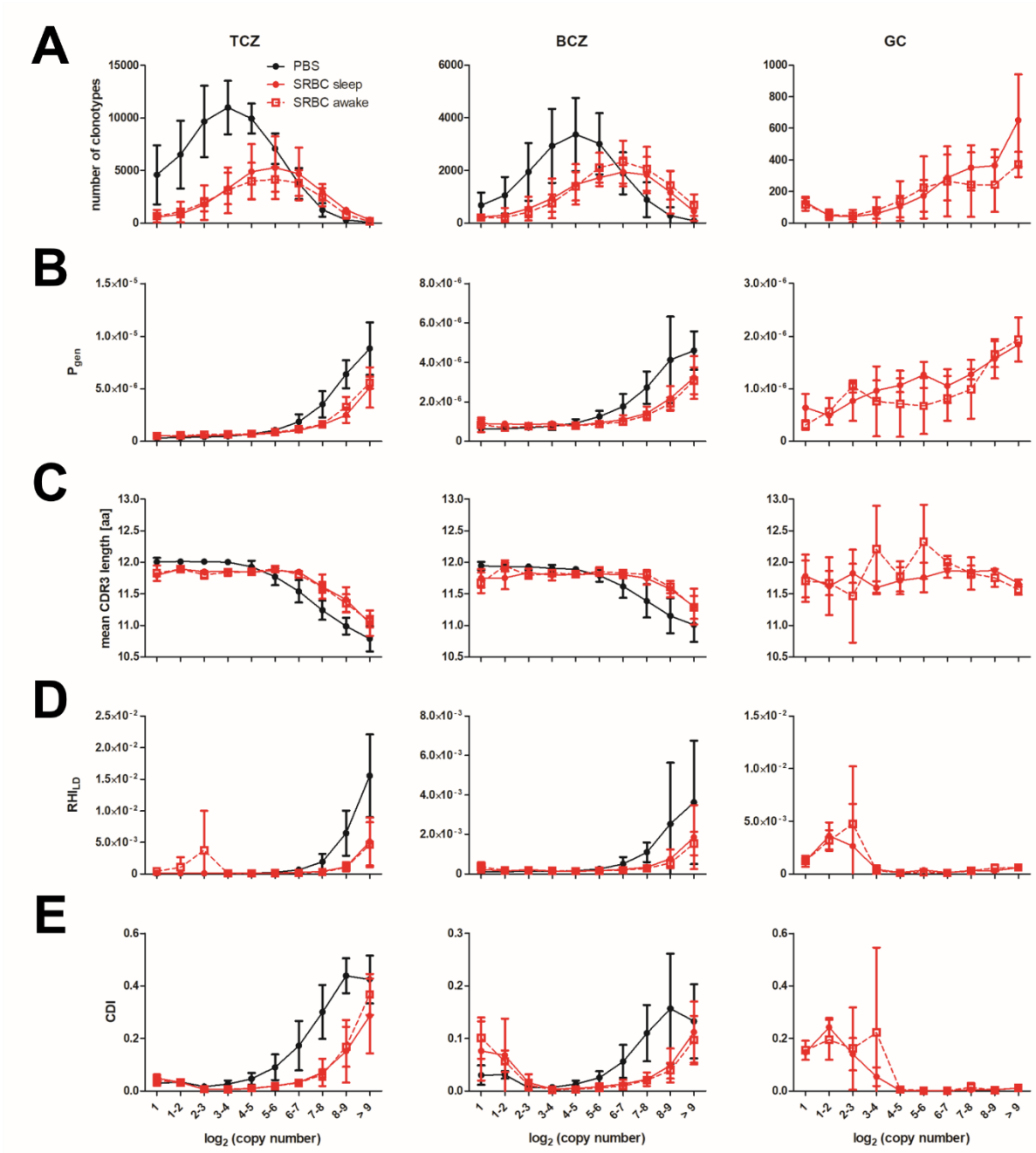

Figure 23: Sleep deprivation does not alter the TCR-R in splenic compartments 7 d after immunization.

Deep sequencing of the complementary determining region 3 (CDR3) β chain of splenic compartments was performed, i.e. T cell zone (TCZ), B cell zone (BCZ) and germinal center (GC). **(A)** Number of detected T cell clonotypes, **(B)** generation probability, **(C)** mean length and **(D)** homogeneity of CDR3β amino acid sequence as well as **(E)** heterogeneity of nucleotide codings were determined to analyze the T cell receptor repertoire (TCR-R) in naïve mice (n = 8) or 7 days (d) after injection of SRBC in mice with normal sleep ("sleep") or sleep deprivation ("awake") (n = 3 each). Clonotypes are grouped in fractions according to their frequency (log_2 of their copy number). Displayed are means and standard deviations. Within each fraction data were analyzed for effects of sleep(deprivation) using Mann-Whitney-U. aa – amino acids; CDI – coding diversity index; P_{gen} – generation probability; RHI_{LD} – repertoire homogeneity index based on Levenshtein distance.

4. Discussion

With this study we want to shed light on the distribution of the TCR-R in different splenic compartments and its implications for a T cell dependent B cell response. We therefore asked if the TCR-R of TCZ and BCZ already differs at the naïve state and whether this affects the reaction to a blood-born antigen. Since a T cell dependent B cell response forces the development of GCs, we further asked if the TCR-R of Tfh cells holds special features and can also be exchanged between compartments. Aside from this, we monitored the current sleep status as further aspect that might have an effect on the underlying TCR-R as well as the predominant splenic milieu.

4.1. The TCR-R of splenic TCZ and BCZ differs in naïve mice

Our results have shown that T cells are not only found in splenic TCZ, but also to a lower amount (~ 1/15) in the B cell follicle of unimmunized mice, which is in agreement with former studies [7, 79-81]. Since we have calculated a 3-fold difference in clonotype number between the two compartments – with overall less varying T cell clonotypes detected in the BCZ – already under steady-state conditions, the diversity of the underlying TCR-R in B cell follicles is absolutely reduced (Figure 6).

4.1.1. The TCR-R of BCZs mainly features more “public” characteristics with respect to the TCZ

These clonotypes seem to hold features of so called “public” clonotypes, resulting in remarkable differences in sequence characteristics compared to their counterparts detected in the TCZ (Figure 7).

“Public” clonotypes are usually known to occur in higher frequencies and have fewer nucleotide additions and thus a shorter CDR3 sequence length, accompanied with a skewed or restricted VJ segment usage. These amino acid sequences are typically coded by many different nucleotide sequences and appear in families of related sequences or encompassing shared sequence motifs, thus resulting in an overall more homogeneous repertoire. Those high frequent “public” clonotypes are said to develop due to biases in recombination processes, favoring the generation of certain sequences [12, 40, 74, 77, 82-84].

What could be the reasons leading to the detected differences in the naïve repertoire of TCZ and BCZ? Factors differentially affecting the diversity of the TCR-R might be variances in migration patterns of T cells or a different $CD4^+/CD8^+$ T cell ratio in TCZ and BCZ. In addition, different retention periods or local proliferation might also be drivers of diversification between splenic compartments [5, 40, 77, 85]. These options will be discussed in the following section.

Lymphocytes continuously circulate through the blood to migrate between different lymphatic and non-lymphatic organs, resulting in an exchange of almost all T cells present in an individual

per day (~ 500 x 10^9) [5, 85]. By stochastically trafficking between and randomly walking within tissues, they scan their environment for cognate antigen [81, 85-87]. Under steady-state conditions, random migration should outpace other criteria like e.g. local proliferation, thus diversity is simply a matter of chance [40, 85]. If there is free exchange between splenic compartments and T cells just randomly enter and exit B cell follicles, the TCR-R in the BCZ should reflect the repertoire found in TCZ with all their characteristics, so that such profound differences were hardly possible.

Although naïve $CD4^+$ T cells are found to migrate almost twice as fast as $CD8^+$ T cells to and within lymph nodes, no differences in their anatomical localization or intranodal migration behavior were found so far [87, 88]. A similar distribution of both lymphocyte subsets can be noted for both splenic TCZ and BCZ, with $CD4^+$ T cells far exceeding the amount of $CD8^+$ T cells [7]. Hence, it seems to be unlikely that this ratio accounts for the differences found in the TCR-R.

If differential migration or entry rate does not result in the detected repertoire pattern, variable proliferation pattern or retention periods could be the cause. Naïve T cells randomly enter the B cell follicle, and most of them constantly leave the tissue as they do not find a suitable antigen. But if cognate antigen is presented, T cells bearing the right TCR are retained and accumulate in this area [5, 85, 86, 88]. It is likely that B lymphocytes bearing small peptides of endogenous antigen on their MHC make contacts with some T cells, resulting in their activation and retainment. It has been postulated that “public” clonotypes are associated with self- or self-like antigen classes [12, 82, 89], therefore especially clonotypes holding those features might be forced to stay within the B cell follicle. While a potpourri of T cell clonotypes with various characteristics is present in the TCZ, the BCZ repertoire is mainly built by TCR sequences with “public” properties that were preferentially retained. Hence, those dwell time differences can account for the higher generation probability, shorter mean CDR3 sequence length, and overall more homogenous repertoire with a skewed V segment usage in the BCZ (Figure 7).

4.1.2. Fractioning the T cell clonotypes according to their copy number reveals that also “private” features can be detected in high copy clonotypes of BCZs

In a former study we already have shown that fractioning the TCR-R is an efficient method to investigate even small changes that could be missed when looking only at the T cell clonotypes in total, because observations might be dominated by those clonotypes making up the majority of the predominant repertoire [74]. Hence, we grouped the detected T cell clonotypes into ten fractions according to their frequency (log_2 of their copy number) and analyzed these categories separately (Figure 8).

Both in TCZ and BCZ we detected a rise with copy number in T cell clonotypes holding “public” characteristics. Since the aforementioned biases in recombination processes are resulting in a higher probability of being generated for those sequences, a correlation of high abundance and “publicness” [77], and thus the observed accumulation in fractions containing clonotypes with highest copy number, is not surprising. Furthermore, the distribution of T cell clonotypes within the BCZ supports our theory of selectively accumulating and expanding T cells with “public” features here. T cell clonotypes are rarely found in fractions of lowest copy number, thus T cells are unlikely to just randomly accumulate within the B cell follicle without being activated or started to proliferate.

Interestingly, the pattern found for the total repertoire is only expressed for T cell clonotypes appearing in low or medium copy numbers, which make up the majority of TCR sequences (> 90 % of T cell clonotypes) in both compartments (Figure 8 and Figure 9). In contrast to that, the more frequent T cell clonotypes in the BCZ show characteristics that resemble “private” sequences compared to their counterpart in the TCZ.

“Private” clonotypes represent the analog to “public” clonotypes, with usually more nucleotide additions and thus a longer CDR3 sequence length. These amino acid sequences are typically coded by only one dominant nucleotide sequence and do not show shared sequence motifs, thus resulting in an overall more heterogenous repertoire [74, 89]. They are said to have a lower probability of being generated, resulting in a variability in copy number they occur with [12, 40, 74, 82, 84, 89]. Those “private” clonotypes are moreover associated with all categories of antigens [12, 82, 89].

Finding T cell clonotypes of highest copy number with more “private” characteristics in the B cell follicle compared to the TCZ might give a hint to a selective advantage. Most immune responses, even to endogenous or environmental antigens that are presented in the BCZ, are composed of a mixture of both “private” and “public” TCR sequences [90]. Recognizing their cognate antigen results in the activation and expansion of the respective T cell [90, 91]. Thus, T cells with “private” features of their TCR can be likewise activated and forced to proliferate after antigen recognition, which is beneficial compared to naïve “public” clonotypes without antigen engagement. Hence, even if not being as much “public” than others, i.e. not inherently occurring in large numbers, proliferation results in the accumulation of these clonotypes in fractions of highest copy number. Thus, T cell clonotypes of highest frequency can be found both within “public” and “private” sequences [74, 82]. Compared to the BCZ, where proliferating T cells have been detected in the naïve state (Supplement Figure 1B) and thus also providing an explanation for the overall reduced CDI (Figure 7D), almost no activation and consequent proliferation is seen in the TCZ (Supplement Figure 1A). Consequently, only T cell clonotypes having a higher probability of being generated per se, i.e. holding “public” features, manage to reach high frequencies here.

Comparing the TCR-R between compartments of different animals to that within TCZ or BCZ of the same mouse confirms this theory (Figure 10). In the TCZ the Jaccard index increases with copy number, thus showing a higher overlap for those T cell clonotypes that are defined to hold “public” characteristics. “Public” clonotypes are also known to be more likely shared by individuals, since they have an overall higher probability of being independently generated at different locations [74, 77, 84]. Thus, the repertoire overlap found for the T cell clonotypes of the TCZ is in range with the sharing level observed in mice and humans for “public” sequences [77, 82]. As seen in a former study by Textor *et al.* [40], almost no difference could be detected when comparing naïve TCZs of the same mouse or between different animals. Thus, finding same TCR sequences in different compartments is just a consequence of “publics” amounting for the majority of high copy T cell clonotypes within the TCZ. In contrast to that, the clonal overlap does not increase with raising copy number when comparing BCZs of different animals (Figure 10B). The B cell follicle is composed of a smaller number of T cells than the corresponding TCZ, thus reducing the chance that the same TCR sequence occurs in both compartments, as “publicness” and associated sharing probability also depend on sample size [77, 92]. In addition, we have shown that high copy clonotypes within the BCZ show “private” characteristics, which are known to be realized only in a few individuals at a given timepoint [74, 84]. Hence, the probability of being independently generated and retained in the B cell follicles of at least two mice is considerably lower for the more “private” T cell clonotypes found here. On the other hand, comparing two BCZs within the same mouse shows the former mentioned increase in overlap for high copy clonotypes. Within the same animal, even “private” T cell clonotypes that we supposed to proliferate, are able to exchange between different compartments, resulting in the occurrence of similar TCR sequences in more than one single BCZ.

To conclude, at steady-state conditions, the majority of T cell clonotypes within the naïve B cell follicle generally holds more “public” characteristics, which might be due to the presentation and subsequent recognition of endogenous antigen, whereas the repertoire found in the naïve TCZ is composed of a sequence mixture of non-activated T cells. Nevertheless, also a minority of T cell clonotypes showing more “private” features is present in the BCZ, which presumably likewise responds to e.g. environmental antigen, resulting in subsequent proliferation. This differential accumulation might account for the difference in the TCR-R between TCZ and BCZ in naïve mice.

4.2. The effect of immunization on the TCR-R in splenic compartments after SRBC-injection

Since the TCR-R already differs between TCZ and BCZ in naïve animals, we wondered if these variances result in differences during an immune reaction. To locally induce a T cell dependent immune response in the spleen, which is exclusively mediated by $CD4^+$ T cells, we used intravenous injection of high dosed SRBC [6, 39, 93].

4.2.1. Immunization induces a shift and the expansion of "private" clonotypes in the TCR-R of TCZ and BCZ

As shown before for whole splenic slices, SRBC-injection results in an immune response that is mainly built by "private" T cell clonotypes [41, 74, 94]. Due to activation and subsequent proliferation of antigen-specific T cells, the diversity of the underlying TCR-R decreases over time, resulting in the accumulation of those "private" T cell clonotypes (Figure 11). As the amount of responding T cells usually is very low compared to the total number of T cells present in an individual, even after expansion antigen-specific T cells might not outstrip non-reacting clonotypes in frequency, making their detection in an heterogenous population a challenge. Thus, we took advantage of the fact that the used parameters are very sensitive to measure even minimal alterations in sequence characteristics which are caused by displacements within the repertoire due to expanding antigen-specific clonotypes [74, 91].

The aforementioned effect of accumulating "private" T cell clonotypes can first be noticed 3 d after immunization in the fraction of highest copy number within the TCZ (Figure 12), when T cell proliferation and IL4 expression is known to peak in the SRBC-model [39, 91]. However, the impacts of immunization are more pronounced after 7 d (Figure 13): The overall decrease in clonotype number but shift to higher copy number fractions confirms the expansion and thus accumulation of reacting SRBC-specific T cells. As in the naïve repertoire, clonotypes of highest frequency are holding more "public"-like properties, revealing that even in a so called "private" immune response those clonotypes can accumulate alike. However, compared to PBS, changes in sequence characteristics towards "private" characteristics here clearly demonstrate that "private" SRBC-specific T cells replace the former predominance of naïve "public" ones [74, 89]. Recognizing their cognate antigen facilitates their expansion, gaining a selective advantage over naïve "public" T cell clonotypes that only reach higher frequencies due to being more likely generated in general. In addition, the immune response not only effectuates the enrichment of specific sequence features for high copy clonotypes, but also in the low copy fractions a difference between PBS- and SRBC-injected mice could be detected. In contrast to T cell clonotypes of highest frequency, the repertoire existing of low copy number clonotypes seems to be more "public" after induction of the immune response, shown e.g. by a decrease in CDR3 sequence length and a simultaneous rise in generation probability. Thus,

it is likely that accumulation of expanding SRBC-specific T cell clonotypes with “private” characteristics in higher copy numbers represses the former predominant naïve clonotypes, so that their “public” properties can only be detected in lower frequencies [74]. Interestingly, these effects are not exclusively found within the TCR-R of the TCZ, but also for the B cell follicle, where all alterations happen on a lower level, presumably representing the differences in the prevalent overall degree of “publicness” between these compartments. Since “private” TCR sequences are known to share less similarities with other sequences, they are found to soften cluster structures of “public” networks [89]. This can be confirmed by our cluster analysis, where TCZs 7 d after SRBC-injection drift off their former cluster. Thus, immunization induces a heterogenization of the underlying TCR-R, revealing an overall scattered pattern as found for the BCZ (Figure 11C).

To sum up, the former heterogenous naïve population that was built of a mixture of TCR sequences with variable frequencies changes as response to the presented foreign antigen to a different composite. Though being still heterogenous, this repertoire is mainly made up by “private” T cell clonotypes that replace the former predominant ones.

4.2.2. The TCR-R of Tfh cells during the GC reaction

During the course of the immune response, interaction of antigen-specific T and B lymphocytes induces the development of GCs within the B cell follicles as early as 4 d post injection (*p.i.*), which reaches a peak around 7 to 10 d [95, 96]. These well-defined structures not only contain B cells undergoing cycles of proliferation, but also T cells that drive their selection to high-affinity antibody producing plasma cells [23, 28, 36]. Within the GC, we detected about 3,600 T cells/mm^2, which is in line with a former study using a different mouse strain [81]. However, for the first time these numbers were quantified in comparison to other splenic compartments at the peak of GC reaction (Figure 14). While the TCZ naturally accommodates the highest number of T lymphocytes, GCs were colonized by twice as many T cells than the adjacent BCZs. Giving the free exchange seen between TCZ and BCZ, these lymphocytes are likely to be recruited from surrounding follicles and retained to take part in the GC reaction where they deliver help to cognate B cells [23, 27, 79]. To analyze the underlying TCR-R of GCs in detail for the first time, we pooled compartmental samples that belong to an anatomical unit, i.e. an individual TCZ with surrounding B cell follicles and GCs. Thus, on average 2.6 ± 1.0 (mean and standard deviation) GCs that encompass a single TCZ were sampled, containing about 12,500 T cells. Although this is in the same magnitude as T cells sampled from B cell follicles, fewer T cell clonotypes could be detected here. However, the GC is not monoclonal either. A multitude of different TCR sequences highlights the heterogeneity of this splenic population, which interestingly is in the same range as the repertoire induced in an autoimmune skin disease model within GCs of popliteal lymph nodes [97]. Thus, it is likely that almost all TCRs of reacting antigen-specific T lymphocytes are represented in the GC repertoire [96, 97], which

in our case comprises about 2,000 SRBC-specific T cell clonotypes. Accordingly, the effects of the “private” immune response induced by injection of SRBC are even more pronounced here than already seen for TCZ and BCZ (Figure 15). Both RHI_{LD} and CDI stayed at a very low level, and almost no alterations in sequence length and generation probability were visible for high copy Tfh cell clonotypes. This confirms our finding of mainly antigen-specific Tfh cells bearing characteristics of “private” clonotypes within the GC.

However, for low copy clonotypes we detected a rise in repertoire homogeneity and nucleotide coding. These T cell clonotypes were also tested to show sequence similarities to TCR sequences of highest copy number (data not shown). Though a TCR generally has its unique specificity, it can respond to a variety of ligands in different extents [73, 98]. Thus, these TCRs might also show cross reactivity to the presented peptides, since SRBC offer a multitude of different epitopes [42, 43, 91, 93]. Due to the fact that clonal expansion depends on TCR signaling strength and T cell clonotypes reacting to peptides they are not absolutely specific for are known to have a lower affinity of their TCR [91], they are at a disadvantage over higher affinity SRBC-specific T cell clonotypes while taking part in a clonal competition. As continuous selection forms the TCR-R of GCs, Tfh cells holding “private” features are overall dominating and are repressing these lower affinity T cell clonotypes to low copy number fractions. However, the underlying cause is not exclusively clarified yet.

4.3. Allocation of Tfh cell-like clones outside the GC highlights the distribution of activated antigen-specific T cell clones

In the history of T cell biology research, most studies have focused on characterizing different $CD4^+$ T cell subsets on the basis of secreted cytokines or the expression of surface molecules and transcription factors [15, 99]. For example, Th1 cells are characterized by production of IFNγ, while Th2 cells preferentially secrete IL4 and IL10. IL10 is also known to be produced by Treg cells that show a pronounced expression of transcription factor FoxP3 (i.e. Forkhead box protein P3), whereas Th17 cells primary use IL17 and IL21 [15, 21, 25].

Tfh cells are typically defined by the $BCL6^+$ $CXCR5^{hi}$ $PD1^{hi}$ phenotype but are also known to adopt cytokine profiles that are prominent for other lineages [20, 36, 96, 100, 101]. However, both phenotype and function are plastic features since TCR signaling, co-stimulation and local cytokine milieu affect the differentiation of $CD4^+$ T cells, resulting in the same cell type showing different phenotypic profiles in different compartments [19, 36, 101-103]. Thus, e.g. Yeh *et al*. [100] found out that to some extent up to 65 % of T lymphocytes bearing the GC-like phenotype are not resident within the GC. Research during the last few years has provided evidence for T lymphocytes with Tfh cell-like characteristics at different anatomical locations, e.g. lymph node follicle, tonsils, or even circulating in the blood, indicating that the phenotype likely overestimates the true Tfh cell population within the GC [96, 100, 102-106].

We therefore combined laser microdissection and deep sequencing to accurately analyze the Tfh cell repertoire, as the TCR does not change with cellular localization or differentiation [102, 103]. By precisely isolating the GC compartment, it is possible to quantify the definite number of Tfh cell clonotypes that are resident within the GC, and in addition to keep information about the microenvironment they were sampled from. Consequently, the local distribution of T cell clonotypes remains undisturbed and potential loss of cells due to conventional isolation techniques and thus biases in the TCR-R can be avoided [91].

4.3.1. Tfh cells proliferate within the GC

During the GC reaction, B lymphocytes are known to extensively expand while undergoing cycles of proliferation and affinity maturation [27, 28]. However, little is known about the proliferative potential of Tfh cells within the GC. Some studies suggest that only pre-Tfh cells are able to proliferate and stop expanding before GCs have fully developed [19, 100]. In contrast to that, Merkenschlager *et al.* [95] found the expression of proliferation marker Ki67 to be increased for T cells bearing the phenotype of Tfh cells in lymph nodes. In addition, their expression paralleled that of GC B cells and their expansion was shown to be controlled by quality of TCR signaling and interaction with B lymphocytes in response to antigen exposure. Hence, these analyses are giving a hint towards the capability for proliferation of Tfh cells during the peak of GC reaction, though not definitely demonstrating that the analyzed

proliferating Tfh cells are indeed located in the GC. Our analysis of the TCR-R of Tfh cells now highlights that there is also a grown number of GC clonotypes occurring in high copy number fractions (Figure 16B), which is accompanied by a reduced nucleotide coding (Figure 15E). This likewise points towards proliferation, as the copy number that is assigned to a T cell clonotype depends both on its mRNA-load, that will rise due to activation, and on the number of T cell siblings bearing the same TCR, and thus being coded by the same nucleotide sequence [82]. Further quantification of splenic cryosections that were immunofluorescently stained for both T cell marker CD4 and proliferation marker Ki67 finally revealed that more than 70 % of Tfh cells found within the GC are indeed proliferating (Figure 16C+D).

4.3.2. GC clones likely exchange between different splenic compartments

Given the theory that Tfh cell numbers have to be limited to present optimal help to GC B cells [24, 107, 108], the extent of Tfh cells proliferating in the GC is surprising. Hence, we asked if Tfh cells are able to exit the GC and migrate to other anatomical locations where they might likewise take over effector functions. Our methodical approach therefore enables the isolation of two distantly located anatomical units, each containing a single TCZ with surrounding B cell follicles and GCs. Thus, we are even able to determine the relationship between the predominant T cell clonotypes of the different splenic compartments. For this reason, we also switched from amino acid sequence level (= T cell clonotype) to nucleotide sequence level (= T cell clone). Due to the degeneracy of the genetic code, T cells bearing the same TCR amino acid sequence do not necessarily have the same underlying nucleotide sequence, and thus no statement can be made about a potential relationship. Indeed, during our analyses we figured out that e.g. 50 % of T cell clonotypes within the BCZ do not share the same nucleotide sequence as Tfh cell clonotypes within the GC, though carrying an identical TCR on the amino acid level (data not shown). That is why for further investigations we defined that only T cell clones having both the same TCR nucleotide sequence and VJ segment usage can be related at all.

To answer the question of potential migrational behavior of GC Tfh cells, we defined two subsets of Tfh cell clones according to their compartmental distribution (Figure 17): Tfh cell clones that were exclusively present in the GC of origin (GC_{in}), and T cell clones that were also found in at least one other splenic compartment in addition to the original GC (GC_{+out}). In fact, about 80 % of Tfh cell clones were resident in the GC whereas 20 % of GC clones were also identified outside. This subgrouping on a clonal basis provides a more accurate picture of the diverse Tfh cell population, while it also confirms the finding by Yeh *et al.* [100] of GC resident and GC-like migrating Tfh cells that were based on the expression of surface marker CD90. In their study they also mentioned that migrating Tfh-like cells are able to expand continuously. In accordance with this outcome, we found GC_{+out} clones occurring with an overall higher copy number than GC resident ones, illustrating their predominance for activation and thus

expansion (Figure 18C). However, T cell clones that we detected both within and outside the GC showed a higher generation probability, a shorter CDR3 sequence length, and an altered VJ segment usage compared to their GC_{in} counterparts, with all parameters indicating “public” characteristics (Figure 18).

This finding of “public”-like features for T cells within and outside the GC immediately raises the question if this distribution is just a matter of chance, with T cells within different splenic compartments developing independently from each other. Due to biases in recombination processes, certain TCR sequences are favored to be more likely generated than others and thus having a higher chance of autonomously developing at different locations. These sequences are known to more likely feature “public” properties [12, 77, 82, 84]. Thus, the overall naïve TCR-R of the spleen might be that wide-ranging so that antigen-driven selection results in same T cell clones being present in different compartments [97]. However, the features of “public”-like T cell clones are not as pronounced here as seen e.g. for the naïve repertoire within TCZ and BCZ, and the GC is also known to harbor mainly SRBC-specific Tfh cells with “private” properties, especially for high copy clones where we likewise can distinguish between T cell clones in- and outside the GC (see sections 4.1 and 4.2). Furthermore, even when comparing T cell clones of GCs that are only present in one additional compartment with those occurring in the totality of compartments analyzed, despite a significant difference in copy number, no discrepancy in their generation probability can be measured here (Supplement Figure 2). If the occurrence of “GC clones” in other compartments is indeed just a matter of being considered a “public” subgroup, we would have expected the generation probability of the TCR sequences that are present in all compartments to be considerably increased. That is why it is rather unlikely that biases in recombination processes and thus generation probability can exclusively account for finding T cell clones with common TCR sequences both within and outside the GC. Therefore, we expect the allocation of GC Tfh cell-like clones within different splenic compartments to more likely result from exchange between anatomical locations.

For that matter, recent studies have started to illustrate that the Tfh cell repertoire undergoes dynamic changes during the GC reaction [95, 96]. We hypothesized that Tfh cells leave the GC and migrate to other compartments, resulting in the detection of overlapping TCR sequences between the analyzed samples. Therefore, we further investigated the clonal distribution of the defined GC_{+out} subset, of which 30 % to 40 % were detected within neighboring follicles and the adjacent TCZ (Figure 19A). We thereby confirmed and further extended a former study of Shulman *et al.* [96] who analyzed Tfh cell dynamics in murine popliteal lymph nodes. Using photoactivation experiments they have shown that Tfh cells are able to leave the GC and emigrate to neighboring follicles and adjacent GCs within 1 d. In contrast to our analysis, they only rarely detected GC cells migrating to the TCZ. However, the

time frame to analyze photoactivated T cells is very limited [96]. Thus, we can complementarily show that T cell exchange between GCs and neighboring splenic compartments is still measurable 7 d *p.i.* and thus during the peak of GC reaction. In addition, Merkenschlager *et al.* [95] compared the distribution of polyclonal Tfh cell clones in two halves of the spleen 7 d after immunization with 4-hydroxy-3-nitrophenylacetyl-ovalbumin (NP-OVA). By purification and sorting of isolated T cells they have noted that Tfh cells from distant splenic halves share multiple TCR sequences. However, no exact statement was made about the specific compartments that the shared clones were detected in. We now confirmed that GC clones were not only present within neighboring compartments but can be also found in TCZ and BCZs as well as GCs located distantly (Figure 19A). Interestingly, we also detected about 30 % of GC_{+out} clones outside the spleen, attending the mln-repertoire. Since SRBC are a blood-born antigen that induces a quick and locally restricted immune response in the spleen [6, 39, 40, 93], the detection of antigen-specific T cell clones in other lymphatic tissues like the mln is only possible when lymphocytes have entered circulation. Thus, this finding also indicates that T cell exchange between distantly located splenic compartments must take place via the blood. Textor *et al.* [40] already found the number of SRBC-specific TCR sequences identified in the TCZ also expanding in the blood after immunization. They hypothesized that T cell clones proliferating in the TCZ in response to antigen exposure egress to the blood to reach other TCZs. Thus, it is likely that also Tfh cells exit the GC via the surrounding BCZ into the TCZ, from where lymphocytes can egress into circulation by the splenic venous system. In fact, recent research points towards the existence of circulating Tfh cell subsets [102-106]. Their true descendance is not fully clarified yet, but at least some of them are most likely clonally related to GC Tfh cells. Thus, it can be also hypothesized that some of the former GC Tfh cells emigrate to build a pool of circulating memory Tfh cell that can become activated Tfh cells again after rechallenge [104, 109]. In addition, Tfh cells that have left the GC and entered the circulation can likewise join lymphatic tissue again, thus arriving through branches of the central artery and the marginal zone in the splenic TCZ and passing the B cell follicle to finally immigrate into another GC.

Taken together, we conclude that after proliferation within the GC some Tfh cells emigrate to execute effector functions at other locations, even in a distantly located GC. Thereby they might also adopt a circulating profile to facilitate their exchange via the blood, by this likewise enabling their detection within mln. Our analysis highlights that resident and migrating GC Tfh cells might even be distinguishable on a clonal basis.

However, we can not finally exclude the possibility that instead of showing emigrating GC clones, progenies of T cells that have been activated elsewhere, e.g. in the TCZ, separately migrated to distantly located compartments and even independently entered different GCs [97, 102]. In addition, migratory movement might already occur before T cells

have finally differentiated and even before mature GCs have formed [97, 103, 110]. Differentiation of Tfh cells is a multi-step process, requiring the interaction with both DCs and B lymphocytes to finally become a GC Tfh cell. Accordingly, not all antigen-specific T cells are forced to become a Tfh cell, and furthermore, not every pre-Tfh cell might complete its differentiation [19, 36, 97, 100, 101, 103]. These lymphocytes might likewise adopt effector functions outside the GC, albeit sharing the TCR sequence with their “siblings” inside. Nevertheless, many aspects like e.g. a strong proliferation capacity are in favor for the ability of GC Tfh cells to migrate to other anatomical locations. To finally determine the real extent of emigrating and immigrating Tfh cell clones, experiments using barcoding of sequenced TCRs should be added in the future.

4.3.3. Distribution of antigen-specific T cell clones is rather independent of generation probability

To further contextualize the finding of T cell exchange between different splenic compartments, we did not only analyze Tfh cells of GCs, but also investigated T cell clones occurring in BCZs and TCZ. As done for the TCR-R within the GC, the same criterion was used for grouping T cell clones of BCZs and TCZ to define two clonal subsets (Figure 19B+C): T cell clones that were exclusively present in the BCZ or TCZ of origin (BCZ_{in} and TCZ_{in}, respectively), and T cell clones that were also found in at least one other splenic compartment in addition to the original one (BCZ_{+out} and TCZ_{+out}, respectively). Interestingly, almost the same ratio of exclusively resident and shared T cell clones was detected for all comparisons. However, when looking at their appearance in the other compartments, the distributional pattern of T cell clones from BCZs and TCZ clearly contrasts the allocation found for GC clones. While the lowest percentage of BCZ_{+out} and TCZ_{+out} clones was determined for GCs, more T cell clones were found in TCZ and BCZs, regardless of being close or distantly located. The highest number of TCZ and BCZ clones was detected outside the spleen in the mln-repertoire. Thus, it is likely that the opposing distributional pattern of especially TCZ clones follows from differences in the overall composition of T cells present in these compartments. To further investigate this aspect, we analyzed the generation probability of the different clonal subgroups within all compartments, with the found pattern surprisingly being almost the same for GC, BCZ and TCZ clones (Figure 19D-F). While the detected pattern is in line with the distribution of T cell clones identified from BCZ and TCZ, top and bottom levels of P_{gen} are contrary to the found clonal allocation of GC Tfh cell clones. We thus expect this allocation within different splenic compartments to be mostly independent of generation probability, consequently highlighting the distribution of antigen-specific T cell clones that are known to account for the majority of Tfh cells within the GC. Accordingly, about 1,200 T cell clones of the GC have the ability for migrating unlimitedly to other anatomical locations, resulting in their overall uniform distribution. However, this competency does not apply for all T cell clones. In contrast to the GC, the TCZ

harbors a multitude of different T lymphocytes, with GC clones and thus in our case SRBC-specific ones making up only a minor part of the repertoire (~ 1 % of T cell clones within the TCZ). Thus, the allocational pattern found for clones identified from the TCZ likely shows how T cells generally distribute within splenic compartments according to their probability of being generated. In accordance with this finding, the distribution of T cell clones originally detected in the BCZ illustrates a pattern in between, as this compartment is already containing more antigen-specific T cells with an overall increased proliferation capacity than the adjacent TCZ (Supplement Figure 1B). However, more analyses have to be performed to confirm this hypothesis.

4.3.4. Dynamics in the TCR-R during the GC reaction – summing-up the highlights

The GC represents distinctive features among the compartments of lymphatic tissues. Besides harboring a multitude of B lymphocytes undergoing cycles of proliferation and affinity maturation, it also contains T cells that deliver help and provide selection signals to cognate B cells. For splenic GCs, we quantified twice as many T cells than for the adjacent BCZs, however given rise to only a fifth in number of different clonotypes. With about 2,000 different T cell clonotypes with mainly “private”-like characteristics detected within the GC, we nevertheless highlighted the polyclonality of this repertoire. In addition, we showed that the majority of these antigen-specific Tfh cells are able to proliferate and a minor part of the expanding T cell clones might also exit the GC. Our findings imply that these emigrating GC clones enter the circulation to finally arrive at distantly located splenic compartments and even in another GC, where they can likewise adopt effector functions. Thus, the detection of T cell clones within different compartments that share the same TCR with GC Tfh cell clones highlights the distribution of antigen-specific T cells, that we showed to be independent of generation probability.

Taken together, our findings highlight that analyzing GC Tfh cells on a clonal basis provides a detailed insight into the dynamic changes occurring during the GC reaction and even reveals that Tfh cells are likely able to migrate between anatomical locations.

4.4. The effect of sleep on a T cell dependent B cell response

Our findings so far have shown that the repertoire of T lymphocytes is affected by both environmental and genetic stimuli, i.e. in our case the compartment they are located in and their functional status as immunization forms the diversity of the underlying TCR-R. Previous research indicates that also sleep has an important regulatory effect on the immune system, both the innate and the adaptive part, and that sleep deprivation consequently leads to its impairment [reviewed in 46, 59]. Studies investigating the impact of sleep on various immune parameters detected e.g. alterations in cytokine levels and distribution of leukocytes [60, 62, 111-113]. In addition, in their study about sleep boosting immunological memory after vaccination, Lange *et al.* [63] mention that the formation of the immunological synapse determines both quantity and quality of an immune response, thus representing a critical regulatory checkpoint that might be influenced by sleep. Since this formation takes place in SLOs like lymph nodes or spleen, it will be advantageous to analyze the effect of sleep on the site of impact.

We therefore asked if short-term sleep deprivation affects a T cell dependent B cell response within splenic compartments, and thus might especially influence the immunization-induced changes in the underlying TCR-R.

4.4.1. Analyzing key molecules involved in the immune response

Hence, we first started our analysis under steady-state conditions by monitoring the mRNA-expression of a set of genes that are involved in key functions of T and B lymphocytes, commencing at 3 d when first alterations in the TCR-R had been identifiable.

4.4.1.1. Shortly after immunization-induced activation of lymphocytes, cell interactions are reduced during the first proliferation period 3 d after SRBC-injection

To assess lymphocyte activation, we determined the expression levels of *ciita* and *zap70*.

The class II MHC transactivator CIITA is a complex, short-lived protein that is expressed on APCs like DCs or B lymphocytes. It is the master regulator of the expression of MHC class II genes and also acts as a transcription factor for many other immunologically important genes [114-116]. Fundamental downstream functions include the presentation of antigenic peptides and the consequent activation and proliferation of cognate T lymphocytes [64, 115].

As the TCR engages with the specific pMHC complex, signal transduction within the T cell is activated. Since the TCR has no intrinsic enzymatic activity, signaling is based on additional molecules [14, 117]. By forming an immunological synapse between the pMHC and the TCR complex, including co-receptors like CD3 and CD4, the lymphocyte-specific protein tyrosine kinase Lck is positioned near this complex [117-120]. Lck is thus forced to phosphorylate the tyrosines of immunoreceptor tyrosine-based activation motifs (ITAMs) of the zeta chain,

consequently setting up a docking site for ZAP70. ZAP70 is a tyrosine kinase that usually exists in an autoinhibited form in the cytoplasm, but ITAM phosphorylation results in the recruitment of ZAP70 to the TCR complex, where it is also activated and stabilized by phosphorylation via Lck. Activated ZAP70 consequently phosphorylates downstream molecules like linker of activated T cell (LAT), thus continuing this signaling cascade and causing the activation of the T lymphocyte [117-119, 121, 122].

Both in the naïve state and 3 d after SRBC-injection, we only detected differences in the compartmental distribution of cells expressing *ciita* and *zap70*, i.e. APCs and T lymphocytes, respectively, but no effects of immunization (Figure 20A and Supplement Table 1). It might be reasonable that both *ciita* and *zap70* expression returned to baseline levels once the first activation period is completed, as presentation of antigenic peptides and subsequent triggering of TCR signaling usually debuts early after antigen uptake, presumably within the first 24 h [107]. In addition, especially the expression of MHC class II genes is regulated strongly depending on the cell's immunological status, and it e.g. has been shown that the expression of *ciita* is actively silenced during the terminal differentiation of B lymphocytes into antibody producing plasma cells [114, 116]. Thus, 3 d after immunization with SRBC when T cell proliferation is known to peak in the TCZ and also expansion of B cells reaches its first maximum [91, 123], mRNA-expression of activation markers might be already flattened.

The interaction of T cells and APCs is not restricted to the entanglement of TCR and pMHC. Different co-stimulatory molecules are involved in forming the immunological synapse as well as in initiating and maintaining a humoral immune response [37, 124, 125]. Thus, we assessed the mRNA-expression of two genes coding for important co-stimulatory molecules, *cd40lg* and *icoslg*.

CD40 is constitutively expressed on APCs like DCs, B cells and macrophages, while its ligand, the transmembrane protein CD40L, also known as CD154, is transiently expressed on primarily activated T cells, especially the $CD4^+$ subset [91, 107, 126-128]. Like CD40L, ICOS is induced on activated T lymphocytes, while it contacts with ICOSL that is constitutively expressed on APCs [93, 99, 124, 125, 129, 130]. Whereas CD40-CD40L interactions provide contact-dependent help, ICOS-ICOSL interactions ensure the entangled mode of the immunological synapse with short but extensive surface engagement between both cell types. Accordingly, a positive feedback loop between CD40L- and ICOS-dependent signals promotes the functional exchange of stimulatory signals [23, 36, 129].

Interestingly, while the differences detected between TCZ and BCZ are likely caused by the different numbers of *cd40lg* or *icoslg* expressing cells within the compartments, the mRNA-expression levels of these co-stimulatory molecules were significantly reduced 3 d after SRBC-injection compared to the naïve state (Figure 20B and Supplement Table 1).

Since expression of CD40L is directly regulated as response of TCR activation, its maximum mRNA-level is already reached within 6 h of constant stimulation [107]. Accordingly, the expression returned back to baseline levels after 12 h, as above all a high degree of mRNA decay shortly after T cell activation was noted [107], that still is reflected in the detected decline 3 d *p.i.* Furthermore, ICOS-ICOSL engagement is known to directly affect the differentiation of T lymphocytes and thus their bipolarization into Tfh cells or effector T cells [99, 130]. Our findings of reduced mRNA-expression of both markers *cd40lg* and *icoslg* at this time point might consequently not only reflect a decline in cell interactions during the proliferation period, but also provide evidence for the differential status of the predominant lymphocytes. As both timing and level of induced signaling affects the fate of T and B cells [126, 130, 131], it might be assumed that expression rates are lowered to primarily induce a first wave of SRBC-specific effector lymphocytes. We in fact not only noticed a significant reduction for *cd40lg* and *icoslg*, but also for Tfh cell migration marker CXCR5 gene *cxcr5* (data not shown), whose induction is regulated by ICOS signaling [130]. Priming of T cells by DCs initiates signaling of ICOS that in turn induces the induction of BCL6, the major transcription factor of Tfh cells. BCL6 thus inhibits the expression of PR domain zinc finger protein 1 (*prdm1*) gene that is coding for the BCL6-antagonist and major transcription factor of effector T and B cells, BLIMP1. In addition, it also promotes the induction of CXCR5 and hence both differentiation and subsequent migration of Tfh cells into the follicle [130]. As minimized ICOS-signaling, as seen 3 d after SRBC-injection, impedes BCL6-induction and thus differentiation of Tfh cells, T lymphocytes might be primarily pushed into the effector cell lineage. In accordance with this, not only *icoslg* and *cxcr5* mRNA-expression was significantly reduced, but we also found a tendency for increased expression of effector lineage marker *prdm1* 3 d after immunization that became significant one day later (data not shown).

Another important modification tool for humoral immune responses is glycosylation. This enzymatic process defines the post-translational modification of surface glycans where glycosyltransferases build glycosyl linkages between these polysaccharides and other molecules like proteins or lipides [132-134]. We therefore analyzed the mRNA-expression of genes coding for two important glycosyltransferases which are transferring galactose and sialic acid to glycans, respectively, i.e. *b4galt1* and *st6gal1*.

We do not detect any differences in the compartmental distribution of their mRNA-expression, neither in the naïve state nor 3 d after SRBC-injection (Figure 20C and Supplement Table 1), as both enzymes are constitutively expressed in most tissues and thus are not specific to certain types of immune cells [135, 136]. Nevertheless, the diverse repertoire of glycans can be changed as response to environmental and genetic stimuli and thus during development, activation and differentiation of all possible cell types [132, 133]. It is highly linked to the function of immune cells and consequently involved in the regulation of key sites in T cell and

B cell biology. Glycosylation not only effectuates post-translational modifications of TCR and BCR and hence is involved in selection processes during thymocyte development, the consequent discrimination of self and non-self, as well as modifications of antibodies, but also modifies cell-cell-interactions by affecting cell adhesion and trafficking as well as the stability of the immunological synapse [132-134, 137-141]. These functions do not depend on a specific type of glycan, but rather rely on the corresponding glycoprotein and their interaction with other molecules [133]. However, the fact that *b4galt1*- and *st6galt1*-expression and thus the induction of glycosyltransferases that are known to affect cell contacts by regulating their adhesion capability are showing constant levels 3 d *p.i.* as well, further confirms the former assumption that the interaction between immune cells is reduced during the proliferation period.

4.4.1.2. Immunization facilitates activation, interaction and modification of T and B lymphocytes during the GC response 7 d after SRBC-injection

While we detected a decline in immune cell activation and interaction 3 d after SRBC-injection by analyzing the mRNA-expression of genes coding for key molecules of T and B lymphocytes, deep sequencing revealed that immunization already started to form the underlying TCR-R, resulting in profound alterations a few days later. Accordingly, we did not only find major changes in the TCR-R during the peak of GC reaction at 7 d, but also detected differences in the expression of all genes analyzed. Due to the fact that the GC reaction is known to be the driver of the ongoing T cell dependent B cell response that requires both successful activation of and effective interaction between T and B lymphocytes [23, 27, 28, 36], immunization with SRBC induces a significant increase in mRNA-expression levels here (Figure 21 and Supplement Table 2).

While the priming of T lymphocytes first primarily takes place by DCs when cognate B cells are still rare, the increased number of antigen-specific B lymphocytes due to extensive clonal expansion within the GC causes a transition in presenting antigenic peptides to appropriate T cells [100, 101, 126, 130]. Accordingly, a higher amount of *ciita* is found especially in the BCZ, hence inducing the expression of MHC class II genes. As B lymphocytes co-localize with Tfh cells, engagement of pMHC and TCR complex results in the activation of T cells by stimulating TCR signal transduction [126], seen in increased *zap70* mRNA-levels. Increased TCR signaling and thus *zap70*-expression is of course not only limited to Tfh cells, but also present for T lymphocytes accumulating in the TCZ. While priming and activation of T and B cells can be independent of CD40 and ICOS, co-stimulatory signals are important to maintain, pursue and strengthen humoral immune responses, i.e. Tfh cell differentiation, B cell expansion and consequent GC formation and affinity maturation [81, 126, 130, 131]. In contrast to the first proliferation period 3 d after immunization with SRBC, *cd40lg*- and *icoslg*-expression are significantly increased during the GC reaction, emphasizing the importance of T cell –

B cell interactions here [93, 126]. In addition, restimulation of T cells with cognate antigenic peptides is known to stabilize CD40L's transcript stability and thus prevents the aforementioned decay occurring shortly after activation [107]. Furthermore, CD40L-mediated stimulation is particularly crucial when antigen availability fades at later stages of the immune response [127]. Absence of CD40/CD40L or ICOS/ICOSL thus results in smaller and less efficient GCs as well as impaired development of Tfh cells and GC B cells [91, 93, 99, 123, 126]. In addition, increased mRNA-levels for genes coding for glycosyltransferases that are known to modify cell interactions underly these findings. Via B4GALT1 galactosylated glycans are commonly recognized by selectins, thus promoting both adhesion, interaction and cell trafficking [132, 138, 139, 142, 143]. The expression of *b4galt1* was indeed shown to correlate with adhesion of $CD4^+$ T cells [142], which is in line with increased levels found especially in the TCZ. ST6GAL1 also promotes cell adhesion and communication but is also known to modulate the threshold of BCR activation by providing sialylated ligands for CD22, an inhibitory receptor for BCR signaling [132, 139, 141]. Aside from that, the inflammatory grade correlates with the degree of sialylated Ig antibodies [132, 141]. Hence, ST6GAL1 plays a pivotal role in B cell biology, likely explaining the increased expression of *st6gal1* in the BCZ during the peak of GC reaction.

Taken together, after initial activation of lymphocytes, the interaction of immune cells seems to be flattened during the first proliferation period of a primary immune response against SRBC, whereas an ongoing GC reaction requires extensive contact-dependent help between T and B lymphocytes. Accordingly, activation of and interaction between these cells is significantly increased at the 7 d timepoint, resulting in their clonal expansion that we are also able to see in our analysis of the TCR-R.

4.4.2. Short-term sleep deprivation dampens important T cell functions like TCR signaling and trafficking during the peak of GC reaction

As we now gained detailed knowledge about how immunization influences key molecules of a T cell dependent B cell response within the different splenic compartments, we were able to go a step further by analyzing the impact of sleep on these parameters.

We therefore subjected mice to 6 h of sleep deprivation after SRBC-injection, and thus during the time of formation of the immunological synapse [37, 41], to monitor if the current sleep status impacts both the predominant splenic milieu and the underlying TCR-R that is induced by immunization. Previous studies have shown that neither injection nor sleep deprivation induces significant levels of stress [41], thus the results obtained in this work are rather the consequence of being sleep-deprived than representing methodical artifacts.

While no differences in the expression of genes that are relevant for key functions of T and B cell biology were detected in the naïve state or 3 d *p.i.* (data not shown), sleep deprivation

resulted in changes at the peak of GC reaction. The immunization-induced increase in expression of *zap70* and *b4galt1* that was present at 7 d, was lowered back to naïve like levels in sleep-deprived animals (Figure 22 and Supplement Table 3).

By reducing expression levels and thus likely also diminishing the amount of functional protein, sleep deprivation might have profound effects on various T cell features occurring downstream of ZAP70 and B4GALT1 functions. These findings can be added to previous work mentioning an effect of sleep deprivation on both distribution and function of T cells. It has been predicted that sleep facilitates the recruitment of lymphocytes to SLOs, thus supporting the interaction of APCs with cognate T cells [52, 59, 60, 111, 112]. Impaired leukocyte trafficking, as indicated by a reduced expression of *b4galt1* for sleep-deprived animals, might consequently result in fewer cells being found within the spleen compared to normal sleep and thus impeding the formation of an immunological synapse here [134, 139]. In line with this, a few studies detected an increased number of circulating T cells and thus a reduced tissue homing after sleep deprivation [60, 62, 111-113]. In addition, ZAP70 is also involved in the control of the T lymphocytes mobility and of the formation of functional immunological synapses [119, 120]. Reduced *zap70*-expression and thus impaired T cell signaling after shortened sleep duration might consequently show that sleep not only affects the development of the immunological synapse but also its functions [119]. As both ZAP70 and B4GALT1 are involved in processes causing the activation and thus also proliferation of T lymphocytes [117, 120, 142], minor levels might likewise lead to a reduction in important downstream functions. A lowered proliferation capability after sleep deprivation was indeed noticed by some studies [144, 145].

Furthermore, deficiency of functional tyrosine kinase ZAP70 and galactosyltransferase B4GALT1 is known to fatally impact various parameters of a T cell dependent B cell response that might boost serious diseases. For example, mice deficient for ZAP70 or lacking functional proteins due to mutations do not only show severed T cell signaling with e.g. reduced Ca^{2+} concentrations, but it has also been shown that T cell development is blocked, resulting in dysfunctional $CD4^+$ or absent peripheral $CD8^+$ T cells as well as augmented autoreactive T lymphocytes [117-119, 121]. Accordingly, abnormal levels of ZAP70 can be related to autoimmune diseases [121]. As cell – cell interactions are important for a multitude of different lymphocyte functions, and its decrease might hence cause serious consequences, B4GALT1-defiency was shown to result in reduced recruitment of leukocytes and thus impairment of both acute and chronic inflammatory responses [132, 142, 146]. In addition, decelerated growth and increased lethality of mice with knockout mutations highlight the importance of glycosylation for a variety of immune functions [136], and abnormal levels of B4GALT1 as well as mutations in the respective gene are even able to induce the pathology of certain diseases [132, 147]. Thus, reducing the duration of sleep periods might cause similar consequences.

However, though we are not able to make a statement about the continuing effects yet, finding changes in the mRNA-expression of functionally important genes that are even still noticeable 7 d after merely short-term sleep-deprivation, is impressive.

4.4.3. Short-term sleep deprivation does not affect the TCR-R recruited into the immune response

Detecting flattened expression levels in sleep-deprived mice for *zap70* and *b4galt1* which are coding for proteins regulating crucial T cell features, legitimates to additionally investigate if short-term sleep deprivation might also have an effect on the composition of the TCR-R.

Despite thoroughly checking TCZ, BCZ and GC separately and using our in-depth analysis tool of both fractioning the clonotypes according to their copy number and determining sensitive sequence parameters, we did not detect any differences in the underlying TCR-R between sleep-deprived mice and control animals, neither 3 d (data not shown) nor 7 d after SRBC-injection (Figure 23). Immunization likewise reduced the number of different T cell clonotypes and induced a shift to high copy number fractions with same changes in sequence characteristics occurring for both groups, i.e. high copy “private” SRBC-specific T cells replacing the former predominant “public” naïve lymphocytes (confer section 4.2). Thus, we have to assume that short-term sleep deprivation does not affect the TCR-R in this manner, thereby confirming our previous findings for whole splenic slices [41, 94].

However, it might be quite possible that T lymphocytes at the peak of GC reaction are rather affected by qualitative changes than by quantitative ones. We can not entirely exclude the possibility that the affinity of the T cell clonotypes might be affected by sleep, even though this might be at least slightly visible in their distribution throughout the fractions within the GC. Another possibility would be that sleep deprivation only changes the functional state of the responding T lymphocytes and thereby e.g. facilitating their transition into a state of unresponsiveness. The induction of this phenomenon called anergy is known to be strongly dependent on TCR signaling strength and thus on signal transduction via functional ZAP70, as it shall prevent peripheral autoreactive cells [121]. In accordance with this, ZAP70-deficiency is associated with dysfunctional $CD4^+$ T cells [117-119] which might be possible here as well since these lymphocytes might share the same TCR sequence like functional ones and thus impeding their detection with our analysis tool.

Furthermore, the effects induced by short-term sleep deprivation might be too subtle to be found within the whole repertoire, and the high dosed injection of SRBC might even mask possible dampening effects. This has already been noted as ceiling effect by Tune *et al.* [41] even though they have only analyzed whole splenic sections instead of separately looking at different compartments with more specific analytical methods.

However, although finding changes in the mRNA-expression of genes induced by sleep deprivation that are still measurable 7 d later, the effect might not be one-to-one transferable to functional differences occurring on the protein level and thus possibly effecting the repertoire. There are of course more options possible, like post-translational modifications that might affect the final outcome of this immune response, and even the presence of other molecules that might take over corresponding effector functions to compensate dampening effects.

In addition, finding different changes when inverting the order of sleep deprivation and immunization [94] highlights the complexity of regulatory mechanisms that control a T cell dependent B cell response and thus possible checkpoints sleep might be able to affect. Consequently, addressing effects of sleep on the immune system is a complicated field of research, with minimal changes in study protocols resulting in profound differences. Duration of sleep deprivation period, timepoint and location of sampling as well as type of immunization are some of many factors that strongly influence the potential outcome [reviewed in 46]. Accordingly, it is hard to directly compare studies analyzing sleep effects and many different results can be found, reaching from no effects on lymphocytes to impaired reaction to pathogens after sleep deprivation [148-152]. While humans can be easily asked to stay awake for whole nights, extending the sleep deprivation periods in mice might result in the induction of stress and thus a complication in correctly working out possible effects of sleep. This of course might be a small disadvantage in our study since 6 h of sleep deprivation might be too short to induce measurable effects e.g. in the TCR-R.

But taken together, our analysis indicates that even short-term sleep deprivation affects certain aspects of a T cell dependent B cell response during the peak of GC reaction and further investigations like e.g. focusing on T cell subsets like Tfh cells or their migrational pattern might reveal more insides into the exact regulatory mechanisms.

4.5. Concluding remarks and perspectives

For the first time, our studies reveal an extensive insight into the TCR-R of splenic compartments both within the naïve state and after immunization with a complex, non-replicating blood-born antigen. Using an in-depth analysis tool, we were not only able to characterize the different T cell clonotypes present within the TCZ, but also to demonstrate that the repertoire of the BCZ, consisting of both “public” and “private” TCR sequences, is similarly affected by injection of high dosed SRBC. Although we already have shown for whole splenic slices that SRBC cause the induction of T cell clonotypes with mainly “private” characteristics [41, 74, 94], the results are not one-to-one transferable to compartmental analysis. Even the repertoire found for the TCZ, though containing the largest number of T lymphocytes and thus being the most suitable for comparisons, does not fully reflect the results detected in former studies [41, 74, 94]. This clearly emphasizes the importance of locally analyzing splenic compartments to get an entire picture of the TCR-R that is recruited into an immune response. In addition, while we so far simply tested the parameters for size dependency and used the fractioning strategy to prevent biases, further extensive analyses like e.g. statistical simulations should proof the whole extent of size versus biological effect. However, we also highlight that the GC, though being limited in size, harbors a multitude of antigen-specific Tfh cells. These lymphocytes are also able to migrate to other compartments and even enter distantly located GCs, thus shaping the underlying TCR-R and facilitating a polyclonal immune response. Furthermore, one might argue that these findings are only due to the use of SRBC as antigen that offers a huge number of different epitopes to respond at [42, 43, 91, 93]. But injecting mice with ovalbumin (OVA) solved in alum, and thus a substantially smaller antigen [153, 154], also results in an immune response that is primarily built by “private” T cell clonotypes that show the same characteristical sequence patterns within the splenic compartments (data not shown).

The knowledge we gained by analyzing both the TCR-R and the predominant microenvironment of the splenic compartments as well as the basic hints towards Tfh cell migrational behavior can be of consequence for further investigations, e.g. regarding autoimmune diseases that are known to play a major role in today’s society. A diverse TCR-R is important to ensure sufficient protection against invading pathogens, but autoimmunity likely results in its restriction [155-158]. One of the most common neuro-inflammatory diseases in early adulthood is multiple sclerosis (MS) with inflammation, demyelination and axonal loss of the central nervous system (CNS) as typical hallmarks [159-161]. T lymphocytes are one of the key players in MS, as myelin-specific T cells become reactivated by recognition of its self-antigen in the CNS, triggering the recruitment of innate immune cells that can mediate the aforementioned axonal damage [160-162]. In the spleen, phenotypic changes of autoreactive T cells take place, which allow them to transgress the blood-brain-barrier, representing an

important step in the course of disease [162-165]. In addition, these lymphocyte infiltrates within the CNS sometimes also are involved in forming kind of tertiary lymphatic organs at later disease stages [166-168]. Therefore, it can be of note to transfer our fundamental knowledge about the TCR-R within the splenic compartments and its ability to exchange due to migration of antigen-specific lymphocytes to those ectopic lymphoid structures in experimental autoimmune encephalomyelitis (EAE), an MS animal model [161, 169], thereby testing for possible checkpoints to interfere in the course of disease. Transferring our specific analyzing methods to other anatomical locations might moreover be advantageous for disease therapies as clinical alterations can be identified very early, thus e.g. helping to prevent relapses in MS or ensuring lower pharmaceutical dose rates. Furthermore, as sleep disorders and an increased risk of developing autoimmune diseases are supposed to be associated [66, 170, 171], our findings regarding the impact of shortened sleep duration on parameters influencing the T cell dependent B cell response within the spleen might be as well useful to be considered for future investigations.

5. Supplement

Supplement Table 1: Statistical results of gene expression analysis, investigating possible effects of compartment and immunization status 3 d after SRBC-injection.

Gene	Tested effect	p-value
ciita	immunization	0.072
	compartment	**0.00000001**
	interaction	0.449
zap70	immunization	0.125
	compartment	**0.00000291**
	interaction	0.516
cd40lg	immunization	**0.036**
	compartment	**0.0000000000682**
	interaction	0.272
icoslg	immunization	**0.000409**
	compartment	**0.0000279**
	interaction	0.118
b4galt1	immunization	0.307
	compartment	0.114
	interaction	0.743
st6gal1	immunization	0.119
	compartment	0.096
	interaction	0.544

Two-way ANOVA was performed for each gene. Significant p-values highlighted using bold print.

Supplement Table 2: Statistical results of gene expression analysis, investigating possible effects of compartment and immunization status 7 d after SRBC-injection.

Gene	Tested effect	p-value
ciita	immunization	**0.031**
	compartment	**0.0000668**
	interaction	0.589
zap70	immunization	**0.043**
	compartment	**0.000815**
	interaction	0.193
cd40lg	immunization	**0.000435**
	compartment	**0.000444**
	interaction	**0.008**
icoslg	immunization	**0.002**
	compartment	**0.005**
	interaction	0.508
b4galt1	immunization	**0.012**
	compartment	**0.002**
	interaction	0.484
st6gal1	immunization	**0.00016**
	compartment	0.061
	interaction	0.651

Two-way ANOVA was performed for each gene. GC compartment excluded from calculations. Significant p-values highlighted using bold print.

Supplement Table 3: Statistical results of gene expression analysis, investigating possible effects of compartment, immunization, and sleep status 7 d after SRBC-injection.

Gene	Tested effect	p-value	
zap70	immunization	**0.046**	
	compartment	**0.000000181**	
	sleep(deprivation)	**0.011**	
	interaction		
	immunization – compartment	0.195	
	interaction		
	immunization – sleep(deprivation)	**0.029**	
		within PBS	0.843
		within SRBC	**0.001**
	interaction		
	compartment – sleep(deprivation)	0.112	
	interaction		
	immunization – compartment – sleep(deprivation)	0.187	
b4galt1	immunization	**0.014**	
	compartment	**0.000000175**	
	sleep(deprivation)	**0.033**	
	interaction		
	immunization – compartment	0.173	
	interaction		
	immunization – sleep(deprivation)	**0.02**	
		within PBS	0.798
		within SRBC	**0.002**
	interaction		
	compartment – sleep(deprivation)	0.948	
	interaction		
	immunization – compartment – sleep(deprivation)	0.931	

Three-way ANOVA was performed for each gene. GC compartment excluded from calculations. Significant p-values highlighted using bold print.

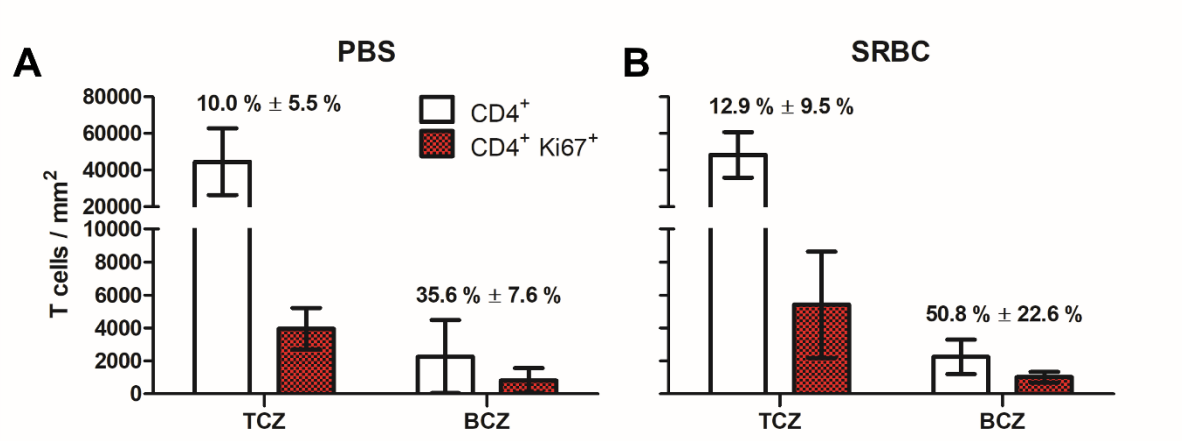

Supplement Figure 1: Proliferating T cells in TCZ and BCZ of naïve and immunized mice.
Splenic cryosections were immunofluorescently stained for T cells ($CD4^+$) and proliferating cells (Ki67). Quantification with ImageJ was performed to assess number of proliferating T cells in T cell zone (TCZ) and B cell zone (BCZ) for **(A)** naïve and **(B)** immunized mice 7 days (d) after SRBC-injection (n = 4 each). Displayed are means and standard deviations. Numbers above the graphs indicate percentage of proliferating $CD4^+$ T cells. CD – cluster of differentiation.

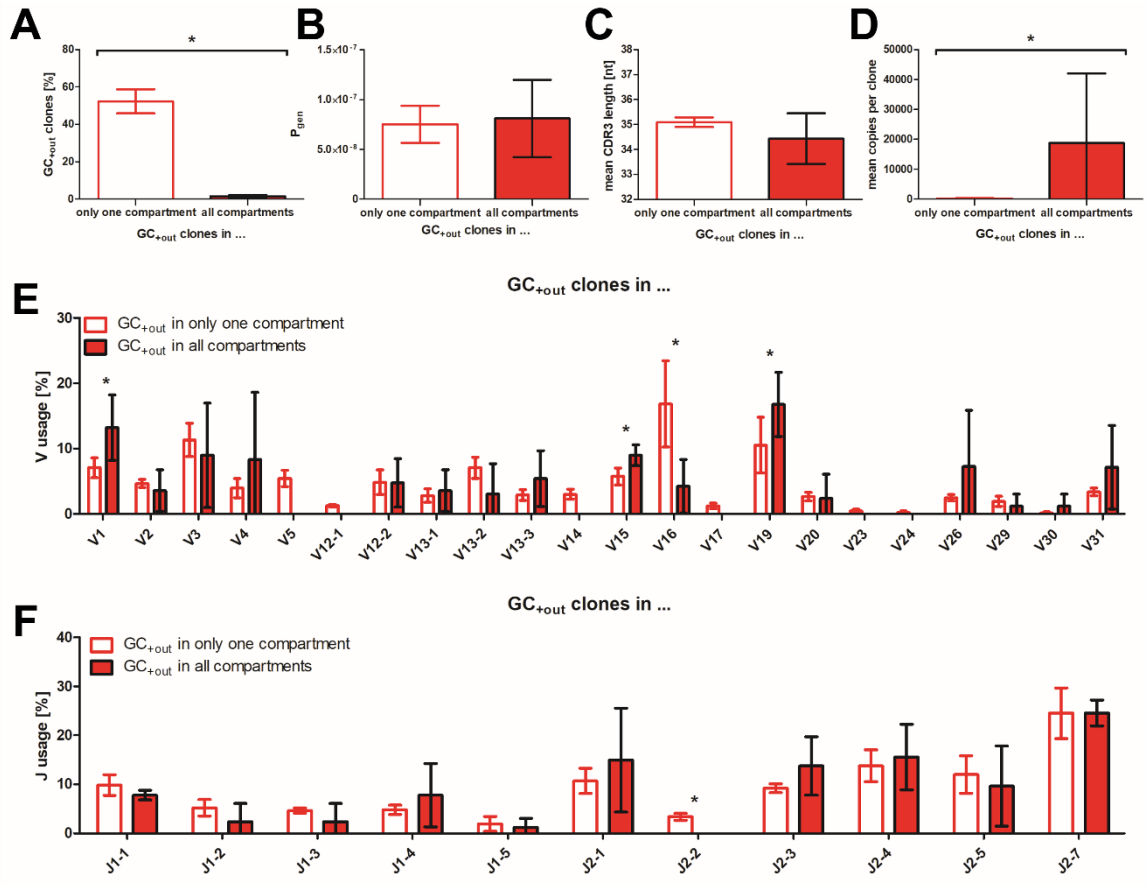

Supplement Figure 2: Distribution of GC clones is independent of generation probability.
Deep sequencing of the complementary determining region 3 (CDR3) β chain of splenic compartments was performed, i.e. T cell zone (TCZ), B cell zone (BCZ) and germinal center (GC), with two independent compartments each being isolated. Each T follicular helper (Tfh) cell clone was tested to be also present in at least one of the remaining compartments and thus denoted as "GC_{+out}". Those clones were further divided into subgroups according to their distribution: Tfh cell clones only occurring in one single compartment besides GC of origin on the one hand, and Tfh cell clones found in all six compartments analyzed on the other hand. **(A)** Percentage of Tfh cell clones found in these subgroups in relation to total number of Tfh cell clones found outside the GC (GC_{+out}), **(B)** generation probability, **(C)** mean length and **(D)** copy number of respective CDR3β nucleotide sequences as well as distribution of used **(E)** V and **(F)** J segments were determined 7 days (d) after SRBC-injection (n = 6). Displayed are means and standard deviations. Data were analyzed using Mann-Whitney-U, with * $p < 0.05$ indicating significant differences between Tfh cell subgroups. nt – nucleotides; P_{gen} – generation probability.

References

1. Murphy K and Weaver C (2016). *Janeway's immunobiology*. Garland science, 9th ed.

2. Schütt C and Bröker B (2011). *Grundwissen Immunologie*. Springer, 3rd ed.

3. Westermann J (2010). *Organe des Abwehrsystems*. In: *Anatomie*. Springer, 355-375.

4. Ruddle NH and Akirav EM (2009). *Secondary lymphoid organs: responding to genetic and environmental cues in ontogeny and the immune response.* J Immunol, 183(4): 2205-2212.

5. Westermann J, Engelhardt B and Hoffmann JC (2001). *Migration of T cells in vivo: molecular mechanisms and clinical implications.* Ann Intern Med, 135(4): 279-295.

6. Van den Eertwegh AJ, Boersma WJ and Claassen E (1992). *Immunological functions and in vivo cell-cell interactions of T cells in the spleen.* Crit Rev Immunol, 11(6): 337-380.

7. Westermann J and Pabst R (1992). *Distribution of lymphocyte subsets and natural killer cells in the human body.* Clin Investig, 70(7): 539-544.

8. Kurosaki T, Kometani K and Ise W (2015). *Memory B cells.* Nat Rev Immunol, 15(3): 149-159.

9. Milićević NM and Westermann J (2016). *Lymph Node Structure*. In: *Encyclopedia of Immunobiology*. Ratcliffe MJH, Editor. Academic Press, 413-419.

10. Arstila TP, Casrouge A, Baron V, Even J, Kanellopoulos J and Kourilsky P (1999). *A direct estimate of the human alphabeta T cell receptor diversity.* Science, 286(5441): 958-961.

11. Nikolich-Zugich J, Slifka MK and Messaoudi I (2004). *The many important facets of T-cell repertoire diversity.* Nat Rev Immunol, 4(2): 123-132.

12. Trofimov A, Brouillard P, Larouche JD, Séguin J, Laverdure JP, Brasey A, Ehx G, Roy DC, Busque L, Lachance S, Lemieux S and Perreault C (2022). *Two types of human TCR differentially regulate reactivity to self and non-self antigens.* iScience, 25(9): 104968.

13. Laydon DJ, Bangham CR and Asquith B (2015). *Estimating T-cell repertoire diversity: limitations of classical estimators and a new approach.* Philos Trans R Soc Lond B Biol Sci, 370(1675).

14. Gaud G, Lesourne R and Love PE (2018). *Regulatory mechanisms in T cell receptor signalling.* Nat Rev Immunol, 18(8): 485-497.

15. Zhu J, Yamane H and Paul WE (2010). *Differentiation of effector CD4 T cell populations (*).* Annu Rev Immunol, 28: 445-489.

16. King C, Tangye SG and Mackay CR (2008). *T follicular helper (TFH) cells in normal and dysregulated immune responses.* Annu Rev Immunol, 26: 741-766.

17. Constant SL and Bottomly K (1997). *Induction of Th1 and Th2 CD4+ T cell responses: the alternative approaches.* Annu Rev Immunol, 15: 297-322.

18. Dong C (2011). *Genetic controls of Th17 cell differentiation and plasticity.* Exp Mol Med, 43(1): 1-6.

19. Schroeder AR, Zhu F and Hu H (2021). *Stepwise Tfh cell differentiation revisited: new advances and long-standing questions.* Fac Rev, 10.

20. Cho YL, Flossdorf M, Kretschmer L, Höfer T, Busch DH and Buchholz VR (2017). *TCR Signal Quality Modulates Fate Decisions of Single CD4(+) T Cells in a Probabilistic Manner.* Cell Rep, 20(4): 806-818.

21. Nakayama T and Yamashita M (2010). *The TCR-mediated signaling pathways that control the direction of helper T cell differentiation.* Semin Immunol, 22(5): 303-309.

22. Yamane H and Paul WE (2013). *Early signaling events that underlie fate decisions of naive CD4(+) T cells toward distinct T-helper cell subsets.* Immunol Rev, 252(1): 12-23.

23. Qi H (2016). *T follicular helper cells in space-time.* Nat Rev Immunol, 16(10): 612-625.

24. Crotty S (2014). *T follicular helper cell differentiation, function, and roles in disease.* Immunity, 41(4): 529-542.

25. Zhang X, Ing S, Fraser A, Chen M, Khan O, Zakem J, Davis W and Quinet R (2013). *Follicular helper T cells: new insights into mechanisms of autoimmune diseases.* Ochsner J, 13(1): 131-139.

26. *Servier Medical Art*. Available from: smart.servier.com.

27. Mesin L, Ersching J and Victora GD (2016). *Germinal Center B Cell Dynamics.* Immunity, 45(3): 471-482.

28. Victora GD and Nussenzweig MC (2012). *Germinal centers.* Annu Rev Immunol, 30: 429-457.

29. Okada T, Miller MJ, Parker I, Krummel MF, Neighbors M, Hartley SB, O'Garra A, Cahalan MD and Cyster JG (2005). *Antigen-engaged B cells undergo chemotaxis toward the T zone and form motile conjugates with helper T cells.* PLoS Biol, 3(6): e150.

30. Vinuesa CG, Tangye SG, Moser B and Mackay CR (2005). *Follicular B helper T cells in antibody responses and autoimmunity.* Nat Rev Immunol, 5(11): 853-865.

31. Heesters BA, Myers RC and Carroll MC (2014). *Follicular dendritic cells: dynamic antigen libraries.* Nat Rev Immunol, 14(7): 495-504.

32. Nurieva RI, Chung Y, Martinez GJ, Yang XO, Tanaka S, Matskevitch TD, Wang YH and Dong C (2009). *Bcl6 mediates the development of T follicular helper cells.* Science, 325(5943): 1001-1005.

33. Yu D, Rao S, Tsai LM, Lee SK, He Y, Sutcliffe EL, Srivastava M, Linterman M, Zheng L, Simpson N, Ellyard JI, Parish IA, Ma CS, Li QJ, Parish CR, Mackay CR and Vinuesa CG (2009). *The transcriptional repressor Bcl-6 directs T follicular helper cell lineage commitment.* Immunity, 31(3): 457-468.

34. Vogelzang A, McGuire HM, Yu D, Sprent J, Mackay CR and King C (2008). *A fundamental role for interleukin-21 in the generation of T follicular helper cells.* Immunity, 29(1): 127-137.

35. Ballesteros-Tato A, León B, Graf BA, Moquin A, Adams PS, Lund FE and Randall TD (2012). *Interleukin-2 inhibits germinal center formation by limiting T follicular helper cell differentiation.* Immunity, 36(5): 847-856.

36. Crotty S (2011). *Follicular helper CD4 T cells (TFH).* Annu Rev Immunol, 29: 621-663.

37. Huppa JB and Davis MM (2003). *T-cell-antigen recognition and the immunological synapse.* Nat Rev Immunol, 3(12): 973-983.

38. Lagrange PH, Mackaness GB and Miller TE (1974). *Influence of dose and route of antigen injection on the immunological induction of T cells.* J Exp Med, 139(3): 528-542.

39. Stamm C, Barthelmann J, Kunz N, Toellner KM, Westermann J and Kalies K (2013). *Dose-dependent induction of murine Th1/Th2 responses to sheep red blood cells occurs in two steps: antigen presentation during second encounter is decisive.* PLoS One, 8(6): e67746.

40. Textor J, Fähnrich A, Meinhardt M, Tune C, Klein S, Pagel R, König P, Kalies K and Westermann J (2018). *Deep Sequencing Reveals Transient Segregation of T Cell Repertoires in Splenic T Cell Zones during an Immune Response.* J Immunol, 201(2): 350-358.

41. Tune C, Meinhardt M, Kalies K, Pagel R, Schierloh LK, Hahn J, Autenrieth SE, Koch CE, Oster H, Schampel A and Westermann J (2020). *Effects of sleep on the splenic milieu in mice and the T cell receptor repertoire recruited into a T cell dependent B cell response.* Brain Behav Immun Health, 5: 100082.

42. Geng T, Guan X and Smith EJ (2015). *Screening for genes involved in antibody response to sheep red blood cells in the chicken, Gallus gallus.* Poult Sci, 94(9): 2099-2107.

43. Yamanaka H and Takeyoshi M (2016). *Identification of sheep red blood cell (SRBC) surface immune-responsive peptides detected by antisera from SRBC-immunized rats.* J Toxicol Sci, 41(1): 13-16.

44. Loetsch C, Warren J, Laskowski A, Vazquez-Lombardi R, Jandl C, Langley DB, Christ D, Thorburn DR, Ryugo DK, Sprent J, Batten M and King C (2017). *Cytosolic Recognition of RNA Drives the Immune Response to Heterologous Erythrocytes.* Cell Rep, 21(6): 1624-1638.

45. Lange T, Dimitrov S and Born J (2010). *Effects of sleep and circadian rhythm on the human immune system.* Ann N Y Acad Sci, 1193: 48-59.

46. Besedovsky L, Lange T and Haack M (2019). *The Sleep-Immune Crosstalk in Health and Disease.* Physiol Rev, 99(3): 1325-1380.

47. Lorton D, Lubahn CL, Estus C, Millar BA, Carter JL, Wood CA and Bellinger DL (2006). *Bidirectional communication between the brain and the immune system: implications for physiological sleep and disorders with disrupted sleep.* Neuroimmunomodulation, 13(5-6): 357-374.

48. Marshall L and Born J (2002). *Brain-immune interactions in sleep.* Int Rev Neurobiol, 52: 93-131.

49. Zielinski MR, McKenna JT and McCarley RW (2016). *Functions and Mechanisms of Sleep.* AIMS Neurosci, 3(1): 67-104.

50. Benington JH and Heller HC (1995). *Restoration of brain energy metabolism as the function of sleep.* Prog Neurobiol, 45(4): 347-360.

51. Diekelmann S and Born J (2010). *The memory function of sleep.* Nat Rev Neurosci, 11(2): 114-126.

52. Akerstedt T and Nilsson PM (2003). *Sleep as restitution: an introduction.* J Intern Med, 254(1): 6-12.

53. Borbély AA (1982). *A two process model of sleep regulation.* Hum Neurobiol, 1(3): 195-204.

54. Cohen DA, Wang W, Wyatt JK, Kronauer RE, Dijk DJ, Czeisler CA and Klerman EB (2010). *Uncovering residual effects of chronic sleep loss on human performance.* Sci Transl Med, 2(14): 14ra13.

55. Kobayashi D, Takahashi O, Deshpande GA, Shimbo T and Fukui T (2012). *Association between weight gain, obesity, and sleep duration: a large-scale 3-year cohort study.* Sleep Breath, 16(3): 829-833.

56. Chao CY, Wu JS, Yang YC, Shih CC, Wang RH, Lu FH and Chang CJ (2011). *Sleep duration is a potential risk factor for newly diagnosed type 2 diabetes mellitus.* Metabolism, 60(6): 799-804.

57. Wang Q, Xi B, Liu M, Zhang Y and Fu M (2012). *Short sleep duration is associated with hypertension risk among adults: a systematic review and meta-analysis.* Hypertens Res, 35(10): 1012-1018.

58. Irwin M (2002). *Effects of sleep and sleep loss on immunity and cytokines.* Brain Behav Immun, 16(5): 503-512.

59. Besedovsky L, Lange T and Born J (2012). *Sleep and immune function.* Pflugers Arch, 463(1): 121-137.

60. Besedovsky L, Dimitrov S, Born J and Lange T (2016). *Nocturnal sleep uniformly reduces numbers of different T-cell subsets in the blood of healthy men.* Am J Physiol Regul Integr Comp Physiol, 311(4): R637-r642.

61. Brown R, Pang G, Husband AJ and King MG (1989). *Suppression of immunity to influenza virus infection in the respiratory tract following sleep disturbance.* Reg Immunol, 2(5): 321-325.

62. Lange T, Perras B, Fehm HL and Born J (2003). *Sleep enhances the human antibody response to hepatitis A vaccination.* Psychosom Med, 65(5): 831-835.

63. Lange T, Dimitrov S, Bollinger T, Diekelmann S and Born J (2011). *Sleep after vaccination boosts immunological memory.* J Immunol, 187(1): 283-290.

64. Bryant PA, Trinder J and Curtis N (2004). *Sick and tired: Does sleep have a vital role in the immune system?* Nat Rev Immunol, 4(6): 457-467.

65. Patel SR, Malhotra A, Gao X, Hu FB, Neuman MI and Fawzi WW (2012). *A prospective study of sleep duration and pneumonia risk in women.* Sleep, 35(1): 97-101.

66. Hsiao YH, Chen YT, Tseng CM, Wu LA, Lin WC, Su VY, Perng DW, Chang SC, Chen YM, Chen TJ, Lee YC and Chou KT (2015). *Sleep disorders and increased risk of autoimmune diseases in individuals without sleep apnea.* Sleep, 38(4): 581-586.

67. Fähnrich A, Krebbel M, Decker N, Leucker M, Lange FD, Kalies K and Möller S (2017). *ClonoCalc and ClonoPlot: immune repertoire analysis from raw files to publication figures with graphical user interface.* BMC Bioinformatics, 18(1): 164.

68. Bolotin DA, Shugay M, Mamedov IZ, Putintseva EV, Turchaninova MA, Zvyagin IV, Britanova OV and Chudakov DM (2013). *MiTCR: software for T-cell receptor sequencing data analysis.* Nat Methods, 10(9): 813-814.

69. Sethna Z, Elhanati Y, Callan CG, Walczak AM and Mora T (2019). *OLGA: fast computation of generation probabilities of B- and T-cell receptor amino acid sequences and motifs.* Bioinformatics, 35(17): 2974-2981.

70. Zhang Z, Procissi D, Li W, Kim DH, Li K, Han G, Huan Y and Larson AC (2013). *High resolution MRI for non-invasive mouse lymph node mapping.* J Immunol Methods, 400-401: 23-29.

71. Schaal S, Kunsch K and Kunsch S (2016). *Der Mensch in Zahlen*. Springer, 4th ed.

72. Simpson EH (1949). *Measurement of Diversity.* Nature, 163: 688-688.

73. Chaudhary N and Wesemann DR (2018). *Analyzing Immunoglobulin Repertoires.* Front Immunol, 9: 462.

74. Meinhardt M, Tune C, Schierloh LK, Schampel A, Pagel R and Westermann J (2022). *The splenic T cell receptor repertoire during an immune response against a complex antigen: Expanding private clones accumulate in the high and low copy number region.* PLoS One, 17(8): e0273264.

75. Levenshtein VI.(1966). *Binary codes capable of correcting deletions, insertions, and reversals*. In: *Soviet physics doklady*. Soviet Union.

76. Navarro G (2001). *A guided tour to approximate string matching.* ACM Comput. Surv., 33(1): 31–88.

77. Elhanati Y, Sethna Z, Callan CG, Jr., Mora T and Walczak AM (2018). *Predicting the spectrum of TCR repertoire sharing with a data-driven model of recombination.* Immunol Rev, 284(1): 167-179.

78. Jaccard P (1908). *Nouvelles recherches sur la distribution florale*. Impr. Réunies.

79. Westermann J, Geismar U, Sponholz A, Bode U, Sparshott SM and Bell EB (1997). *CD4+ T cells of both the naive and the memory phenotype enter rat lymph nodes and Peyer's patches via high endothelial venules: within the tissue their migratory behavior differs.* Eur J Immunol, 27(12): 3174-3181.

80. Willführ KU, Westermann J and Pabst R (1990). *Absolute numbers of lymphocytes subsets migrating through the compartments of the normal and transplanted rat spleen.* Eur J Immunol, 20(4): 903-911.

81. Banczyk D, Kalies K, Nachbar L, Bergmann L, Schmidt P, Bode U, Teegen B, Steven P, Lange T, Textor J, Ludwig RJ, Stöcker W, König P, Bell E and Westermann J (2014). *Activated CD4+ T cells enter the splenic T-cell zone and induce autoantibody-producing germinal centers through bystander activation.* Eur J Immunol, 44(1): 93-102.

82. Madi A, Shifrut E, Reich-Zeliger S, Gal H, Best K, Ndifon W, Chain B, Cohen IR and Friedman N (2014). *T-cell receptor repertoires share a restricted set of public and abundant CDR3 sequences that are associated with self-related immunity.* Genome Res, 24(10): 1603-1612.

83. Venturi V, Kedzierska K, Price DA, Doherty PC, Douek DC, Turner SJ and Davenport MP (2006). *Sharing of T cell receptors in antigen-specific responses is driven by convergent recombination.* Proceedings of the National Academy of Sciences, 103(49): 18691-18696.

84. Greiff V, Weber CR, Palme J, Bodenhofer U, Miho E, Menzel U and Reddy ST (2017). *Learning the High-Dimensional Immunogenomic Features That Predict Public and Private Antibody Repertoires.* J Immunol, 199(8): 2985-2997.

85. Westermann J and Bode U (1999). *Distribution of activated T cells migrating through the body: a matter of life and death.* Immunol Today, 20(7): 302-306.

86. Westermann J, Söllner S, Ehlers EM, Nohroudi K, Blessenohl M and Kalies K (2003). *Analyzing the migration of labeled T cells in vivo: an essential approach with challenging features.* Lab Invest, 83(4): 459-469.

87. Textor J, Henrickson SE, Mandl JN, von Andrian UH, Westermann J, de Boer RJ and Beltman JB (2014). *Random migration and signal integration promote rapid and robust T cell recruitment.* PLoS Comput Biol, 10(8): e1003752.

88. Mandl JN, Liou R, Klauschen F, Vrisekoop N, Monteiro JP, Yates AJ, Huang AY and Germain RN (2012). *Quantification of lymph node transit times reveals differences in antigen surveillance strategies of naive CD4+ and CD8+ T cells.* Proc Natl Acad Sci U S A, 109(44): 18036-18041.

89. Madi A, Poran A, Shifrut E, Reich-Zeliger S, Greenstein E, Zaretsky I, Arnon T, Laethem FV, Singer A, Lu J, Sun PD, Cohen IR and Friedman N (2017). *T cell receptor repertoires of mice and humans are clustered in similarity networks around conserved public CDR3 sequences.* Elife, 6.

90. Thomas N, Best K, Cinelli M, Reich-Zeliger S, Gal H, Shifrut E, Madi A, Friedman N, Shawe-Taylor J and Chain B (2014). *Tracking global changes induced in the CD4 T-cell receptor repertoire by immunization with a complex antigen using short stretches of CDR3 protein sequence.* Bioinformatics, 30(22): 3181-3188.

91. Fähnrich A, Klein S, Sergé A, Nyhoegen C, Kombrink S, Möller S, Keller K, Westermann J and Kalies K (2018). *CD154 Costimulation Shifts the Local T-Cell Receptor Repertoire Not Only During Thymic Selection but Also During Peripheral T-Dependent Humoral Immune Responses.* Front Immunol, 9: 1019.

92. Greiff V, Miho E, Menzel U and Reddy ST (2015). *Bioinformatic and Statistical Analysis of Adaptive Immune Repertoires.* Trends Immunol, 36(11): 738-749.

93. Akiba H, Takeda K, Kojima Y, Usui Y, Harada N, Yamazaki T, Ma J, Tezuka K, Yagita H and Okumura K (2005). *The role of ICOS in the CXCR5+ follicular B helper T cell maintenance in vivo.* J Immunol, 175(4): 2340-2348.

94. Tune C, Hahn J, Autenrieth SE, Meinhardt M, Pagel R, Schampel A, Schierloh LK, Kalies K and Westermann J (2021). *Sleep restriction prior to antigen exposure does not alter the T cell receptor repertoire but impairs germinal center formation during a T cell-dependent B cell response in murine spleen.* Brain Behav Immun Health, 16: 100312.

95. Merkenschlager J, Finkin S, Ramos V, Kraft J, Cipolla M, Nowosad CR, Hartweger H, Zhang W, Olinares PDB, Gazumyan A, Oliveira TY, Chait BT and Nussenzweig MC (2021). *Dynamic regulation of T(FH) selection during the germinal centre reaction.* Nature, 591(7850): 458-463.

96. Shulman Z, Gitlin AD, Targ S, Jankovic M, Pasqual G, Nussenzweig MC and Victora GD (2013). *T follicular helper cell dynamics in germinal centers.* Science, 341(6146): 673-677.

97. Niebuhr M, Belde J, Fähnrich A, Serge A, Irla M, Ellebrecht CT, Hammers CM, Bieber K, Westermann J and Kalies K (2021). *Receptor repertoires of murine follicular T helper cells reveal a high clonal overlap in separate lymph nodes in autoimmunity.* Elife, 10.

98. Birnbaum ME, Mendoza JL, Sethi DK, Dong S, Glanville J, Dobbins J, Ozkan E, Davis MM, Wucherpfennig KW and Garcia KC (2014). *Deconstructing the peptide-MHC specificity of T cell recognition.* Cell, 157(5): 1073-1087.

99. Nurieva RI, Mai XM, Forbush K, Bevan MJ and Dong C (2003). *B7h is required for T cell activation, differentiation, and effector function.* Proc Natl Acad Sci U S A, 100(24): 14163-14168.

100. Yeh CH, Finney J, Okada T, Kurosaki T and Kelsoe G (2022). *Primary germinal center-resident T follicular helper cells are a physiologically distinct subset of CXCR5(hi)PD-1(hi) T follicular helper cells.* Immunity, 55(2): 272-289.e277.

101. Crotty S (2019). *T Follicular Helper Cell Biology: A Decade of Discovery and Diseases.* Immunity, 50(5): 1132-1148.

102. Brenna E, Davydov AN, Ladell K, McLaren JE, Bonaiuti P, Metsger M, Ramsden JD, Gilbert SC, Lambe T, Price DA, Campion SL, Chudakov DM, Borrow P and McMichael AJ (2020). *CD4(+) T Follicular Helper Cells in Human Tonsils and Blood Are Clonally Convergent but Divergent from Non-Tfh CD4(+) Cells.* Cell Rep, 30(1): 137-152.e135.

103. Vella LA, Buggert M, Manne S, Herati RS, Sayin I, Kuri-Cervantes L, Bukh Brody I, O'Boyle KC, Kaprielian H, Giles JR, Nguyen S, Muselman A, Antel JP, Bar-Or A, Johnson ME, Canaday DH, Naji A, Ganusov VV, Laufer TM, Wells AD, Dori Y, Itkin MG, Betts MR and Wherry EJ (2019). *T follicular helper cells in human efferent lymph retain lymphoid characteristics.* J Clin Invest, 129(8): 3185-3200.

104. Heit A, Schmitz F, Gerdts S, Flach B, Moore MS, Perkins JA, Robins HS, Aderem A, Spearman P, Tomaras GD, De Rosa SC and McElrath MJ (2017). *Vaccination establishes clonal relatives of germinal center T cells in the blood of humans.* J Exp Med, 214(7): 2139-2152.

105. Hill DL, Pierson W, Bolland DJ, Mkindi C, Carr EJ, Wang J, Houard S, Wingett SW, Audran R, Wallin EF, Jongo SA, Kamaka K, Zand M, Spertini F, Daubenberger C, Corcoran AE and Linterman MA (2019). *The adjuvant GLA-SE promotes human Tfh cell expansion and emergence of public TCRβ clonotypes.* J Exp Med, 216(8): 1857-1873.

106. Hu M, Notarbartolo S, Foglierini M, Jovic S, Mele F, Jarrossay D, Lanzavecchia A, Cassotta A and Sallusto F (2023). *Clonal composition and persistence of antigen-specific circulating T follicular helper cells.* Eur J Immunol, 53(2): e2250190.

107. Vavassori S and Covey LR (2009). *Post-transcriptional regulation in lymphocytes: the case of CD154.* RNA Biol, 6(3): 259-265.

108. Pratama A and Vinuesa CG (2014). *Control of TFH cell numbers: why and how?* Immunol Cell Biol, 92(1): 40-48.

109. Hale JS, Youngblood B, Latner DR, Mohammed AU, Ye L, Akondy RS, Wu T, Iyer SS and Ahmed R (2013). *Distinct memory CD4+ T cells with commitment to T follicular helper- and T helper 1-cell lineages are generated after acute viral infection.* Immunity, 38(4): 805-817.

110. Suan D, Nguyen A, Moran I, Bourne K, Hermes JR, Arshi M, Hampton HR, Tomura M, Miwa Y, Kelleher AD, Kaplan W, Deenick EK, Tangye SG, Brink R, Chtanova T and Phan TG (2015). *T follicular helper cells have distinct modes of migration and molecular signatures in naive and memory immune responses.* Immunity, 42(4): 704-718.

111. Born J, Lange T, Hansen K, Mölle M and Fehm HL (1997). *Effects of sleep and circadian rhythm on human circulating immune cells.* J Immunol, 158(9): 4454-4464.

112. Dimitrov S, Lange T, Nohroudi K and Born J (2007). *Number and function of circulating human antigen presenting cells regulated by sleep.* Sleep, 30(4): 401-411.

113. Ruiz FS, Andersen ML, Martins RC, Zager A, Lopes JD and Tufik S (2012). *Immune alterations after selective rapid eye movement or total sleep deprivation in healthy male volunteers.* Innate Immun, 18(1): 44-54.

114. Nash G, Paidimuddala B and Zhang L (2022). *Structural aspects of the MHC expression control system.* Biophys Chem, 284: 106781.

115. Devaiah BN and Singer DS (2013). *CIITA and Its Dual Roles in MHC Gene Transcription.* Front Immunol, 4: 476.

116. LeibundGut-Landmann S, Waldburger JM, Krawczyk M, Otten LA, Suter T, Fontana A, Acha-Orbea H and Reith W (2004). *Mini-review: Specificity and expression of CIITA, the master regulator of MHC class II genes.* Eur J Immunol, 34(6): 1513-1525.

117. Au-Yeung BB, Shah NH, Shen L and Weiss A (2018). *ZAP-70 in Signaling, Biology, and Disease.* Annu Rev Immunol, 36: 127-156.

118. Béné MC (2006). *What is ZAP-70?* Cytometry B Clin Cytom, 70(4): 204-208.

119. Fischer A, Picard C, Chemin K, Dogniaux S, le Deist F and Hivroz C (2010). *ZAP70: a master regulator of adaptive immunity.* Semin Immunopathol, 32(2): 107-116.

120. Gangopadhyay K, Roy S, Sen Gupta S, Chandradasan AC, Chowdhury S and Das R (2022). *Regulating the discriminatory response to antigen by T-cell receptor.* Biosci Rep, 42(3).

121. Ashouri JF, Lo WL, Nguyen TTT, Shen L and Weiss A (2022). *ZAP70, too little, too much can lead to autoimmunity.* Immunol Rev, 307(1): 145-160.

122. Courtney AH, Lo WL and Weiss A (2018). *TCR Signaling: Mechanisms of Initiation and Propagation.* Trends Biochem Sci, 43(2): 108-123.

123. Garside P, Ingulli E, Merica RR, Johnson JG, Noelle RJ and Jenkins MK (1998). *Visualization of specific B and T lymphocyte interactions in the lymph node.* Science, 281(5373): 96-99.

124. Smith KM, Brewer JM, Webb P, Coyle AJ, Gutierrez-Ramos C and Garside P (2003). *Inducible costimulatory molecule-B7-related protein 1 interactions are important for the clonal expansion and B cell helper functions of naive, Th1, and Th2 T cells.* J Immunol, 170(5): 2310-2315.

125. Okazaki T, Iwai Y and Honjo T (2002). *New regulatory co-receptors: inducible co-stimulator and PD-1.* Curr Opin Immunol, 14(6): 779-782.

126. Elgueta R, Benson MJ, de Vries VC, Wasiuk A, Guo Y and Noelle RJ (2009). *Molecular mechanism and function of CD40/CD40L engagement in the immune system.* Immunol Rev, 229(1): 152-172.

127. Howland KC, Ausubel LJ, London CA and Abbas AK (2000). *The roles of CD28 and CD40 ligand in T cell activation and tolerance.* J Immunol, 164(9): 4465-4470.

128. Cheng G and Schoenberger SP (2002). *CD40 signaling and autoimmunity.* Curr Dir Autoimmun, 5: 51-61.

129. Liu D, Xu H, Shih C, Wan Z, Ma X, Ma W, Luo D and Qi H (2015). *T-B-cell entanglement and ICOSL-driven feed-forward regulation of germinal centre reaction.* Nature, 517(7533): 214-218.

130. Choi YS, Kageyama R, Eto D, Escobar TC, Johnston RJ, Monticelli L, Lao C and Crotty S (2011). *ICOS receptor instructs T follicular helper cell versus effector cell differentiation via induction of the transcriptional repressor Bcl6.* Immunity, 34(6): 932-946.

131. Marsman C, Verstegen NJ, Streutker M, Jorritsma T, Boon L, Ten Brinke A and van Ham SM (2022). *Termination of CD40L co-stimulation promotes human B cell differentiation into antibody-secreting cells.* Eur J Immunol, 52(10): 1662-1675.

132. Marth JD and Grewal PK (2008). *Mammalian glycosylation in immunity.* Nat Rev Immunol, 8(11): 874-887.

133. De Bousser E, Meuris L, Callewaert N and Festjens N (2020). *Human T cell glycosylation and implications on immune therapy for cancer.* Hum Vaccin Immunother, 16(10): 2374-2388.

134. Pereira MS, Alves I, Vicente M, Campar A, Silva MC, Padrão NA, Pinto V, Fernandes Â, Dias AM and Pinho SS (2018). *Glycans as Key Checkpoints of T Cell Activity and Function.* Front Immunol, 9: 2754.

135. Furukawa K and Sato T (1999). *Beta-1,4-galactosylation of N-glycans is a complex process.* Biochim Biophys Acta, 1473(1): 54-66.

136. Hennet T (2002). *The galactosyltransferase family.* Cell Mol Life Sci, 59(7): 1081-1095.

137. Rudd PM, Elliott T, Cresswell P, Wilson IA and Dwek RA (2001). *Glycosylation and the immune system.* Science, 291(5512): 2370-2376.

138. Nilius V, Killer MC, Timmesfeld N, Schmitt M, Moll R, Lorch A, Beyer J, Mack E, Lohoff M, Burchert A, Neubauer A and Brendel C (2018). *High β-1,4-Galactosyltransferase-I expression in peripheral T-lymphocytes is associated with a low risk of relapse in germ-cell cancer patients receiving high-dose chemotherapy with autologous stem cell reinfusion.* Oncoimmunology, 7(5): e1423169.

139. Sperandio M, Gleissner CA and Ley K (2009). *Glycosylation in immune cell trafficking.* Immunol Rev, 230(1): 97-113.

140. Gómez-Henao W, Tenorio EP, Sanchez FRC, Mendoza MC, Ledezma RL and Zenteno E (2021). *Relevance of glycans in the interaction between T lymphocyte and the antigen presenting cell.* Int Rev Immunol, 40(4): 274-288.

141. Jones MB (2018). *IgG and leukocytes: Targets of immunomodulatory α2,6 sialic acids.* Cell Immunol, 333: 58-64.

142. Han Y, Zhou X, Ji Y, Shen A, Sun X, Hu Y, Wu Q and Wang X (2010). *Expression of beta-1,4-galactosyltransferase-I affects cellular adhesion in human peripheral blood CD4+ T cells.* Cell Immunol, 262(1): 11-17.

143. Cheng X, Wang X, Han Y and Wu Y (2010). *The expression and function of β-1,4-galactosyltransferase-I in dendritic cells.* Cell Immunol, 266(1): 32-39.

144. Bollinger T, Bollinger A, Skrum L, Dimitrov S, Lange T and Solbach W (2009). *Sleep-dependent activity of T cells and regulatory T cells.* Clin Exp Immunol, 155(2): 231-238.

145. Wilder-Smith A, Mustafa FB, Earnest A, Gen L and Macary PA (2013). *Impact of partial sleep deprivation on immune markers.* Sleep Med, 14(10): 1031-1034.

146. Khoder-Agha F, Harrus D, Brysbaert G, Lensink MF, Harduin-Lepers A, Glumoff T and Kellokumpu S (2019). *Assembly of B4GALT1/ST6GAL1 heteromers in the Golgi membranes involves lateral interactions via highly charged surface domains.* J Biol Chem, 294(39): 14383-14393.

147. Staretz-Chacham O, Noyman I, Wormser O, Abu Quider A, Hazan G, Morag I, Hadar N, Raymond K, Birk OS, Ferreira CR and Koifman A (2020). *B4GALT1-congenital disorders of glycosylation: Expansion of the phenotypic and molecular spectrum and review of the literature.* Clin Genet, 97(6): 920-926.

148. Renegar KB, Floyd RA and Krueger JM (1998). *Effects of short-term sleep deprivation on murine immunity to influenza virus in young adult and senescent mice.* Sleep, 21(3): 241-248.

149. Ackermann K, Revell VL, Lao O, Rombouts EJ, Skene DJ and Kayser M (2012). *Diurnal rhythms in blood cell populations and the effect of acute sleep deprivation in healthy young men.* Sleep, 35(7): 933-940.

150. Ricardo JS, Cartner L, Oliver SJ, Laing SJ, Walters R, Bilzon JL and Walsh NP (2009). *No effect of a 30-h period of sleep deprivation on leukocyte trafficking, neutrophil degranulation and saliva IgA responses to exercise.* Eur J Appl Physiol, 105(3): 499-504.

151. Heiser P, Dickhaus B, Schreiber W, Clement HW, Hasse C, Hennig J, Remschmidt H, Krieg JC, Wesemann W and Opper C (2000). *White blood cells and cortisol after sleep deprivation and recovery sleep in humans.* Eur Arch Psychiatry Clin Neurosci, 250(1): 16-23.

152. Heiser P, Dickhaus B, Opper C, Hemmeter U, Remschmidt H, Wesemann W, Krieg JC and Schreiber W (2001). *Alterations of host defence system after sleep deprivation are followed by impaired mood and psychosocial functioning.* World J Biol Psychiatry, 2(2): 89-94.

153. Sun LZ, Elsayed S, Aasen TB, Van Do T, Aardal NP, Florvaag E and Vaali K (2010). *Comparison between ovalbumin and ovalbumin peptide 323-339 responses in allergic mice: humoral and cellular aspects.* Scand J Immunol, 71(5): 329-335.

154. Yang M and Mine Y (2009). *Novel T-cell epitopes of ovalbumin in BALB/c mouse: potential for peptide-immunotherapy.* Biochem Biophys Res Commun, 378(2): 203-208.

155. Merkenschlager J and Kassiotis G (2015). *Narrowing the Gap: Preserving Repertoire Diversity Despite Clonal Selection during the CD4 T Cell Response.* Front Immunol, 6: 413.

156. Imberti L, Sottini A and Primi D (1993). *T cell repertoire and autoimmune diseases.* Immunol Res, 12(2): 149-167.

157. Zhao Y, Nguyen P, Vogel P, Li B, Jones LL and Geiger TL (2016). *Autoimmune susceptibility imposed by public TCRβ chains.* Sci Rep, 6: 37543.

158. Planas R, Metz I, Martin R and Sospedra M (2018). *Detailed Characterization of T Cell Receptor Repertoires in Multiple Sclerosis Brain Lesions.* Front Immunol, 9: 509.

159. Jick SS, Li L, Falcone GJ, Vassilev ZP and Wallander MA (2015). *Epidemiology of multiple sclerosis: results from a large observational study in the UK.* J Neurol, 262(9): 2033-2041.

160. Sospedra M and Martin R (2005). *Immunology of multiple sclerosis.* Annu Rev Immunol, 23: 683-747.

161. Goverman J (2009). *Autoimmune T cell responses in the central nervous system.* Nat Rev Immunol, 9(6): 393-407.

162. Flügel A, Berkowicz T, Ritter T, Labeur M, Jenne DE, Li Z, Ellwart JW, Willem M, Lassmann H and Wekerle H (2001). *Migratory activity and functional changes of green fluorescent effector cells before and during experimental autoimmune encephalomyelitis.* Immunity, 14(5): 547-560.

163. De Vos AF, van Riel DA, van Meurs M, Brok HP, Boon L, Hintzen RQ, Claassen E, t Hart BA and Laman JD (2005). *Severe T-cell depletion from the PALS leads to altered spleen composition in common marmosets with experimental autoimmune encephalomyelitis (EAE).* J Neuroimmunol, 161(1-2): 29-39.

164. Guo J, Zhao C, Wu F, Tao L, Zhang C, Zhao D, Yang S, Jiang D, Wang J, Sun Y, Li Z, Li H and Yang K (2018). *T Follicular Helper-Like Cells Are Involved in the Pathogenesis of Experimental Autoimmune Encephalomyelitis.* Front Immunol, 9: 944.

165. Lodygin D and Flügel A (2017). *Intravital real-time analysis of T-cell activation in health and disease.* Cell Calcium, 64: 118-129.

166. Pipi E, Nayar S, Gardner DH, Colafrancesco S, Smith C and Barone F (2018). *Tertiary Lymphoid Structures: Autoimmunity Goes Local.* Front Immunol, 9: 1952.

167. Kuerten S, Rottlaender A, Rodi M, Velasco VB, Jr., Schroeter M, Kaiser C, Addicks K, Tary-Lehmann M and Lehmann PV (2010). *The clinical course of EAE is reflected by the dynamics of the neuroantigen-specific T cell compartment in the blood.* Clin Immunol, 137(3): 422-432.

168. Kuerten S, Schickel A, Kerkloh C, Recks MS, Addicks K, Ruddle NH and Lehmann PV (2012). *Tertiary lymphoid organ development coincides with determinant spreading of the myelin-specific T cell response.* Acta Neuropathol, 124(6): 861-873.

169. Tsunoda I, Libbey JE, Kuang LQ, Terry EJ and Fujinami RS (2005). *Massive apoptosis in lymphoid organs in animal models for primary and secondary progressive multiple sclerosis.* Am J Pathol, 167(6): 1631-1646.

170. Pedroni MN, Hirotsu C, Porro AM, Tufik S and Andersen ML (2017). *The role of sleep in pemphigus: a review of mechanisms and perspectives.* Arch Dermatol Res, 309(8): 659-664.

171. Sangle SR, Tench CM and D'Cruz DP (2015). *Autoimmune rheumatic disease and sleep: a review.* Curr Opin Pulm Med, 21(6): 553-556.

List of Figures

List of Tables

Acknowledgements

First of all, I want to thank my supervisor Prof. Dr. med. Jürgen Westermann for giving me the possibility to do a PhD in the Institute of Anatomy. With productive discussions, his support, and his competence to put information in a nutshell he promoted this work while always lending an ear for upcoming problems.

Furthermore, I appreciate being two years part of the research training group “Modulation of Autoimmunity”. The chance to present my own work to receive feedback for the experiments as well as gaining new input from people of different fields of knowledge was instrumental in making massive strides. My mentors Dr. rer. nat. Andrea Schampel and PD Dr. Ing. Antje Müller should especially set apart here.

A special thanks goes to the members of the Institute of Anatomy, in particular Dr. rer. nat. Andrea Schampel, Dr. rer. physiol. Cornelia Tune, Dr. rer. nat. René Pagel, Dr. med. Martin Meinhardt, Prof. Dr. rer. nat. Kathrin Kalies and Farbod Bahreini. Thank you for your support, expertise, and helpful discussions as well as nice off-topic conversations and activities that ensured a comfortable atmosphere and thus welcomed me in the team.

This of course also applies to Petra Lau, Daniela Rieck and Lidija Gutjahr who together with Dr. rer. nat. René Pagel moreover supported me at various experiments and guided the laboratory work with their technical expertise to success.

In addition, former and actual research assistants that helped me to deal with the bulk of sequencing data should not remain unmentioned here. I especially want to emphasize Johanna Gosten and Ida Happel who did a great job and fought with me through the jungle of programming and statistics. In this context, I also want to thank Dr. rer. nat. Johannes Textor for his great advice and new ideas to analyze and interpret these data.

I also want to express my gratitude to the Department for Infectious Diseases and Microbiology, in particular Dr. rer. nat. Mareike Ohms, for briefing me in using the Agilent 2100 Bioanalyzer for RNA quantification as well as for kindly providing all required reagents. Thank you also to Prof. Dr. rer. nat. Marc Ehlers and Dr. rer. nat. Hanna Lunding from the Laboratories of Immunology and Antibody Glycan Analysis of the Institute for Nutrition Medicine for affording the opportunity to transfer this analysis to a different antigen model.

Finally, sincere thanks are given to both family and friends for their unfailing assistance, encouragement and required distraction whenever needed.